Spring 2017

Dissolution-enlarged fractures imaging using electrical resistivity tomography (ERT)

Elnaz Siami-Irdemoosa

DISSOLUTION-ENLARGED FRACTURES IMAGING USING ELECTRICAL RESISTIVITY TOMOGRAPHY (ERT)

by

ELNAZ SIAMI-IRDEMOOSA

A DISSERTATION

Presented to the Faculty of the Graduate School of the

MISSOURI UNIVERSITY OF SCIENCE AND TECHNOLOGY

In Partial Fulfillment of the Requirements for the Degree

DOCTOR OF PHILOSOPHY

in

GEOLOGICAL ENGINEERING

2017

Approved
Neil L. Anderson, Advisor
J. David Rogers
Norbert H. Maerz
Kelly Liu
Maochen Ge

ABSTRACT

In recent years the electrical imaging techniques have been largely applied to geotechnical and environmental investigations. These techniques have proven to be the best geophysical methods for site investigations in karst terrain, particularly when the overburden soil is clay-dominated. Karst is terrain with a special landscape and distinctive hydrological system developed by dissolution of rocks, particularly carbonate rocks such as limestone and dolomite, made by enlarging fractures into underground conduits that can enlarge into caverns, and in some cases collapse to form sinkholes.

Bedding planes, joints, and faults are the principal structural guides for underground flow and dissolution in almost all karstified rocks. Despite the important role of fractures in karst development, the geometry of dissolution-enlarged fractures remain poorly unknown. These features are characterized by an strong contrast with the surrounding formations in terms of physical properties, such as electrical resistivity.

Electrical resistivity tomography (ERT) was used as the primary geophysical tool to image the subsurface in a karst terrain in Greene County, Missouri. Pattern, orientation and density of the joint sets were interpreted from ERT data in the investigation site. The Multi-channel Analysis of Surface Wave (MASW) method and coring were employed to validate the interpretation results.

Two sets of orthogonal visually prominent joints have been identified in the investigation site: north-south trending joint sets and west-east trending joint sets. However, most of the visually prominent joint sets are associated with either cultural features that concentrate runoff, natural surface drainage features or natural surface drainage.

ACKNOWLEDGMENTS

I would like to express my sincere gratitude to my PhD advisor, Dr. Neil L. Anderson, as well my PhD examination committee members, Dr. Norbert H. Maerz, Dr. J. David Rogers, Dr. Kelly Liu and Dr. Maochen Ge. I would like to thank the Geological Engineering program at Missouri S&T and Dr. Norbert H. Maerz, the former program head, for awarding me the department scholarship in 2013. I would like to acknowledge the Society of Mining, Metallurgy, and Exploration for awarding me "SME-WAAIAMI" scholarship in 2014 and 2016.

I owe much gratitude to my parents, brothers, and my nephew Ilia for their supports. Dear mom, you have brought me up cocooned in you love and motivated by your hard work. Thank you for walking with me and loving me unconditionally. Dear Dad, you have been a rock in my life. Thank you for being a pillar of strength over the last 33 years. It wouldn't have been such a success without you.

Last, but never least, I cannot begin to express my unfailing gratitude and love to my husband Dr. Saeid R. Dindarloo who has constantly supported me and encouraged me. I would also like to thank him for his scientific contributions to this dissertation and related research tasks. I could not overcome insurmountable obstacles in big data analytic processes in this project without his guidance and persistent help.

TABLE OF CONTENTS

LIST OF ILLUSTRATIONS

Page

LIST OF TABLES

Page

1. INTRODUCTION

Karst is terrain with a special landscape and distinctive hydrological system developed by dissolution of rocks, particularly carbonate rocks such as limestone and dolomite, made by enlarging fractures into underground conduits that can enlarge into caverns, and in some cases collapse to form sinkholes [1, 2, and 3]. Downward percolating water slowly dissolves the host rock creating a network of enlarged fractures, fissures and bedding planes.

Bedding planes, joints, and faults are the principal structural guides for underground flow and dissolution in almost all karstified rocks [1 and 2]. Palmer [4] has investigated the pattern of several thousand cave passage and conclude that 57% of cave passage follow bedding planes, 42% are fracture-oriented and only 1% of the total passages are related to porosity of the rock.

Despite the important role of fractures in karst development, the geometry of dissolution-enlarged fractures remain poorly unknown, largely due to inaccessibility of these underground geological features.

McCracken [5] points out that nearly all of the consolidated rock formation of Missouri are jointed. Graves [6] who has studied the Missouri joints in Precambrian distinguishes four joint systems, each consisting of two sets at right angles to each other. The sets strike about N.-S, .E.-W., N. 40° E., N. 50° W., N. 65° W., N. 25° E., N. 65° E., and N. 25° W.

Missouri is located at the central stable region of the United States and western Canada. This region has been fairly stable since the Proterozoic time, with only epeirogenic

movements. Although Missouri is a part of the stable Mid-continent, localized areas have undergone several periods of uplifts and distortion since the Precambrian time.

According to [7], joints in the Cambrian and Ordovician rocks are mainly vertical. In general, there is a persistent set of joints striking approximately N. 20° W. and N. 75 E., and a minor set striking N. 45° E. and N. 60° W., the former set being the more persistent.

Van Horn [8] studied joints of the Mississippian rocks in Moniteau County. He noted four set of vertical or nearly vertical joints in the Burlington limestone of Mississippian age. The strike of major joints is N. 24° W. and N. 64° W., and that of the minor joints is north-south (N. 19° E.) and east-west (N. 70° W.).

Hinds and Greene [9] has studied joints in the Pennsylvanian series in Missouri. According to [9], all of the limestone and some of the sandstone beds of the region are more or less prominently intersected by vertical joint planes. Most of these may be separated in to two principal and two minor sets, those striking about N. 62° E. are the most common, but those whose direction is about N. 3° W. are scarcely less abundant.

Bretz [10] mentioned jointing as influencing the development of many caves including the Cameron and Mark Twain Caves in Marion County and the Bluff Dwellers Cave in McDonald County. Barnholtz [11] related the Ball and Smith [7]'s joint pattern to cavern development and orientation. He found an strong correlation between cave passage direction and surface joint trends. Author concluded that cavern development is influenced a great deal by pre-existing joint systems.

A few research has been carried out on the geometry of dissolution-enlarged fractures in karst terrain, due to inaccessibility of this underground geological features.

These features are characterized by strong contrast with the surrounding formations in terms of physical properties, such as electrical resistivity.

In recent years, the electrical imaging techniques have been largely applied to geotechnical and environmental investigations. These techniques have proven to be the best geophysical methods for site investigations in karst terrain, particularly when the overburden soil is clay-dominated [12, 13, and 14]. The high contrast in resistivity values between carbonate rock and clayey soil makes the resistivity method useful for determining the soil-bedrock contact.

Electrical resistivity tomography (ERT) was used as the primary geophysical tool to image the subsurface in a karst terrain in Greene County, Missouri. A total of 352,015 linear feet of ERT data were acquired along 149 separate traverse. ERT data were acquired mostly along parallel west-east oriented traverses nearly spaced at 100 ft intervals. Several more widely north-south oriented traversed were also selected for data acquisition. Because joint orientation in both north-south and west-east direction are expected in the investigation site.

The collected ERT data were processed to produce a 2D model of the subsurface from the apparent electrical resistivity data. Then, pattern, orientation and density of the joint sets were interpreted from ERT data in the investigation site.

The Multi-channel Analysis of Surface Wave (MASW) method and coring were employed to validate the interpretation results. Soil-rock contacts were determined from ERT data. The determined soil-rock contact from ERT data, MASW data and cores were compared. The variation of the interpreted soil-rock contact in the investigation site was also compared to the interpreted joint sets in the study area.

In order to validate two dimensional ERT data interpretation results, three dimensional ERT data were acquired in a section of the investigation site. The interpreted jointing patterns from the 2D ERT data were compared with the 3D ERT results.

A few number of studies have been carried out on jointing pattern in the karst areas close to the investigation site. A comparative discussion between the previous studies and our results, has been presented.

2. STRATIGRAPHIC AND STRUCTURAL GEOLOGY OF SOUTHWESTERN MISSOURI

2.1. STRATIGRAPHY

Missouri is a part of stable Mid-continent and deeply eroded Ozark uplift is located on it. Deeply eroded Ozark has undergone repeated mild uplift since Precambrian time exposing rocks ranging in age from Precambrian to Paleozoic [5]. The stratigraphic geology of Missouri is presented in the following with an emphasis on the southwestern Missouri, Springfield Plateau [15]:

Precambrian rocks of Missouri appear at the surface in the southeastern part of the states in Washington, Ste. Genevieve, St. Francois, Madison, Wayne, Reynolds, Shannon, dent, and Carter counties. These rocks are mainly porphyries and granites. A long period of erosion followed the formation of the porphyries and granites and, in a part of Missouri where they are now exposed, valleys several hundred feet deep formed. It is probable that hundreds of feet of rock were removed from the tops of the highest hills before the sea came in and sediment were laid down on top of the igneous rocks .

During ***Lower and Middle Cambrian*** time all of the area of Missouri seems to have been undergoing erosion and it was not until lower Upper Cambrian that seas spread over the state. The advancing seas formed conglomerates made of fragments of granite and porphyry, and sandstones made of the small pebbles and only rarely do the largest of them reach a diameter of 5 inches.

The ***Ordovician*** seas seem to have advanced into the state from the south and southeast. A basal conglomerate was to be expected, made up largely of chert fragment, but the conglomerate is not more than a foot thick in most places and in many places is absent.

The only outcrops of ***Silurian*** in Missouri are in the northeastern part of the state in Pike and Lincoln counties and the southeastern part in Ste. Genevieve, Perry, Bollinger, Scott, and Cape Girardeau counties. The Lower Silurian seas came as far as west and probably entered the northwest part of the state from Iowa. The only Middle Silurian known in the state is in Ste. Genevieve, Perry, Bollinger, and Cape Girardeau counties. In the northeastern part of the state two Lower Silurian formation have been recognized, the Edgwood formation and the Sexton Greek limestone.

The ***Devonian*** formation is represented in Missouri from earliest to latest but there are many gaps in the record. Only three Devonian formations have been recognized in southwestern Missouri, and they are thin and patchy in distribution (Fortune formation, Sylamore sandstone, Louisiana limestone).

The ***Mississippian*** system crops out from the northeastern corner of Missouri to the southeastern. The width of Mississippian outcrop belt is highly variable. In places the belt of outcrop is more than 50 miles wide while in other places it is less than five mile wide. The system is less than 400 feet thick and has 26 formations, but not more than 10 are present in any one place. Most of the formations are well differentiated, but some of them cannot be distinguished from adjacent formations. This is true in particular of the Burlington and Keokuk, and the Warsaw and St. Louis are in the same category.

The Mississippian seas invaded from the south and east over a low lying terrain, in a peneplained condition. In the northeastern area, the sea connected northeastern Missouri with central, so that the sand from central Missouri was shifted through shallow seas to the northeastern area. The coarse sand was deposited west and southwest of St. Louis, and the sediment became finer to the northeast making the Hannibal siltstone and shale.

After the sands were all used up, and the sea margins advanced hundreds of miles expecting in central Missouri, silty and argillaceous limestone began to be deposited. The soon gave place to pure limestone and cherty limestone, which continued as long as sea remained over the state, expecting in the southeastern part and, for a time, in the southwestern part.

In the southwestern part, limestone followed the thin sandstone of the Bushberg until a thickness of accumulated clay and silt again came in and formed the Northview formation. The southeastern lowlands must have finished the clastics at the same time that the fine materials were being deposited in northeastern Missouri. The materials of the Northview are almost exactly like those of the Hannibal, and they could have come from no other source. In both regions, limestones were deposited over the clastics. In the central part of the state no sandstone or shale succeeded the thin film of Bushberg sand.

It is not known that how much Middle Mississippian was deposited over the central and western parts of the state, because in most places all overlying formation above the Burlington had been removed before the Pennsylvanian seas came in. In the eastern and southeastern parts of the state a complete succession of Mississippian sediments seems to have formed. Some erosion took place, however, before the Upper Mississippian seas came in.

Much of the Upper Mississippian is clastics in southeastern Missouri, where the sea occupied the lower areas; but the shallow seas filled up in the early part of the Upper Mississippian, and the shore line was east of Missouri in the last two-thirds of the Upper Mississippian. Over the southwestern Missouri the Upper Mississippian seas advanced for about 50 miles, filling the depression in the surface of the older rocks with boulders,

cobbels, and sands, finally clearing and allowing limestones to form. Probably the seas were filled before the middle of the Upper Mississippian. All of Missouri was land at the end of the Mississippian, and none of it was high.

At the opening of ***Pennsylvanian*** time, all of Missouri was land, but none of it was very high. Mississippian and Ordovician rocks formed most of the surface. Probably about as much pre-Cambrian and Cambrian were at the surface as at the present time, and Devonian and Silurian rocks formed the surface in small areas of eastern Missouri. A great many sink holes were present in Ordovician and Mississippian areas but as all of the northwestern part of the state is deeply covered with Pennsylvanian sediments the pre-Pennsylvanian topography is unknown there. As most of the Mississippian and Ordovician rocks are cherty, a rather thick chert mantle covered a great deal of the Mississippian and Ordovician areas. When the Pennsylvanian seas came in, they washed the cherts into the valleys and sink holes and left the top of the hills bare until water covered them and fine sediments were moved for some distance to make a sandstone over the chert conglomerates and hilltops. Apparently, the land was well covered with vegetation in the late Mississippian.

Moore considers the Admire of northwestern Missouri as ***Permian*** but none of the other students of Permian has published concurring opinion [15]. No ***Triassic*** or ***Jurassic*** seas reached Missouri. Continental deposits must have formed in many places in the state but no remnants of these are known. In Crowleys Ridge of southeastern Missouri there are several areas of outcrops of ***Cretaceous*** sediments and no other marine Cretaceous sediments have been found in the state. The sediments are alternating sands and clays containing some mica and glauconite, one bed of lignite, and some limonite.

Eocene formations are present in Missouri only in the southeastern lowlands. Three formations are present, Clayton, Porters, Creek, and Wilcox. Their Maximum thickness is about 460 feet.

Table 2.1 summarize Missouri stratigraphic units. Springfield Plateau units have been shown in bold font.

Table 2.1. General section of Missouri stratigraphic units [15 and 16]

Geologic time	System	series	Geologic unit
Cenozoic			
	Pliocene and Pleistocene		Lafayette formation
			Glacial drifts of Missouri
	Eocene		Clayton formation
			Porter's Creek clay
			Wilcox group
Mesozoic			
	Tertiary		
	Cretaceous		Ripley formation
			Owl Creek formation
			Dakota sandstone
			Continental Cretaceous
Paleozoic			
	Pennsylvanian		
	Mississippian	Chesterian	
		Meramecian	
		Osagean	**Keokuk Limestone**
			Burlington Limestone
			Grand Falls Formation
			Reeds Spring Formation
			Pierson Formation
		Kinderhookian	**Northview Formation**
			Sedalia Formation

Table 2.1 General section of Missouri stratigraphic units [15 and 16] (cont.)

Geologic time	System	series	Geologic unit
			Compton Formation
			Hannibal Formation
	Devonian		
	Silurian		
	Ordovician		
		Cincinnatian	Orchard Creek Shale
			Thebes Sandstone
			Maquoketa Shale
			Cape Limestone
		Champlainian	Kimmswick Formation
			Decorah Formation
			Plattin Formation
			Joachim Dolomite
			Dutchtwon Formation
			St. Peter Sandstone
			Everton Formation
		Canadian	Smithville Formation
			Powell Dolomite
			Cotter Dolomite
			Jefferson City Dolomite
			Roubidoux Fromation
			Gasconade Dolomite
			Gunter Sandstone member
	Cambrian	Upper Cambrian	**Eminence Dolomite**
			Potosi Dolomite
			Derby-Doerun Dolomite
			Davis Formation
			Bonneterre Formation
			Lamotte Sandstone
Precambrian			**Igneous**, metasediments, and other metamorphic rock

Ozark Plateaus lies mainly between Missouri, Mississippi, and Arkansas River and contains parts of the state of Missouri, Oklahoma, Arkansas, and Illinois. This province has been divided to four sections by regional geologist and each sections has its distinctive geology and topography [17]. These are St. Francois Mountains, Salem Plateau, Springfield Plateau, and Boston Mountains sections and can be seen in Figure 2.1.

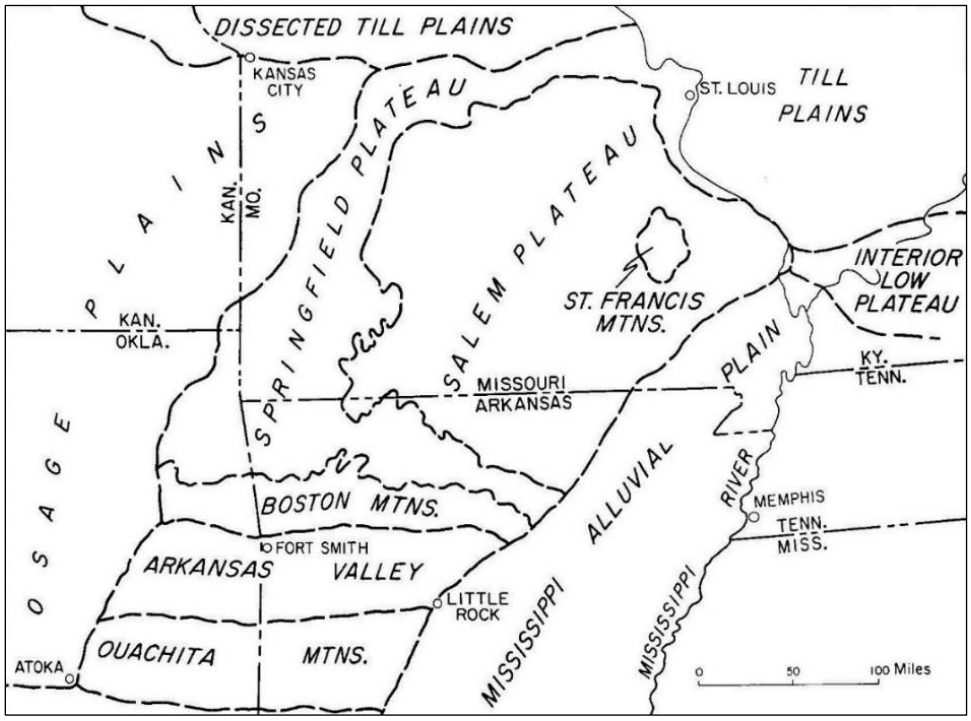

Figure 2.1. Sections of Ozark Plateaus [17]

The Springfield Plateau is the part Ozark which is underlain mostly by rocks of Mississippian age [17]. It is underlain by Precambrian crystalline rock at depth. The Precambrian basement is overlain by the Cambrian age rocks; Lamotte Sandstone, Bonneterre Formation, Davis Formation, Derby-Doerun Dolomite, Potosi Dolomite, and

Eminence Dolomite. The Ordovician-aged Gasconade Fromation overlies the Eminence Formation. Gasconade Formation is underlain by Roubidoux formation, Jefferson City and Cotter Formations.

2.2. STRUCTURAL FEATURES

The continent of North America is made up of a great stable interior and surrounding belts of compressed, intruded, and metamorphosed rock (Fig. 2.2). Belts that border the interior has been active since Proterozoic time and had orogenic movement. The interior has been fairly stable with only epeirogenic movement. The term orogeny and epeirogeny are processes of deformation. Gillbert [18] defined orogeny as the process of mountain building, and epeirogeny as the process of continental displacement to form the large swells and basins. Orogenic structure are visible to the eye, such as faults, folds , and thrusts; whereas epeirogenic structures are so gentle that dips are scarcely noticeable, and are due to broad wrapping [18]. The usage in America today is fairly uniform in the respect that orogenic movement is of the nature of folding, thrusting, and block faulting or rifting, and for the most part take place in the geosynclinal belts. Epeirogenic movement is vertical, of gentle nature, and effects regional parts of the crust. The arches, domes, and large basins of the central stable region of the continent are examples of epeirogenic movements, and the interruption of cycles of erosion in the deformed geosynclinal belt by elevation is an example of epeirogenic movement in the marginal and older orogenic belts [18].

The interior stable region is commonly referred to as the nucleus of the continent, as the craton, or the shield. Shield exist in other continents, but not so effectively surrounded by orogenic belts as that of the North America continent. The stable interior is

divided into three major parts, the Canadian Shield, the central stable region of the United States and western Canada, and the Arctic stable region (Figure 2.2). Missouri is located at the central stable region of the United States and western Canada.

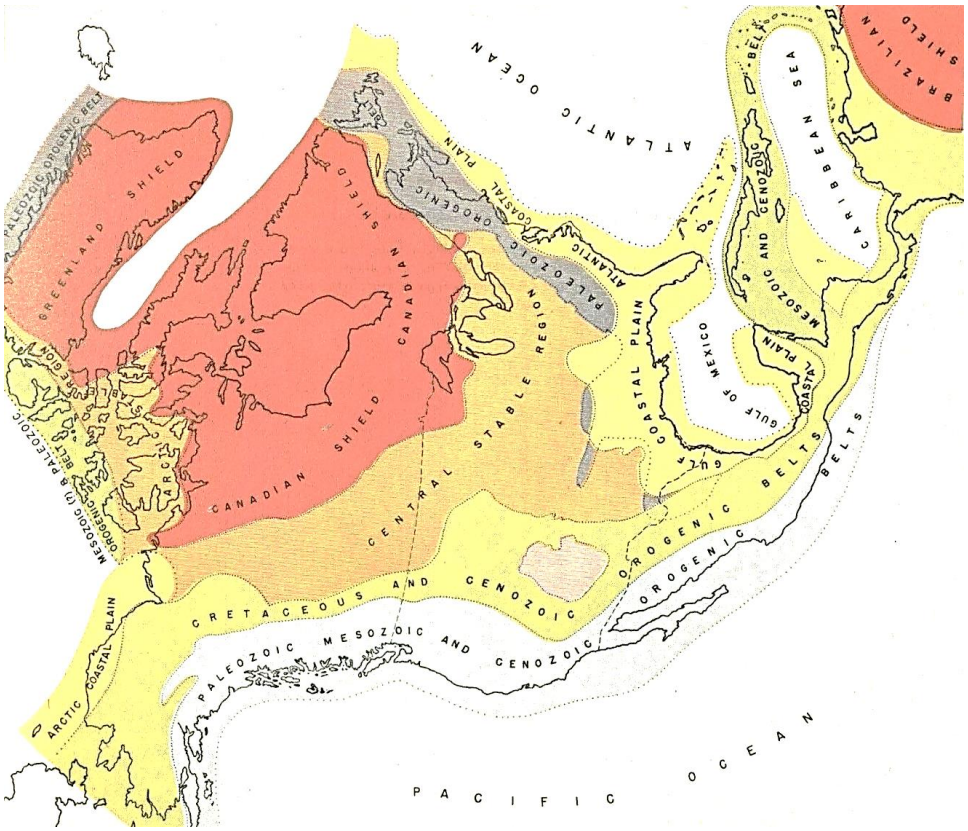

Figure 2.2. Major tectonic division of North America [18]

Figures 2.3.a to 2.3.k illustrate the Paleotectonic maps of North America. Paleotectonic maps represent the crustal unrest and deformation of the earth's crust during Paleozoic and Mesozoic. On each tectonic map are shown the orogenic belts that were active during the time specified, the areas of epeirogenic uplift and erosion, and the areas of subsidence and sedimentation. The orogenic belts are those of sever compression and

igneous activity. The region other than the orogenic belts that suffered erosion were for the most part being uplifted epeirogenically.

The central stable region consist of a foundation of pre-Cambrian crystalline rock with a veneer of sedimentary rock. For the most part, the central stable region has suffered vertical movements, and broad basins and arches have formed. Some of the basins have more than 10,000 feet of strata in them, and in the cores of some of the arches the pre-Cambrian crystalline rock is exposed. Some of the arches and sharper uplifts are not exposed in the surficial layers, and have been revealed only by drilling operations. The arches, basins, other structures of the central stable region, with few expectation, formed during the Paleozoic ear, and many of them yield evidence of a prolonged history of development.

Up to Pennsylvanian time, there was a certain bilateral symmetry to the stable region, with a great medial transcontinental arch, and basins and smaller arches on either side. During Mississippian, Pennsylvanian, and Permian time, great overlaps on some of the arches occurred. Other were either not completely buried or have since been partially exhumed by erosion [18].

Although Missouri is a part of stable Mid-continent localized areas have undergone several periods of uplifts and distortion since Precambrian time. At least six episode of deformation has occurred in Missouri, beginning with intense faulting and volcanic activity in the Precambrian followed by intermittent but persistent uplift of the Ozark region during the Paleozoic and Mesozoic. Sharp rejuvenation of the Mississippi embayment took place in post-Paleocene-pre-Pliocene time. Pleistocene stream terraces, entrenched meanders, and seismic activity all indicate that uplift is continuing [5].

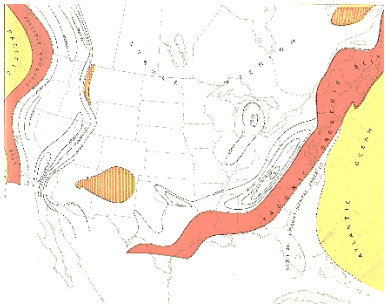

a. Tectonic map of the Cambrian, Ordovician, and Silurian

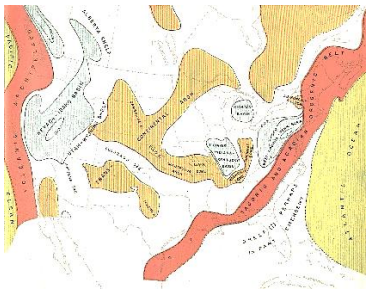

b. Tectonic map of the Devonian

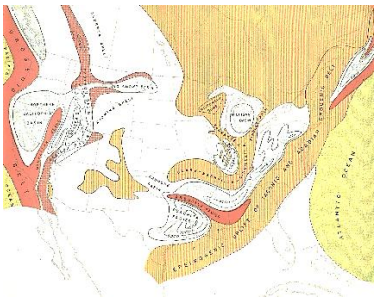

c. Tectonic map of the Mississippian

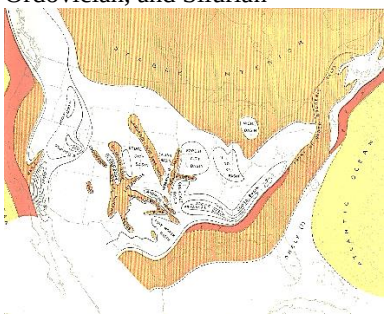

d. Tectonic map of the Early Pennsylvanian

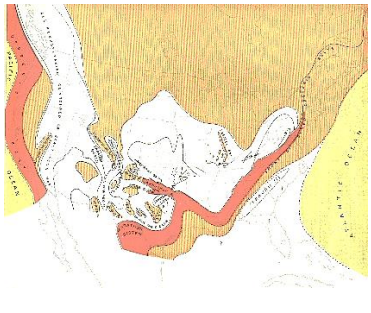

e. Tectonic map of the Late Pennsylvanian

f. Tectonic map of the Permian

g. Tectonic map of the Triassic

h. Tectonic map of the Early and Middle Jurassic

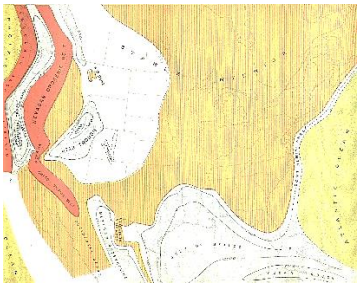

i. Tectonic map of the Late Jurassic

j. Tectonic map of the Early Cretaceous

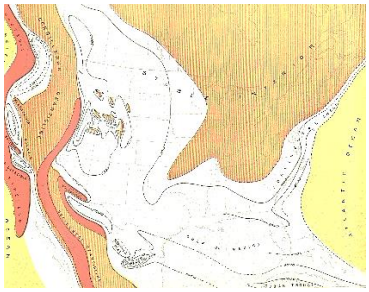

k. Tectonic map of the Late Cretaceous

Figure 2.3. Tectonic maps of the Paleozoic and Mesozoic; Red areas are the orogenic belts; blue are the basins; white area are stable region covered by sediment; orange areas are the epeirogenic uplifts that were subjected to erosion; green areas are the ocean basins [18]

The main periods of deformation are described as follows [5]:

Precambrian: The Precambrian structural framework is aligned northwest-southeast with a subordinate northeast-southwest pattern. There are jointing and some fracturing, both east-west and north-south. Probably the most intense structural deformation occurred in the Precambrian when there was considerable faulting along the lineaments. These was preceded by late Precambrian igneous activity which produced flows of rhyolite, tuffs, and ignimbrites in the Shannon County and St. Francois Mountain area. The large structures trend northwest-southeast. These may be block-faulted structures in the Precambrian with the Paleozoic sediments draped over them producing anticlinal and synclinal structures which persist to the surface.

Post Canadian -- Precambrian: From late Cambrian to middle Ordovician time sediments were essentially conformable, being deposited in a stable structural environment on a gently titled surface and thickening form northwest to southeast Missouri. At the close of Early Ordovician time, the area was subjected to stresses which caused uplift in the Ozark area as well as along an arch extending to the west and passing into Kansas at the west edge of Vernon County, Missouri. The entire area was subjected to erosion at this time and the beginning of Middle Ordovician (Champlainian) time saw the structural picture materially changed. Uplift was especially important in an east-west zone from northern Vernon County to the St. Francois Mountain area. Uplift in the Ozark area was accompanied by the development of a basin in northwestern Missouri which has been named the North Kansas basin. This continued and culminated in Pennsylvanian time as the Forest City basin.

The structurally positive Ozark region restricted sedimentation in Middle and Late Ordovician, Silurian, and early Devonian time to the east, north and northwest flanks of the uplift area. The close of Early Devonian time brought widespread uplift, faulting (especially in southeastern Missouri), erosion, and beveling of beds.

Post Lower Devonian -- Pre Mississippian: A lifting of the Ozark area to northwest in post-Early Devonian time was occurred, accounting for the thick section of the St. Francois Mountain area. The Ste. Genevieve fault system also shows post-Early Devonian movement. There are two age of faulting: one in post-Devonian time to account for the complex faulting in that area, and the other in post-Mississippian time. It is hard to determine the original extent of these Lower Devonian rocks. It should be noted that remnants are preserved in down dropped blocks well beyond the present outcrop area into the Ozark uplands. This would indicate a larger original area of sedimentation which has been stripped away by post-Early Devonian --- pre-Mississippian erosion. Strata ranging in age from Middle Devonian to Early Mississippian overlap the eroded beds, bringing Mississippian overlap the eroded beds, bringing Mississippian beds in contact with Canadian rocks in some areas.

Post Mississippian -- Pre Pennsylvanian: Mississippian deposits were probably laid down across the state under stable structural conditions. At the close of Mississippian time another uplift in the Ozark area resulted in widespread erosion and stripping of the Mississippian rocks from the uplift, and beveling of Mississippian rocks over the rest of the state.

Few structures can be definitely dated as post-Mississippian --- pre-Pennsylvanian. One of these is the Chesapeake fault which is crossed by an undeformed channel sandstone

of Pennsylvanian (Cherokee) age. However, in the northern part of Missouri the Mississippian rocks show a pattern of thinning by erosion over old high areas along anticlinal axes which are probably developed over Precambrian lineaments. It is, therefore, apparent that uplift, faulting, and beveling over either gently folded beds or draped beds over Precambrian structures took place in post-Mississippian time.

Post Pennsylvanian: The Pennsylvanian sea advanced over the state with oldest Pennsylvanian beds being deposited in the Forest City basin and in southwestern Missouri adjacent to the Cherokee basin in Kansas and Oklahoma. The Ozark area was probably only briefly covered at this time. Post-Pennsylvanian structural movements again accented uplift of the Ozark area and this was followed by erosion over the entire state.

Tertiary: The last sea invasion of Missouri was in latest Cretaceous and earliest Tertiary (Paleocene) time. The area must have been essentially a peneplain before Cretaceous and Tertiary sedimentation and remained stable until after Paleocene time. Sharp rejuvenation of the uplift of the Ozarks with differential depression of the Mississippi embayment took place in post-Paleocene -- Pliocene time.

Continued intermittent movement of the Ozark area seems to have gone on until the present. Pleistocene terraces, entrenched meanders, and recent earthquakes all point to continuing uplift of the Ozark.

2.2.1. Uplifts and Basins. Missouri seems like a broad dome with a center in the southeastern quarter of the state. Outward from this center, the layer of sedimentary rock dip away in all direction. To the southeast, dips are steeper, however; to the west and southwest the beds dip gently across the state [19].

The Ozark Plateau which comprise a part of the state of Missouri is an old positive area of repeated mild uplift since Precambrian. The main structural pattern of the state is aligned northwest-southeast with a subordinate northeast-southwest pattern. This is reflected in the pattern of the outcrops of older rocks along anticlinal axes on the geology map of Missouri (Figure 2.4). The most important examples includes, Framington anticline, Lincoln fold, Saline County arch, and the Proctor anticline in Camden and Morgan Counties [5].

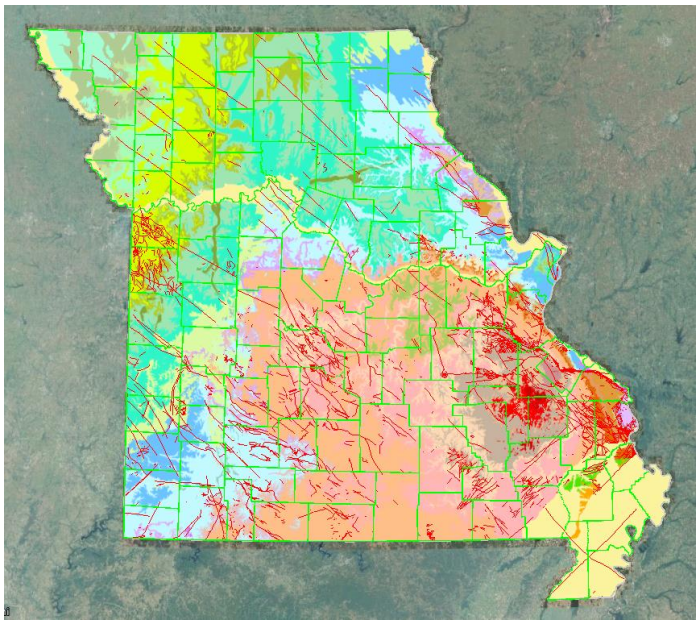

Figure 2.4. Geologic map of Missouri [20]

Forest city basin, is a basinal area in the northwestern quarter of the state which has trapped and preserved sediments of Paleozoic age. This, contains a well-developed and thick sequence of Siluro-Devonian and early Pennsylvanian rocks. It appears to have had its inception as part of a larger basin in post-Canadian time [5].

Missouri also contains, within its extreme southeastern section, a portion of the northern tip of the Mississippi embayment with sediments of Late Cretaceous and Early Tertiary age as well as a thick section of Pleistocene and Holocene alluvium. The embayment and the eastern and southern border of the Ozark uplift are active seismic zones where earthquake occur with moderate frequency [5].

Mary McCracken [5] has reported that there are nearly one hundred named anticline in Missouri, and she locates and describes most of them. This abundance has caused some geologist to refer to the "wrinkled skin" of Missouri [19].

2.2.2. Folds. In general, the rocks of Missouri which fail by folding are of Pennsylvanian age. A few of the large structures, however, show gentle folding in the more competent pre-Pennsylvanian sediments which are predominantly limestones or dolomites with minor amounts of sandstone and only a small percentage of shale. The Pennsylvanian rocks, containing a large percentage of clastic and only thin and minor amounts of limestone, tend to produce gentle folds [5].

The fact that much of Missouri is stable area, moving generally as a block, has kept folding to a minimum and no Alpine structures or tightly folded rocks occur. Steeply dipping beds are restricted to the immediate vicinity of faults; whereas, over most of the state, the regional dip of strata is only a few degree in magnitude. The dip of strata is quaquaversal with respect to the St Francois Mountains area, with steeper dips on the south and east flanks of the Precambrian outcrop area. The general dip is well illustrated by the structure contour map with the base of the Roubidoux formation as a datum [5].

Folding in many cases, may not be so much a result of lateral stress as it is a result of sedimentary rock draping over a block-faulted Precambrian basement of competent crystalline rocks [5].

2.2.3. Faults. Faulting is prevalent in the pre-Pennsylvanian strata of the state because the brittle carbonate and sandstone beds tend to fail primarily by fracture rather than by folding. Many of the faults are not of great throw, but average about 100 feet of displacement. In some instances, faults are accompanied by brecciation of the limestone or dolomite beds which appears to be out of proportion to the throw of the faults [5].

Faulting follows the old Precambrian patterns of predominant northwest-southeast trends with secondary northeast-southwest and east-west trending faults. Many of these faults have had repeated movement. From the southern third of Missouri northward, the trend is predominantly northwest-southeast, with some of the larger fault systems crossing the entire state [5].

Anticlinal structures and faulting in extreme southern Missouri are aligned northeast-southwest. These structural features extend trends present in Oklahoma and Arkansas. The prominence of these northeast-southwest trend is reduced sharply along a line just south of the 37th parallel where the east-west trending Ritchey fault crosses Newton and Lawrence Counties. This fault apparently passes into an anticline to the east and, where passes across the southern extension of the Chesapeake fault and northern extension of the Ten O'Clock Run, obliterates these faults. It is interesting to note that the throw of the Chesapeake fault is exactly opposite of that of the Ten O'Clock Run fault. East-west trends continue in Greene and Webster Counties with the valley Mills fault zone. There has been little except reconnaissance work done in Missouri east of this area, but

detailed work may show that the trend continues to the east. In fact, it may be responsible in part for the northern boundary of the Mississippi embayment [5].

Another east-west structural disturbance related to the faulting passes through Missouri at about the 38th parallel. This is the dominant east-west structural zone within the state. It has also been studied the most. It was recognized as the Bourbon arch in Kansas. It passes through the Decaturville dome area in Camden County, through some east-west faults mapped by Wallace Lee in the Rolla quadrangle, and joins the Plamer fault system at Crooked Creek disturbance in Crawford County. This continue eastward as a major fault system to join the Ste. Genevieve fault system and thence to the Rough Creek fault zone of southern Illinois and Kentucky [5].

This zone shows a change in the alignment of most of the northwest-southeast anticlinal structure which cross it. These are bent northwesterly north of the east-west axis, particularly in the lower Paleozoic, and possibly even more so in the Precambrian. This would indicate an east-west shearing action continuing over a long period of time with lateral displacement of beds and may account for the disturbed structures at Weableau, Decaturville, and Crooked Creek. These three unusual structural complex occur at or near the junction of northwest-southeast structural features with the east-west axis [5].

One other noteworthy feature is that the steep limbs of anticlinal and synclinal axes are reversed in passing over this axis .This chief anticlinal structures in northern Missouri have their steep limbs to the southwest. South of this axis most of the anticlines have their steep limbs to the northeast. This would appear to be a result of shearing stress [5].

Another less apparent east-west axis crosses the state on an approximate line between Kansas and Cap au Gres fault near Winfield, Missouri. This causes an increase in

the westward and northwest-southeast structures, again bending them to the northwest. This has caused possible offsetting of the Precambrian along the Cap au Gres fault of 30 miles. Structure maps (see Figure 2.5) show more offsetting of older Paleozoic than of the younger rocks in the area. This may have a bearing on the peculiar relationships of the Silurian, Devonian, and early Mississippian (kinderhookian) formations in the vicinity of the Lincoln fold. It would appear that some of the Illinois Silurian and Devonian had been displaced westward north of the Cap au Gres fault line [5].

These Structural trends could have been formed by forces from the southwest abutting against the stable Canadian shield area with a secondary stable area in Ozarks. Apparently volcanism in late Precambrian and early Cambrian was concentrated in this central east-west zone. Post-Middle Devonian diatremes are present in Ste. Genevieve County near the fault zone, and an active seismic belt lies along the Ste. Genevieve fault system [5].

The pre-Pennsylvanian rocks of the state are broken by many faults, but they are too small to show on the geologic map. The area east and north of the St. Francois Mountains is intensively faulted, primarily in a northwest-southeast trend. This is also true for of the southwestern part of the state in the Springfield plateau region.

2.2.4. Joints. Joints are another common feature of the consolidated rocks, which are more rigid and less flexible. They are fractures formed in response to pressure or stress. Unlike folds or faults, joints do not involve horizontal or vertical movement. Joints can be seen on the top surfaces of layers of rock, called the bedding planes. McCracken [5] points out that nearly all of the consolidated rock formation of Missouri are jointed. Graves [6] who has studied the Missouri joints in Precambrian distinguishes four joint systems, each

consisting of two sets at right angles to each other. The sets strike about N.-S, .E.-W., N. 40° E., N. 50° W., N. 65° W., N. 25° E., N. 65° E., and N. 25° W. In some localities one set is the most dominant while in others a different set is the most significant.

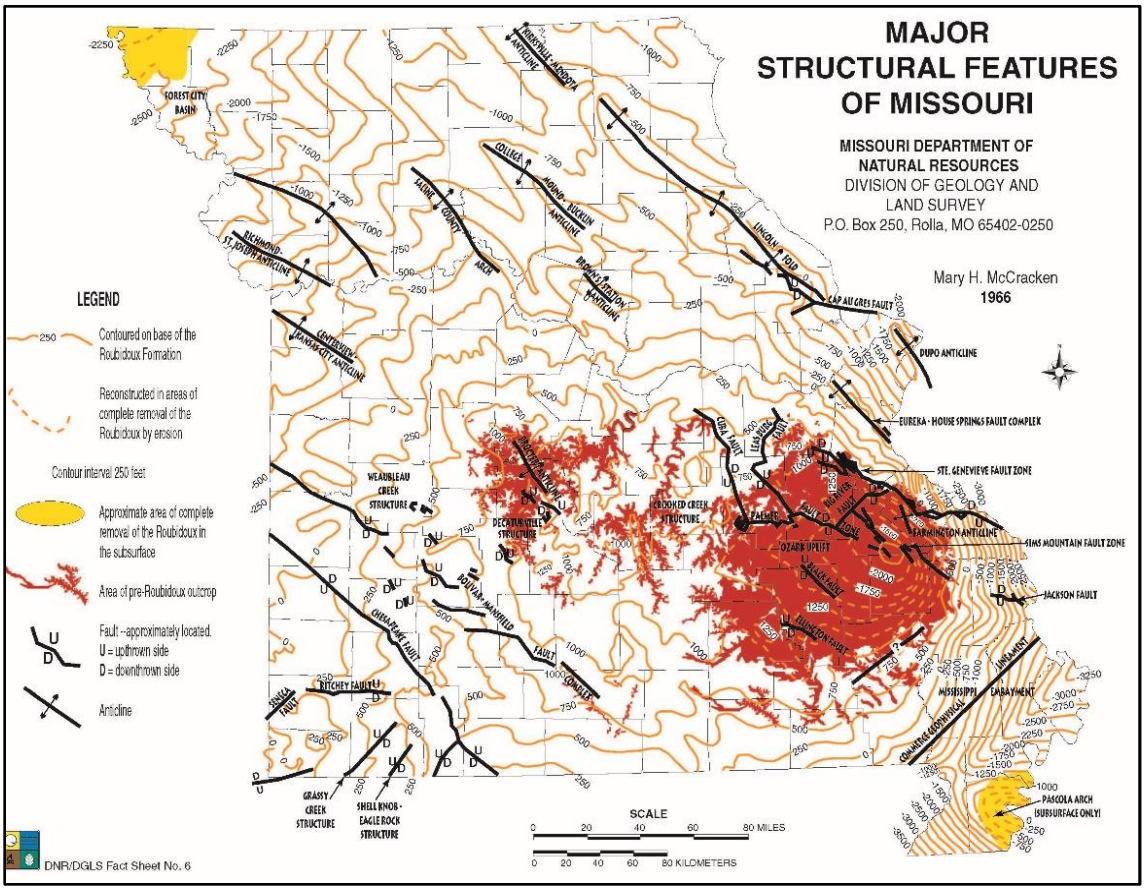

Figure 2.5. Structural features map of Missouri [21].

Jointing in the Cambrian and Ordovician rocks is best developed in the massive dolomite of the Eminence, Potosi, and Gasconade formations. Incidentally, these also are the best cave formers and the host of many of the large springs [5]. Ball and Smith [7] have investigated the joints in this rocks in Miller County. According to [7], joints in the

Cambrian and Ordovician rocks are mainly vertical. In general, there is a persistent set of joints striking approximately N. 20° W. and N. 75 E., and a minor set striking N. 45° E. and N. 60° W. the former set being the more persistent. In the Proctor limestone, the major set of joints strike N. 70° E. and N. 15° W. Two major sets in the Gunter sandstone strike N. 57° E. and N. 25° W. There are two sets of major joints in Gasconade limestone, one striking from N. 38° W. to N. 13° W., and the other from N. 83.5° E. to N. 60° E. These joints strike approximately parallel to the axes of the main folds. They are considered as tension joints due to the tensile forces set up by folding on the convex halves of anticlines and synclines in the zone of fractures. There are two distinct sets of joints in the St. Elizabeth formation which strike N. 20° W. and N. 60° E. Joints in the pitted dolomite beds of Jefferson City formation are poorly developed and a few reading was taken by the authors. The cotton rock of the Jefferson City formation have no well-defined system of joints, although there are more that strike northeast than in any direction [7].

[7] have extended their observation and found that the Proctor limestone possesses joints which do not occur in the overlying formations. The dike-like masses of sandstone fill what appear to be joints which strike N. 45° E. The upper Burlington limestone occupies what appear to be joint-like cavities or enlarged joint in the Jefferson City formation filled with deposits of Saline Creek cave-conglomerate and Coal Measure shale. [7] believes that major joint were formed after the deposition of the Jefferson City formation and prior to that of the Coal Measures rock and probably prior to the deposition of the Upper Burlington limestone. The joints in the Upper Burlington limestone strike differently in each basin. The presence of Upper Burlington chert in the Coal Measure rock may indicate the existence of joints in that formation prior to the Coal Measure subsidence, although the

limestone prior to the Coal Measure deposition may have been changed to chert only along the bedding planes.

During the initial stage of cavern development, solution is most effective along joints, faults, fractures and bedding planes. Barnholtz [11] related Ball and Smith [7]'s joint pattern to cavern development and orientation. He found strong correlation between cave passage direction and surface joint trends. Author concluded that cavern development is influenced a great deal by pre-existing joint systems.

Van Horn [8] studied joints of the Mississippian rocks in Moniteau County. He noted four set of vertical or nearly vertical joints in the Burlington limestone of Mississippian age. The strike of major joints is N. 24° W. and N. 64° W., and that of the minor joints is north-south (N. 19° E.) and east-west (N. 70° W.).

Hinds and Greene [9] has studied joints in the Pennsylvanian series in Missouri.

According to [9], all of the limestone and some of the sandstone beds of the region are more or less prominently intersected by vertical joint planes. Most of these may be separated in to two principal and two minor set, those striking about N. 62° E. are the most common, but those whose direction is about N. 3° W. are scarcely less abundant. Many of the thinner limestones have been cut into rhomboidally-shaped blocks by these joints. The two minor sets strike approximately N. 45° E. and N. 45° W., but vary within a wider range than those of the principal sets. The thicker limestones usually exhibit only the minor jointing.

Bretz [10] mentioned jointing as influencing the development of many caves including the Cameron and Mark Twain Caves in Marion County and the Bluff Dwellers Cave in McDonald County. Bretz [10] wrote: "Both stratification and jointing provide

initial water passages for gravity to move water downward and laterally. . . . Where jointing is dominant, the city street, network pattern characterizes the subsequent growth."

2.2.5. Origin of Structures. Fracturing rocks in laboratory under different states of stress and different conditions make it possible to formulate *fracture criteria*, which define both the stress state at fracture and the orientation of the fractures relative to the principal stresses. Fracture criteria are then applied to infer the conditions in the Earth when fractures formed in the rocks [22]. Fracture criterion is commonly used in structural geology to explain the formation of structure. A number of fracture criteria are briefly described in Appendix A.

When several structures of the same age are present in a region, it is possible to predict the forces producing the structures. *Folding* is caused by compressive stress and the fold axis is parallel to the intermediate stress. *Faulting* consist of movements parallel to the walls of a fracture and is therefore due to shearing. Thrusts faulting is due to compression and result in crustal shortening while normal faulting is due to tension and result in crustal elongation. Both normal and thrust faults are parallel to the shearing planes. *Joints* are formed by tension normal to the joint planes which are oriented parallel to axes of greatest and intermediate stress [6].

It is worth mentioning that in cases of complex deformation history, structures may be difficult to interpret, either because the relative timing of the formation of different structures is obscure or because structures form under one set of conditions and are reactivated under another. Thus, for example, it may be difficult to determine whether a set of fractures were formed before or during folding; fractures may develop as extension fractures and subsequently be reactivated with shearing displacement along them; and

faults initiated with thrust displacement may be reactivated as normal faults. Such complexities make the interpretation of structures challenging and sometimes controversial [22]. A more detail description of fracturing and its relation to other structures has been presented in Appendix B.

Missourian is a part of the central stable region of North America and were not active during Paleozoic and Mesozoic times. Tectonic joint can be find only in the Precambrian rocks of Missouri, therefore. Precambrian structures of Missouri and their relation to the state of stress has been discussed by Graves [6] which is presented in the following:

The structural framework in the Precambrian rocks of Missouri aligned northwest-southeast with a subordinate northeast-southwest pattern. The dominant structural trend is N. 50° W. Precambrian faults and joints strike in this direction, as do bedding planes in the pyroclastics and flow lines in the felsites. Second in importance are N. 40° E. structures which includes flaws and joints, and the majority of basic dikes also strike in this direction. Many of the dikes in the Precambrian rocks follow the northeast set of joints indicating that northeast was the direction normal to tensional stress during the Precambrian. This set may therefore be called the dip set and northwest set the strike set. Fault strike N. 50° W. in both the Precambrian and the Paleozoic rocks, indicating that this direction is parallel to the intermediate axis and that compressive stress acted in northeast-southwest direction. Fault planes in many cases dip to the southwest, therefore, the stress was by compression from the southwest, rather than the northeast.

The presence of dikes in the northeast set of joints may be evidence that this set was formed first and the dikes intruded before the second set was formed. It may, however,

merely indicate that this was the direction normal to tensional stress which favored the intrusion of the dikes. The theory advanced for this type of jointing would require the northeast set of joints to be formed first. The presence of later dikes in the northwest set in a few localities may show that this set was formed later, although these dikes may be in fault planes rather than dikes. Fault trending northwest through the St. Francois Mountains are normal faults due to relief of pressure which elevated the block. This faulting was later than intrusion of the basic dikes and probably of the same age as the northwest set of joints. These relations conform to the theory advanced for the origin of joints.

The block structure of the St. Francois Mountains and Shannon County areas can be explained similarly to the jointing. Thrust faults were formed by pressure from the southwest and were accompanied by vertical, transverses flaws which probably followed previously formed joint planes. Upon relief of the pressure, normal faults were formed parallel to, and southwest of, the thrust faults. This left the block outlined on all four sides. During the later periods there was compression alternately from the southwest and southeast which accentuated the block structure.

There is little distinction between the N. 70° W. and N. 20° E. sets of joints, but the former set is much more abundant and there are dikes parallel to it, thus suggesting that it is the dip set. It seems more probable, however, that the stress acted from the southwest, parallel to the N. 20° E. set. The same set occur in the Wichita Mountains where structures are due to pressure from the southwest. Buckley and Buehler [11] report a southwest dip for a number of the N. 70° W. joints which is further indication that the stress acted form the southwest.

The N.-S. set of joints is more important than the E.-W. and there are dikes in the N.-S. set in the Precambrian rocks. The Palmer fault in Washington and Crawford counties and the Devonian fault in Ste. Genevieve County strike west through part of their length and may both lie above a Precambrian fault.

The N. 70° E. and N. 20° W. system is the least well defined. The N. $60-70^{\circ}$ E. joints at Graniteville may belong to this system or may be of local origin. Joints occurring N. $50-60^{\circ}$ E. may be either of local origin or belong to this system or to the N. 40° E. set. Joints striking N. 80° E. may belong to N. 70° E. set or the E.-W. set. The Springfield anticline strikes about N. 70° E. and it is possible that the joints originated with the anticline during the Tertiary, as there is no definite proof they are Precambrian.

2.2.5.1 Source of stress. The possible source of the stress forming the joints and faults in the Precambrian rock include igneous intrusion, vertical uplift, and horizontal compression. While the minor sets of joints may be the result of intrusion, the major structural systems are too widespread to have been formed by anything but major structural movement. Vertical uplift would produce structures that were unoriented or were radial or tangential to the uplift but structures throughout the state have the same trends indicating horizontal compression over a wide area.

During Precambrian time there were two structural systems developed which were of regional origin. The N. 50° W. and N. 40° E. system is dominant in Missouri and important in the Llano region of Texas. The N. 70° W. and N. 20° E. system is dominant in the Precambrian of the Wichita Mountains of Oklahoma, and of secondary importance in Missouri. These system were developed as a result of compression form the southwest from two somewhat different direction at different times during the Precambrian. The stress

must have originated at a considerable distance southwest of any of the Precambrian localities and probably come from the Pacific Ocean basin.

Joint not belonging to either of the above systems may be of local origin or in the case of the N.-S. and E.-W. sets may be due to a minor, but regional, movement. Many of the joints in the Precambrian rocks may be due to movement at a later time but it seem more probable to consider them all of Precambrian age. Until the age relations of the various Precambrian rocks have been definitely worked out, it is impossible to determine the relative ages of the different ages of the different sets of joints [6].

2.3. KARST FEATURES

Missouri has hundreds of significant caves, thousands of springs, and many other spectacular karst features [23]. The Missouri Speleological Survey (MSS) has made significant contribution to the exploration, mapping, and study of Missouri cave. MSS has modified the karst distribution map of Missouri after Missouri Department of Natural Resource [24], which can be seen in Figure 2.6.

Missouri is divided in to two disparate halves by Missouri River. The northern half is underlain mainly by Pennsylvanian strata, mostly shale and siltstone covered by Quaternary till. Karst features are rare, but some important caves are located close to the Mississippi River. South of the Missouri River called the Ozark Plateau (or “Ozark Maountains”). The Ozark Plateau contains great area of karst. More than 90% of Missouri’s caves are located in this region (Figure 2.6). However, its sinkholes and stream valleys are chocked by up to 30-50 m of residual material [23].

Figure 2.6. Physiographic map of Missouri showing karst distribution [23].

Caves are nearly developed all of the soluble geologic units [23]. Considering the abundance of carbonate rocks in the Ozark Plateaus, particularly in the Springfield and Salem Plateaus, it is surprising that this area is not one of the major karst region in the United States [17].

Certainly most of the conditions essential to maximum development of karst topography are present; a humid climate, soluble rock beneath the surface, deeply entrenched valleys below the limestone or dolomite uplands, and jointed and bedded rocks. It appears that the major reason that some karst features, particularly sinkholes and swallow holes, are so poorly displayed in the Ozark is the abundance of chert in the limestones and dolomites of the Springfield and Salem Plateaus [17].

Chert mantles much of the topography and literally chokes many of the lesser stream valleys. This porous mantle results in reduced concentrated surface runoff; there is mass diversion of surface waters to the subsurface rather than through streams that terminate in swallow holes [17].

Probably it is not correct to say that sinkholes and swallow holes are largely lacking in the Missouri karst; it is likely more correct to say that to a large degree they are obscured by the chert mantle. If this cover were removed probably the limestone surface would show innumerable basins similar to those found on a typical sinkhole plain [17].

2.3.1. Springs. There are springs in many parts of Missouri, but the majority of springs in the state are in the Ozark region. The soluble Cambrian and Ordovician dolomites of this region expedite the movement of water. The Springfield Plateau is the second most abundant spring area. The underlying rock in Springfield Plateau are Mississippian limestone. Figure 2.7 shows the distribution of the so-called “large springs” in Missouri. In this region springs are not as large as the springs of Ozark and their flow is less constant [19]. Although a few spring are in the Springfield Plateau, none of the first magnitude springs is found here. Springs in the Springfield Plateau are associated with the Burlington-Keokuk and Warsaw limestones or cherty limestone formations of Mississippian age [17].

2.3.1. Caverns. Missouri is widely known as “The Cave State” [19]. Caves are developed throughout nearly all the state [23]. Figure 2.8 shows the density of caves in Missouri. Missouri is widely known as “The Cave State” [19]. The more than 400 known caverns in Missouri are distributed through some 55 counties.

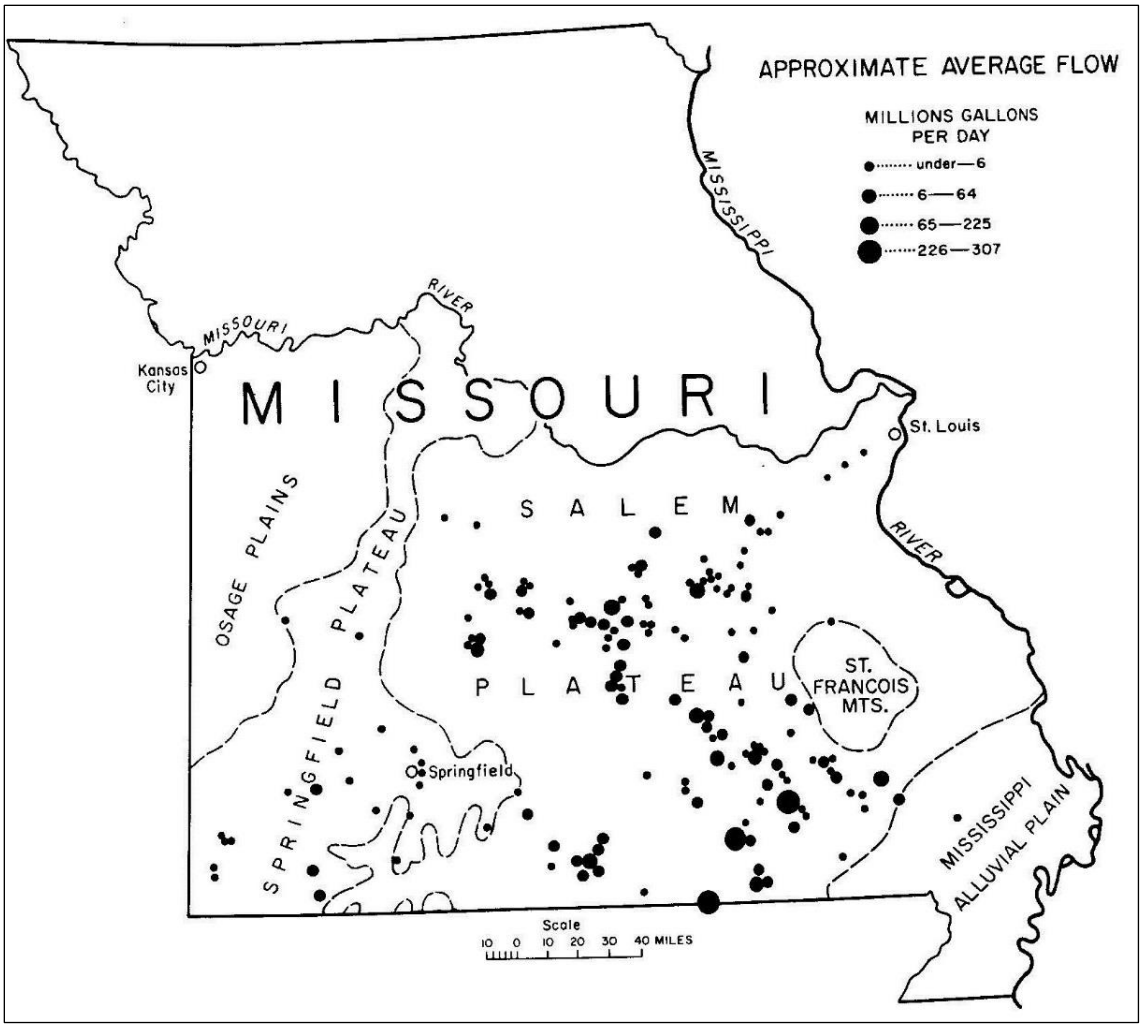

Figure 2.7. Distribution of large springs in Missouri [17].

The major cave area lies in the southern part of the state and is roughly triangular in shape, with its northern apex being near Boonville, its western corner near the southwest edge of the state, and its southeast corner at the contact of coastal plain sediments and Paleozoic rocks of Ozark dome. Within this triangular area caves are especially numerous south and west of Rolla and southwest of Springfield [17].

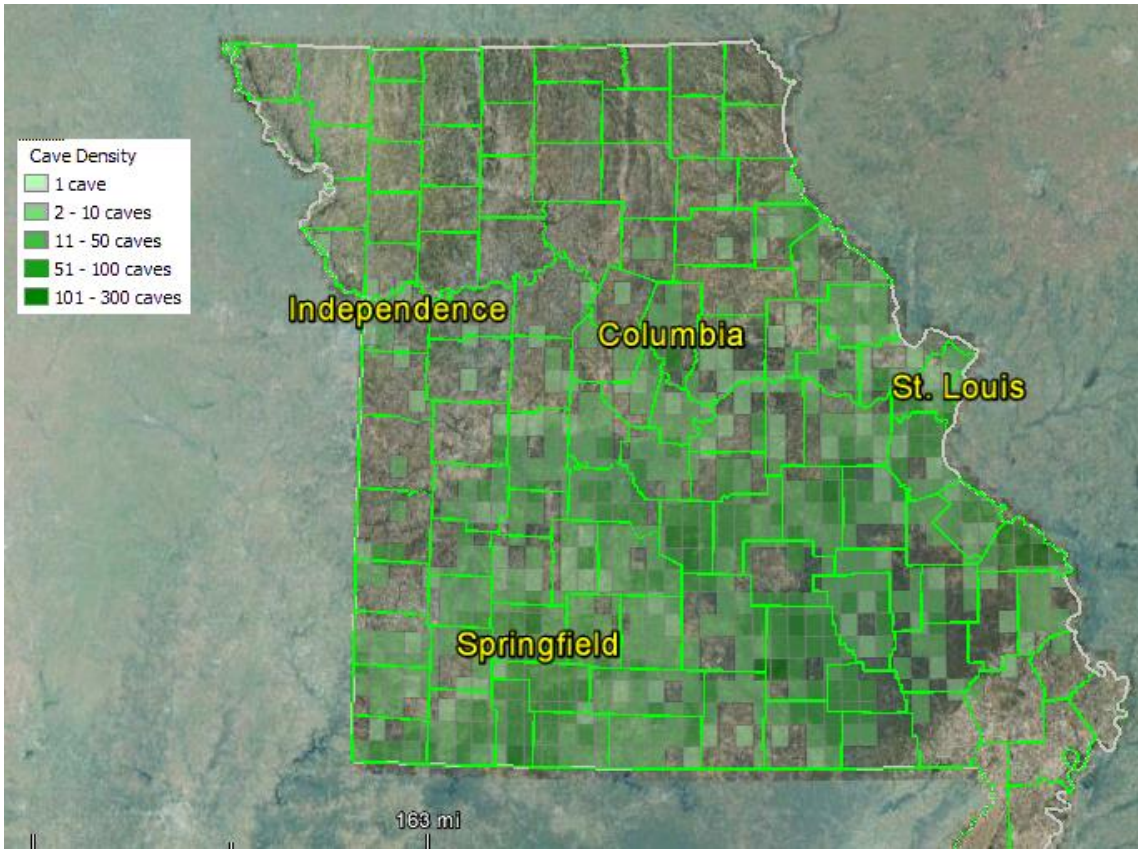

Figure 2.8. Density of caves in Missouri [20].

Almost all of the State is underlain by limestone and dolomite formations in which ground water dissolves out caves. Therefore, the area north of the Missouri River may well contain as large a proportion of caves as do the Ozarks, but the cover of glacial drift and the lack of deep stream valleys north of the river conspire to keep us ignorant of their existence.

A point stressed in the history of almost every cave is that it is older than the latest broad uparching of the Ozark dome. The regional uplift was responsible for the subsequent stream erosion which has toady exposed the cavities that were made before the latest doming occurred.

Most caves contain a partial fill of gravel, sand, mud, or clay; insoluble materials that have collected in them to bury the bedrock floor. Even if a cave has become completely filled with such detrital material, it is still a cave; a consequence of the solvent action of circulation ground water at some earlier time.

Very few Missouri caves are growing today. Open caves almost all are suffering destruction, largely because they have become air-filled. Collapse of roofs has blocked many a cave chamber, sinkhole debris has filled large portion of them, dripstone and flowstone deposits have decreased camber capacities, cave streams have deposited gravel in them, and outside creeks and rivers, by widening their valleys, have shortened cave lengths. Every one of these changes is still going on. The condition of the present time do not favor cave-making in the rock of Missouri's hills, although the collapse of cavern roof may give the impression that caves are still being formed [10].

3. METHODS AND MATERIALS

3.1. DISSOLUTION-ENLARGED FRACTURES

Karst is terrain with a special landscape and distinctive hydrological system developed by dissolution of rocks, particularly carbonate rocks such as limestone and dolomite, made by enlarging fractures into underground conduits that can enlarge into caverns, and in some cases collapse to form sinkholes [1, 2, and 3]. Downward percolating water slowly dissolves the host rock creating a network of enlarged fractures, fissures and bedding planes. Dissolution will continue while voids are too small to sustain a turbulent water flow [25]. Once critical dimension reached, the flow turns into turbulent with a higher velocity boosting mechanical erosion. Man-size conduits can evolve in this stage and enlarging can continue as long as water is able to fill the voids completely [2]. Sedimentation, alluviation and collapse process are characteristics of the final stages of karst development [26]. Figure 3.1 depicts typical karst features.

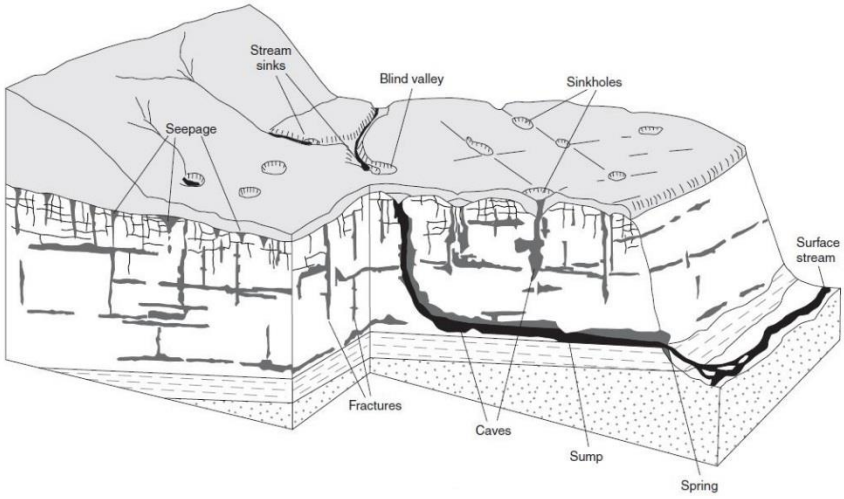

Figure 3.1. Block Diagram of a Karst Landscape in Southern Minnesota with Some Typical Surface and Subsurface Karst Features [27]

Bedding planes, joints, and faults are the principal structural guides for underground flow and dissolution in almost all karstified rocks [1 and 2]. Palmer [4] has investigated the pattern of several thousand cave passage and conclude that 57% of cave passage follow bedding planes, 42% are fracture-oriented and only 1% of the total passages are related to porosity of the rock.

Most karst areas are prevailed by patterns of similar straight joints with identical orientations [2]. ISRM [28] has defined joint as "A discontinuity plane of natural origin along which there has been no visible displacement". Joints generally aligned in a preferred direction as Joint sets forming the jointing pattern. One to three prominent joints sets and one or more minor sets often occur; however, several individual or random joints may be present [29]. Where two or more different set intersect at constant angle they constitute a joint system. A rectangular system of jointing is the most common system in platformal sedimentary rocks such as limestone and dolostones. A system with 60/120 degree is the second common jointing pattern. Combination of these two system which form a more complex patterns is also frequent [2].

Despite the important role of fractures in karst development, the geometry of dissolution-enlarged fractures remain poorly unknown, largely due to inaccessibility of these underground geological features. These features are characterized by strong contrast with the surrounding formations in terms of physical properties, such as electrical resistivity. Electrical Resistivity Tomography (ERT) has been used to image the dissolution-enlarged fractures in this study. Detailed methods used has been presented in the following sections.

3.2. ELECTRICAL RESISTIVITY TOMOGRAPHY (ERT)

In recent years, the electrical imaging techniques have been largely applied to geotechnical and environmental investigations. These techniques have proven to be the best geophysical methods for site investigation in karst terrain, particularly when the overburden soil is clay-dominated [12, 13, and 14]. The high contrast in resistivity values between carbonate rock and clayey soil makes the resistivity method useful for determining the soil-bedrock contact. Archie [30] proposed an empirical formula for the effective resistivity of rocks which take into account the porosity (Ø) the fraction(S) of the pores containing water, and the resistivity of the water (ρ_w):

$$\rho = a\emptyset^{-m}S^{-n}\rho_w \tag{1}$$

where ρ and ρ_w are the effective rock resistivity, and the resistivity of pore water, respectively; Ø is the porosity, S is the volume fraction of pores with water; a, m and n are constants where $0.5 \leq a \leq 2.5, 1.3 \leq m \leq 2.5, and\ n \approx 2$.

In sedimentary rocks, the resistivity of the interstitial fluid is more important than that of the host rock, according to Archie's formula [31]. The value of resistivity increases relatively to the resistivity of clayey soil because it has much smaller primary porosity and fewer interconnected pore space. Moreover, voids have significantly higher resistivity than host rock if they are filled with air and they have much smaller resistivity than surrounded rock if they are filled with clay and/or water [32]. This high resistivity contrast favors the use of resistivity method to delineate the geometry of dissolution-enlarged fractures.

For the traditional resistivity method, four metal stakes or electrodes are coupled into the ground. Two "current electrodes" are used to introduce direct electricity into the

subsurface and two other “potential electrodes” are used to measure the resulting voltage difference in earth. In electrical sounding method, the spacing between the electrodes is changed to gain data at different depths while the center point of the electrode array remains fixed. The measured apparent resistivity are normally plotted as a one-dimensional vertical profile of the electrical resistivity. Another classical method is electrical profiling method. In this method, the spacing between the electrodes remains fixed while the array is moved along a straight line to gain data at different location at the same depth. However, the application of electrical sounding remains limited to simplified earth model with horizontal layers and interpretation of data from electrical profiling is mainly qualitative. Thus, conventional resistivity method cannot proved reliable model of subsurface in area with complex geology, such as karst terrain.

Electrical resistivity method have developed from the conventional techniques that provide two-dimensional and even three-dimensional images of the resistivity pattern in the subsurface. This development started with the appearance of new acquisition system (multi-electrode array configuration) [33 and 34] and followed by post-processing and new tomographic inversion techniques [35]. The Electrical Resistivity Tomography (ERT) have been frequently applied to image the subsurface in area of complex geology [36, 37, 14, 38 and 39].

Figure 3.2 illustrates the data acquisition sequences for the dipole-dipole array in an ERT investigation. Direct current is introduced into the ground via two electrodes “a” feet apart. The potential difference is measured between two other electrodes “a” feet apart in line with current electrodes. The spacing between adjacent electrodes is constant for each traverse “n”. A micro-controller unit select four electrodes to be used for each

measurement and then automatically switches to a different electrode configuration, thus; data acquisition advance very fast today.

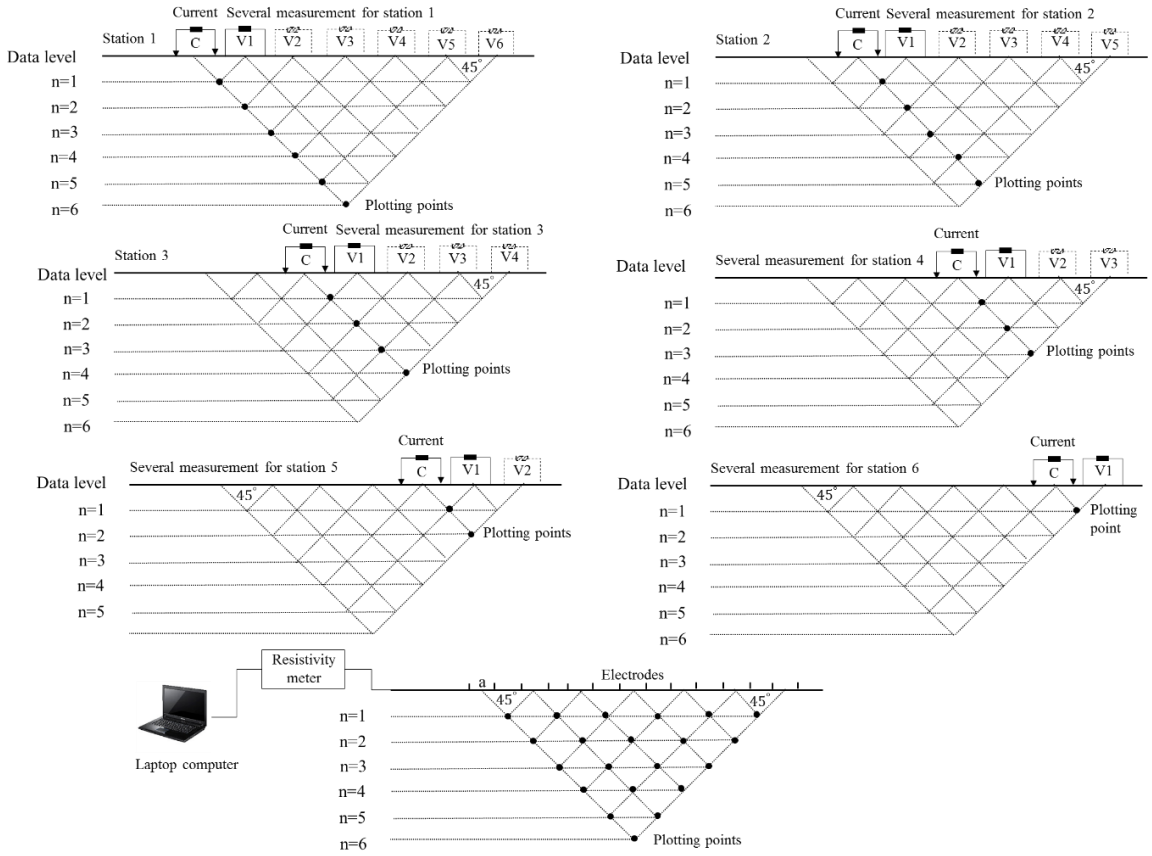

Figure 3.2. ERT data measurement sequence using the dipole-dipole array

The resolution of 2D ERT data is highly affected by the electrode arrangement or electrode geometry. Commonly used arrays are the dipole-dipole, Wenner, and Wenner-Schlumberger arrays. The dipole-dipole array have been selected by many authors to be used in karst terrain exploration [36, 40, 38, 41, 14 and 39] due to its high resolution and

sensitivity to vertical resistivity boundaries as are found at karst features. The dipole-dipole configuration was selected as the most appropriate array four our studies as well.

Two-dimensional measured resistivity data are mainly presented as apparent pseudo-section. This section gives only an approximate picture of the subsurface resistivity that can be sometimes unclear. An inversion procedure is utilized to reconstruct a true model of subsurface that satisfy the observed data in the form of a pseudo-section. Many inversion methods have been proposed to create a 2D tomography [e.g. 42, 43, 44, 45, 46 and 47]. Nearly all proposed algorithm are iterative and follow similar strategies. First an initial resistivity model is assumed and the boundary data is calculated for this starting model. Next the calculated boundary data are compared with the actual measurement. Differences between the measured resistivity and computed resistivity are used to adjust the model until boundary data best fit the observed data. In the present study, we used the algorithm proposed by Lake and barker [35] for 2D inversion of apparent resistivity data which is the most frequently used in geoscience. This method is based on the least-square method with an enforced smoothness constrain and employs a quasi-Newton optimization technique to adjust the model. The difference between measured resistivity values and inverted data or “goodness of fit” is represented by a Root-Mean-Squared (RMS) error.

3.3. FIELD INVESTIGATION

A preliminary geophysical investigation was undertake in a karst terrain with the objective of identifying prominent karst features. Figure 3.3 shows the location of study area in Greene County, Missouri. Electrical Resistivity Tomography (ERT) and Multi-channel Analysis of Surface Waves (MASW) were selected to image the karst features in

the study area. A total of 352,015 linear feet of ERT data were acquired along 149 separate traverse at JTEC. MASW data were acquired at 181 separate grid location. Exploratory borings were also acquired to validate the geophysical data.

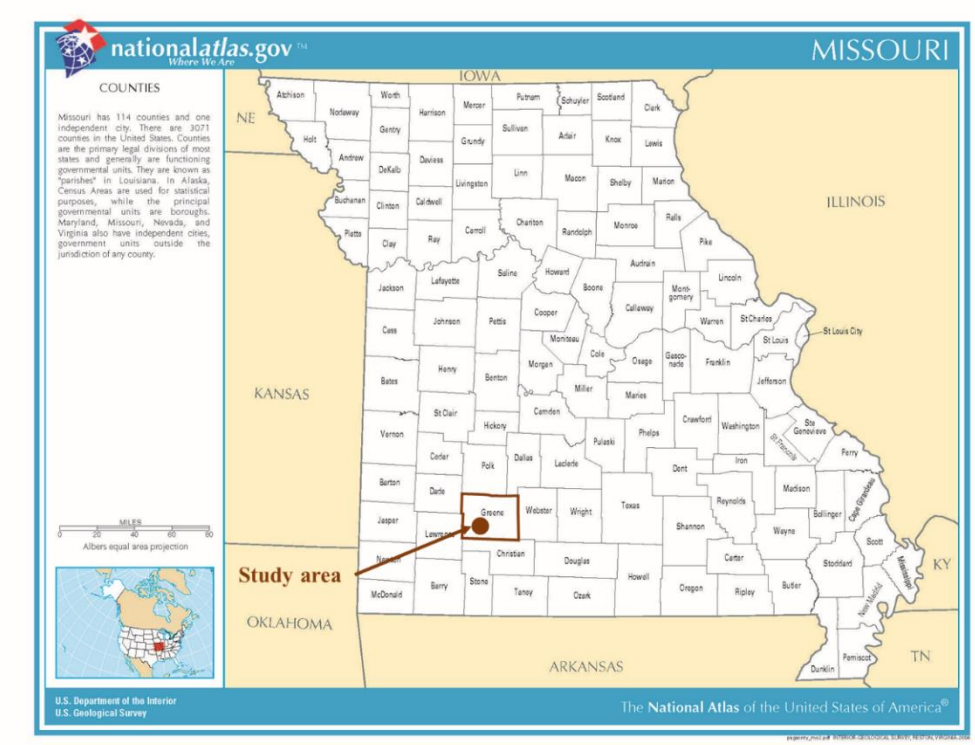

Figure 3.3. Location map of the investigation site in Greene County, Missouri [49]

The investigation site was divided to four areas for the data acquisition and presentation purposes (Figure 3.4). ERT data were acquired mostly along parallel west-east oriented traverses nearly spaced at 100 ft intervals using dipole-dipole array. Several more widely north-south oriented traversed were also selected for data acquisition. Because joint orientation in both north-south and west-east direction are expected in the investigation area.

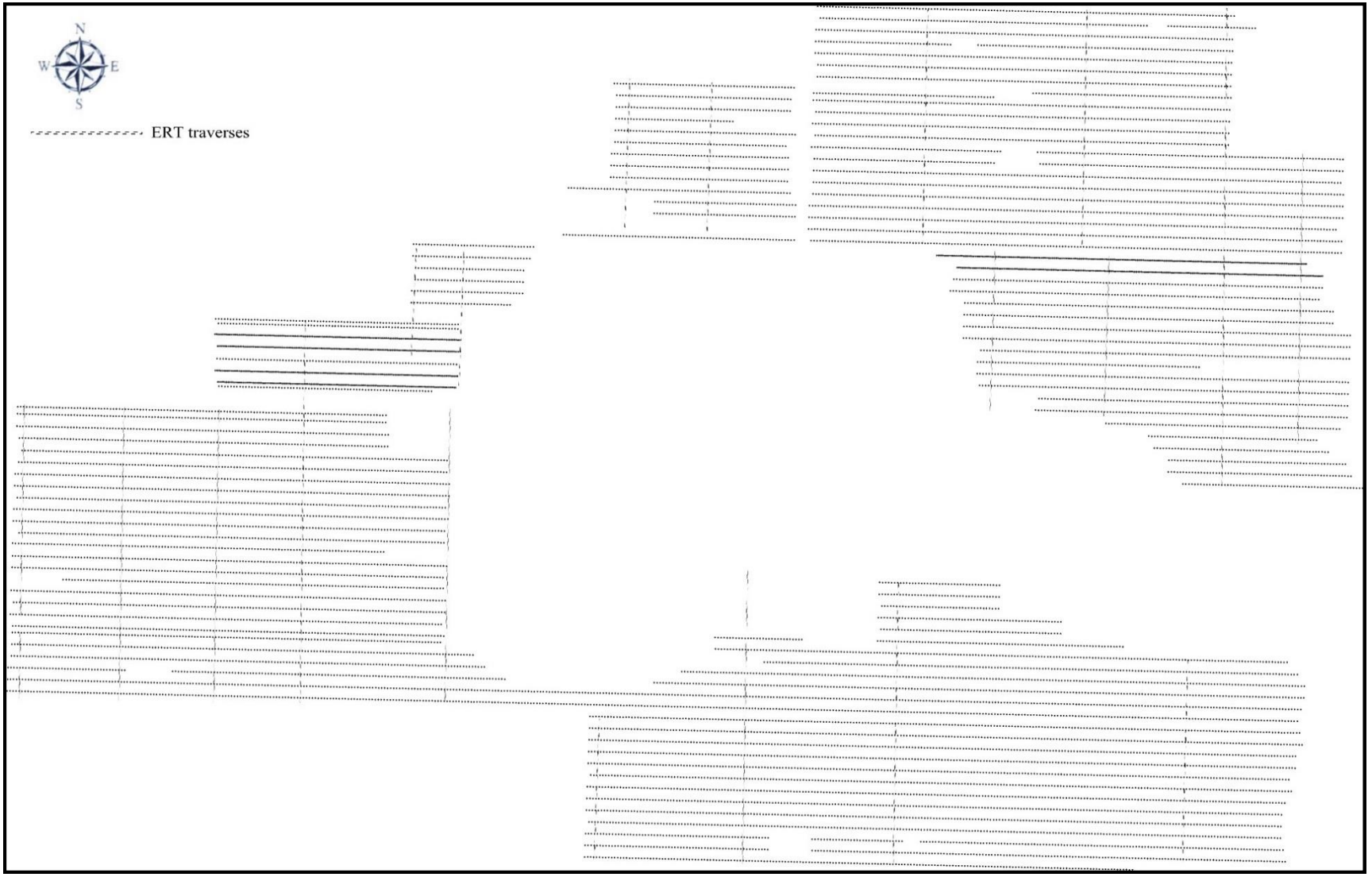

Figure 3.4. Boundary of the investigation site

3.3.1. Regional Geology. The investigation site is located in Springfield Plateau. The Springfield Plateau is a part of the Ozark Plateau with a bedrock surface of thick Mississippian-age limestones and chert limestones above Ordovician and Cambrian-aged strata [17]. Bedrock gently dips toward the west with minor folding and faulting. The predominantly limestone strata of area has been extensively weathered, and irregular bedrock is hidden below a mantling of chert clay residuum with thickness varying from a few to over 40 feet [48].

The Springfield Plateau is underlain by Precambrian crystalline rock at depth. The Precambrian basement is overlain by the Cambrian age rocks; Lamotte Sandstone, Bonneterre Formation, Davis Formation, Derby-Doerun Dolomite, Potosi Dolomite, and Eminence Dolomite. The Ordovician-aged Gasconade Fromation overlies the Eminence Formation. Gasconade Formation is underlain by Roubidoux formation, Jefferson City and Cotter Formations.

In the study area the Cotter Dolomite is unconformably overlain by about 30 feet of the Mississippian-aged Compton Limestone. The Devonian and Silurian Periods are entirely missed from the geologic record. The Compton Limestone is overlain by between 5 and 30 feet of shale and siltstone of the Northview formation. The Northview Formation is overlain by around 100 feet of the Pierson Limestone, which is overlain by the Elsey-Reeds Spring Formation, consisting of up to 200 feet of cherty limestone. Burlington-Keokuk Limestone capes the Elsey-Reeds Formation and forms the bedrock surface across most of the Springfield plateau. Its thickness may be vary from 150 to 250 feet due to high degree of weathering. Most of the karst features in southwest Missouri are developed within this Formations [48 and 50]. The bedrock stratigraphy in the investigation site has been summarized in Figure 3.5.

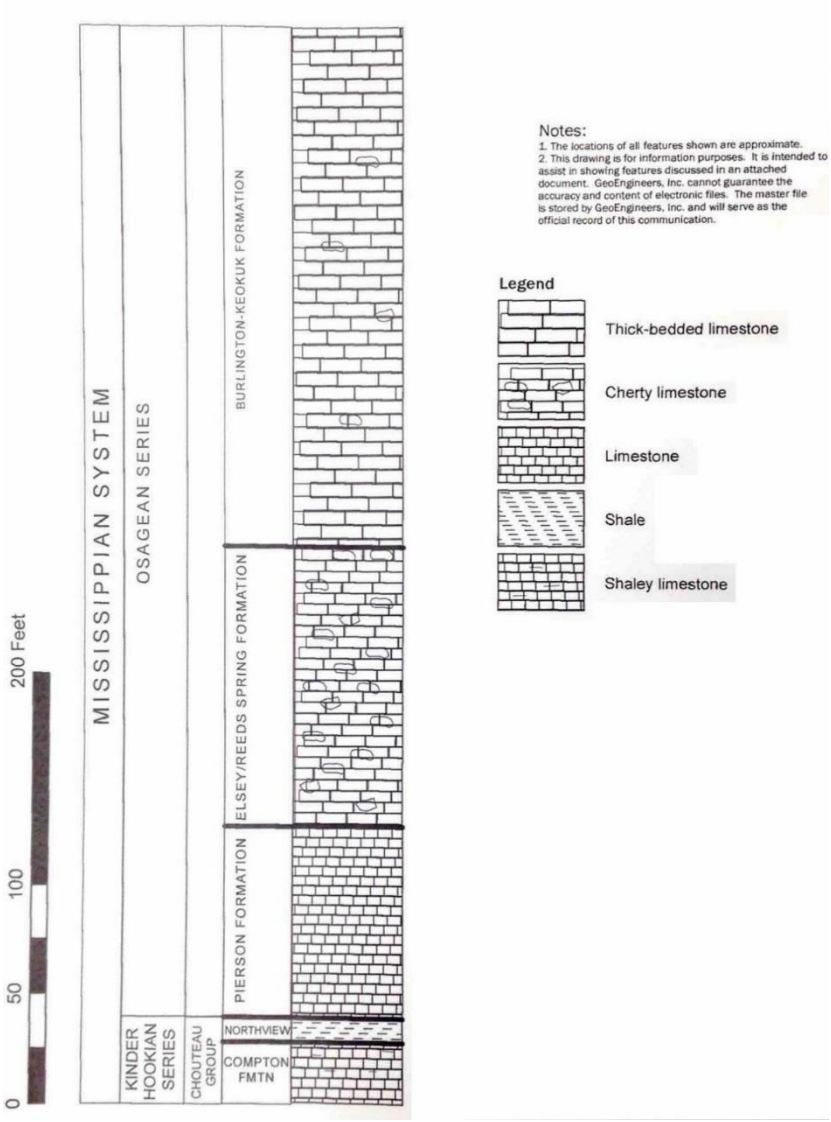

Figure 3.5. Bedrock stratigraphy in the investigation site [48]

Geologic studies and maps of the Springfield 1 degree by 2 degree quadrangle [51 and 52] reveals that the investigation site is located in an area underlain by Mississippian-aged Burlington-Keokuk Limestone. The Burlington-Keokuk consists mainly of calcium carbonate with highly variable thickness due to weathering. Both surface and subsurface drainage in Burlington-Keokuk limestone are influenced by joints. Joint have caused the bedrock surface to be weathered into cutters and pinnacles. Cherty clay residuum consists

of clay loam to silty clay loam containing subangular to angular fragments of chert up to one foot in diameter as individual clasts and relict chert layers [15, 53 and 48]. Surface geology map of the investigation site is illustrated in Figure 3.6.

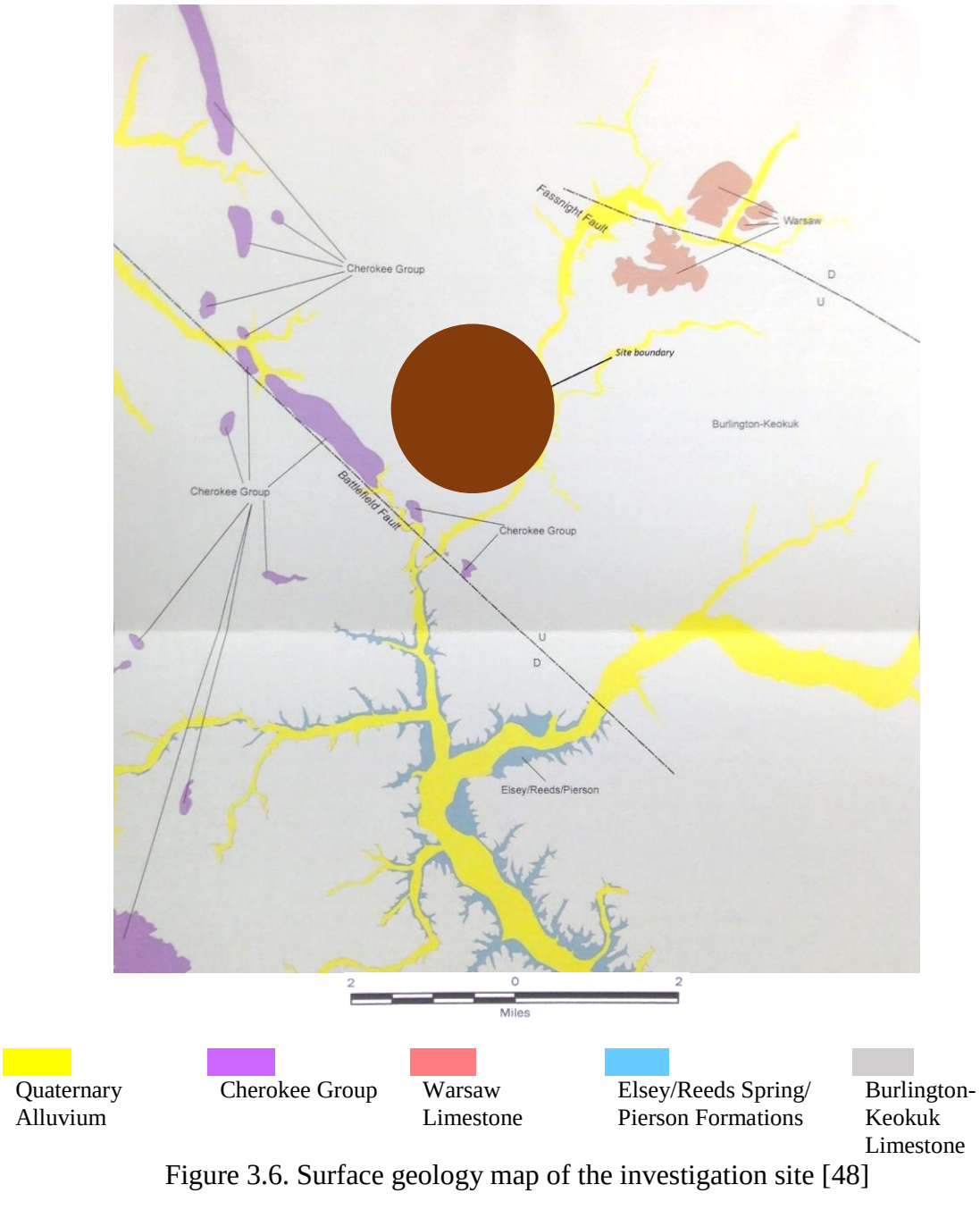

Figure 3.6. Surface geology map of the investigation site [48]

3.3.2. Electrical Resistivity Tomography (ERT). Figures 3.7 to 3.10 show the layout of ERT traverses in the investigation site. The electrode spacing along each traverse was 5 feet. Five feet inter-electrode spacing was used to reach the goal of imaging subsurface to a depth approximately 100 ft. The length of the traverses varied from 625 ft to 8680 ft. In total, 352,015 lineal feet of ERT data were acquired. A Super Sting R8/IP system (manufactured by the AGI, Inc., USA) with up to 68 electrodes was used for data collection. To ensure good galvanic contact between the electrodes and the ground contact resistance test was routinely performed prior to data acquisition and the surface in proximity to each electrodes were periodically wetted on drier days. Technical parameters of data acquisition are described in table 3.1.

Table 3.1. Summary of technical parameters of ERT data acquisition

Parameter	Value
Total number of traverses	149
Number of west-east oriented traverses	127
Number of north-south oriented traverses	22
Total length of traverses	352015
Longest traverse	8680
Shortest traverse	625
Average data quality*	98.43%
Maximum data quality	100%
Minimum data quality	85%
Penetration depth	~104 ft
Array type	Dipole-dipole
Period of measurement	September 2014 to September 2014

*Data quality is a measure of the percentage of useful data point to the total data points acquired along a traverse.

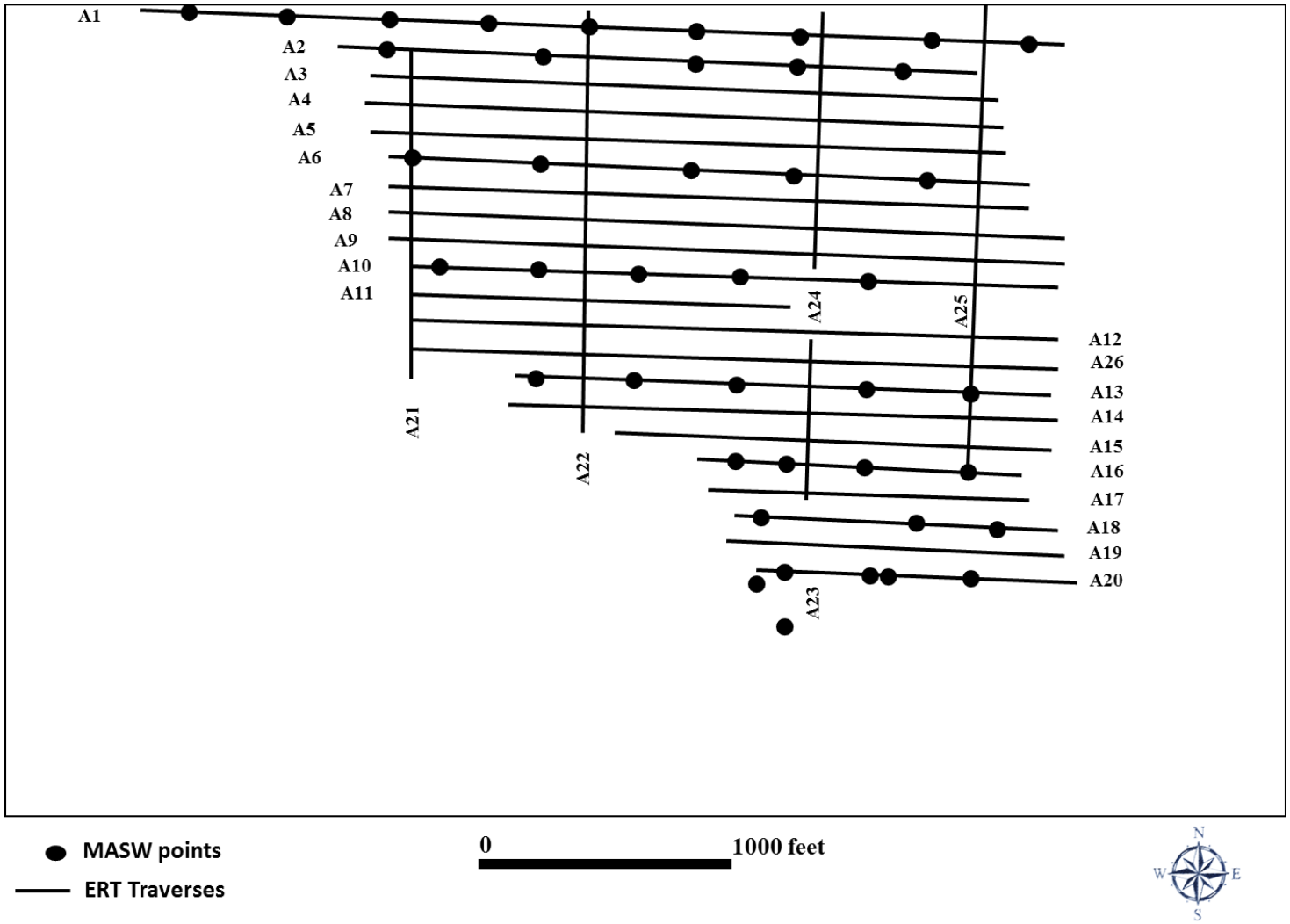

Figure 3.7. Layout of ERT traverses at the investigation site (Area A)

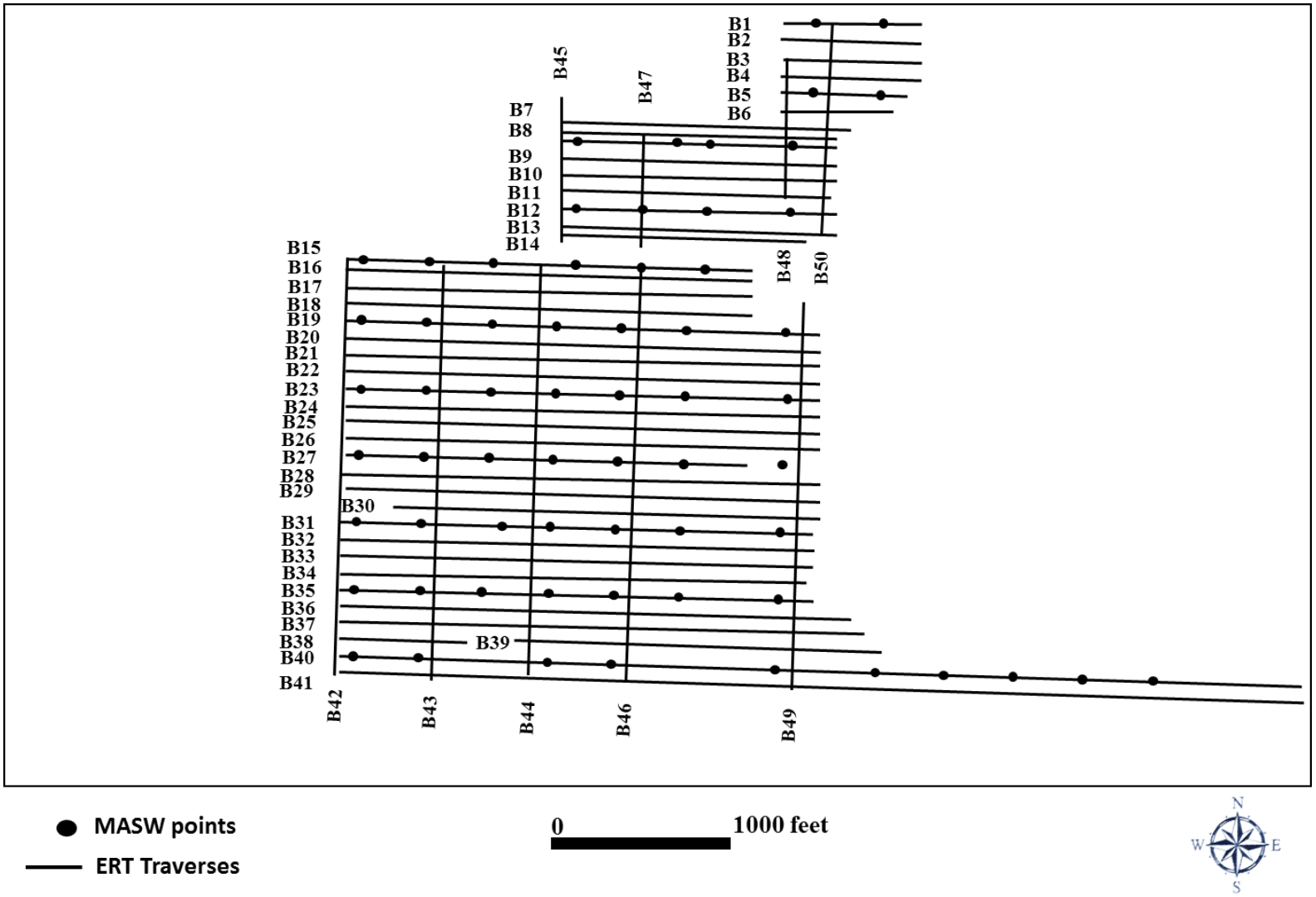

Figure 3.8. Layout of ERT traverses at the investigation site (Area B)

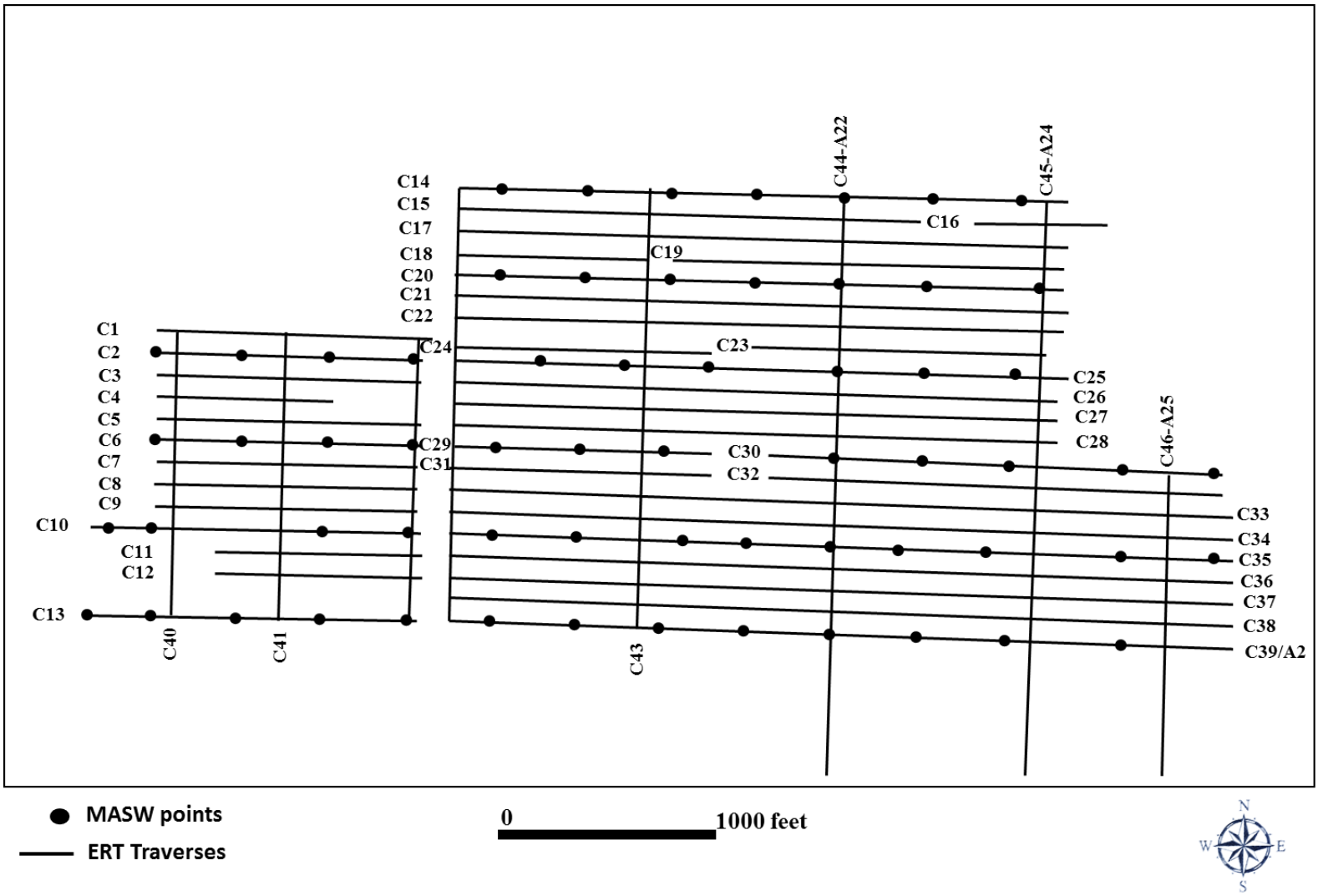

Figure 3.9. Layout of ERT traverses at the investigation site (Area C)

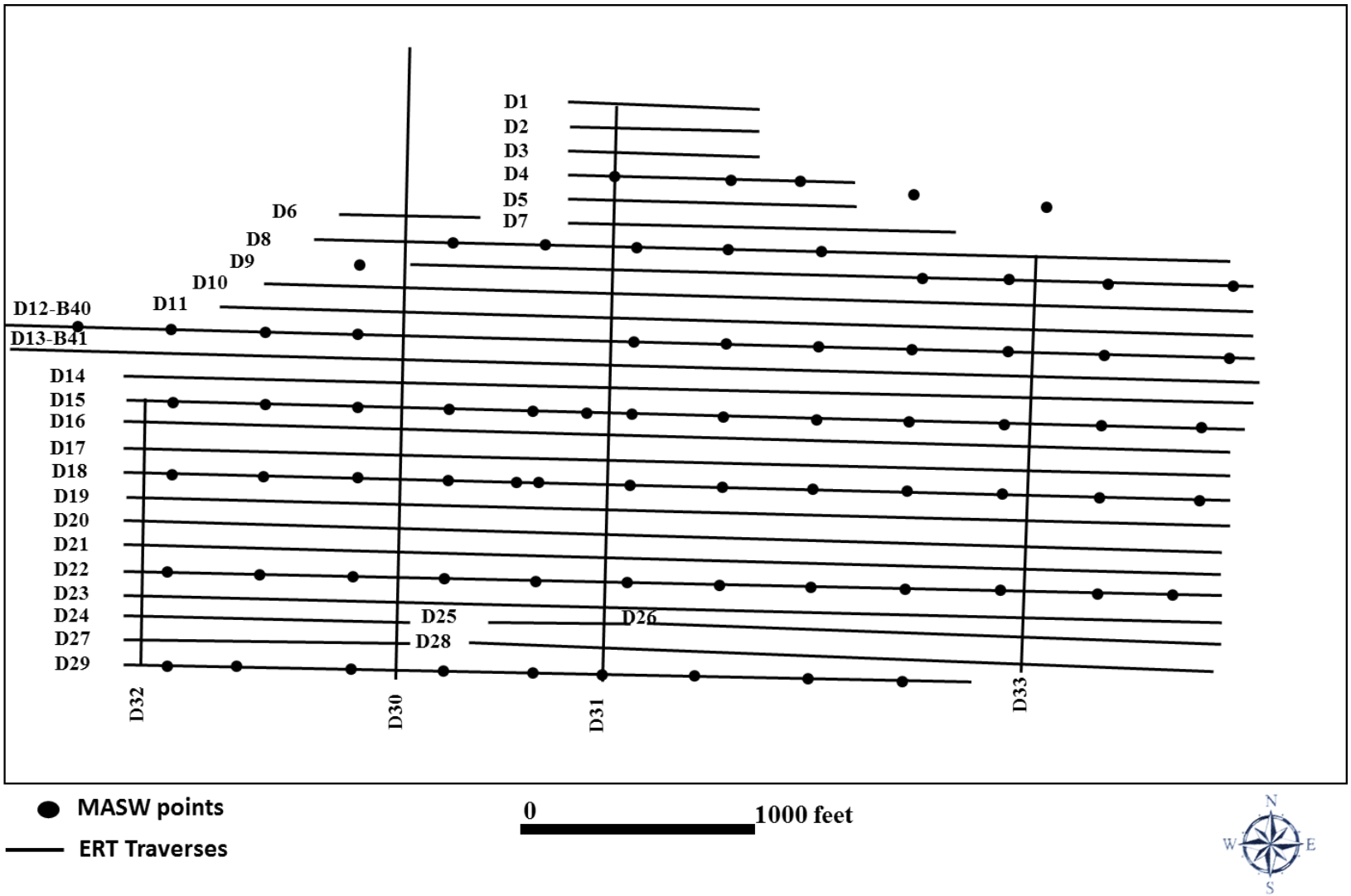

Figure 3.10. Layout of ERT traverses at the investigation site (Area D)

The collected ERT data were processed to produce a 2D model of the subsurface from the apparent electrical resistivity data using Res2Dinv software version 4.03.20 [35]. Due to the topographic change in the field finite element scheme was employed to discretize the model. The grid is distorted base on the Schwarz-Christoffel transformation method to represent topography. The robust constrained and least-square inversion method was used. The iteration process was stopped at iteration no.7. Table 3.2 represent the parameters of data processing.

Table 3.2. Summary of parameters of ERT data processing

Parameter	Value
Inversion method	robust constrained and least-square
Iteration number	7
Ratio of first layer thickness to the unit electrode spacing	0.3418
Rate at the layer thickness increases with depth	1.1
Factor to increase model depth range (1-5)	1.05
Discretization method	Finite Element
Average RMS error	5.5%
Maximum RMS error	10.7%
Minimum RMS error	2.3%

Figures 3.11 illustrates the inverted data of two representative ERT profiles acquired at the Area B. Four distinct level with high resistivity contrast can be identified from the resistivity models in Figures 3.11 and other inverted ERT data. Therefore,

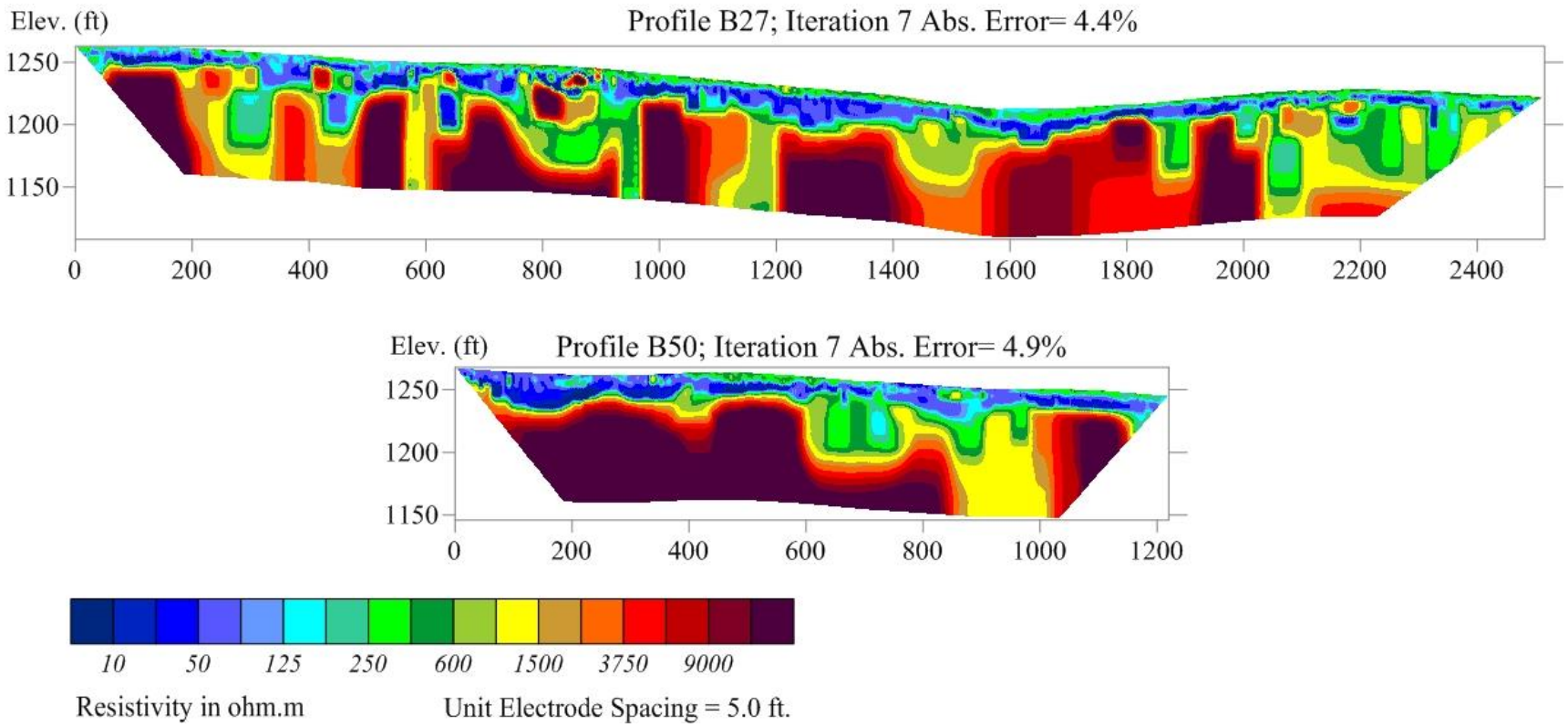

Figure 3.11. Processed west-east oriented ERT profile B27 and north-south oriented ERT profile B50

each profiles were interpreted to four units with distinct resistivity. Interpreted unit 1 has an average resistivity of 60 ohmmeter ($\Omega.m$). Average resistivity of unit 2 is 345 ohmmeter. Average resistivity is 2574 ohmmeter for unit 3. And unit 4 is characterized by an average resistivity of 19794 ohmmeter. Unit one with lowest resistivity was considered as clayey soil; thus, the unit1-unit 2 contact indicates the top of rock or soil-rock contact.

The contacts between the units were digitized manually and digitized data were transformed in a new plot. Figures 3.12 illustrates the interpreted ERT data of two representative ERT profiles acquired at the Area B. Elongated anomalies in term of low resistivity (determined by unit 1 and unite 2 and in some cases by unit 3) are interpreted as areas of high moisture content. It was anticipated that these anomalies would be aligned with the dominant joint sets in the study area. Expectations were that the anomalies would correspond to rock with high moisture content. High conductivity could be attributed to moist piped clay-fill and high clay content. Interpretation results are discussed in more details in next chapter.

3.3.3. Multi-Channel Analysis of Surface Waves (MASW). MASW data were acquired along ERT traverses to validate and constrain the ERT interpretation. In an MASW survey, multiple records (of 12 or more channels) with the same source-receiver configuration are acquired moving successively by a fixed distance interval along linear survey line [54]. All acquired records then go independently through a dispersion-inversion processing to produce a 1-D (depth) shear wave velocity (V_s) profile for each record. Spatial interpolation methods can be used to create 2-D shear wave velocity map by assigning each 1-D V_s profile at the surface coordinate in the middle the receiver spread used to acquire the corresponding record [55].

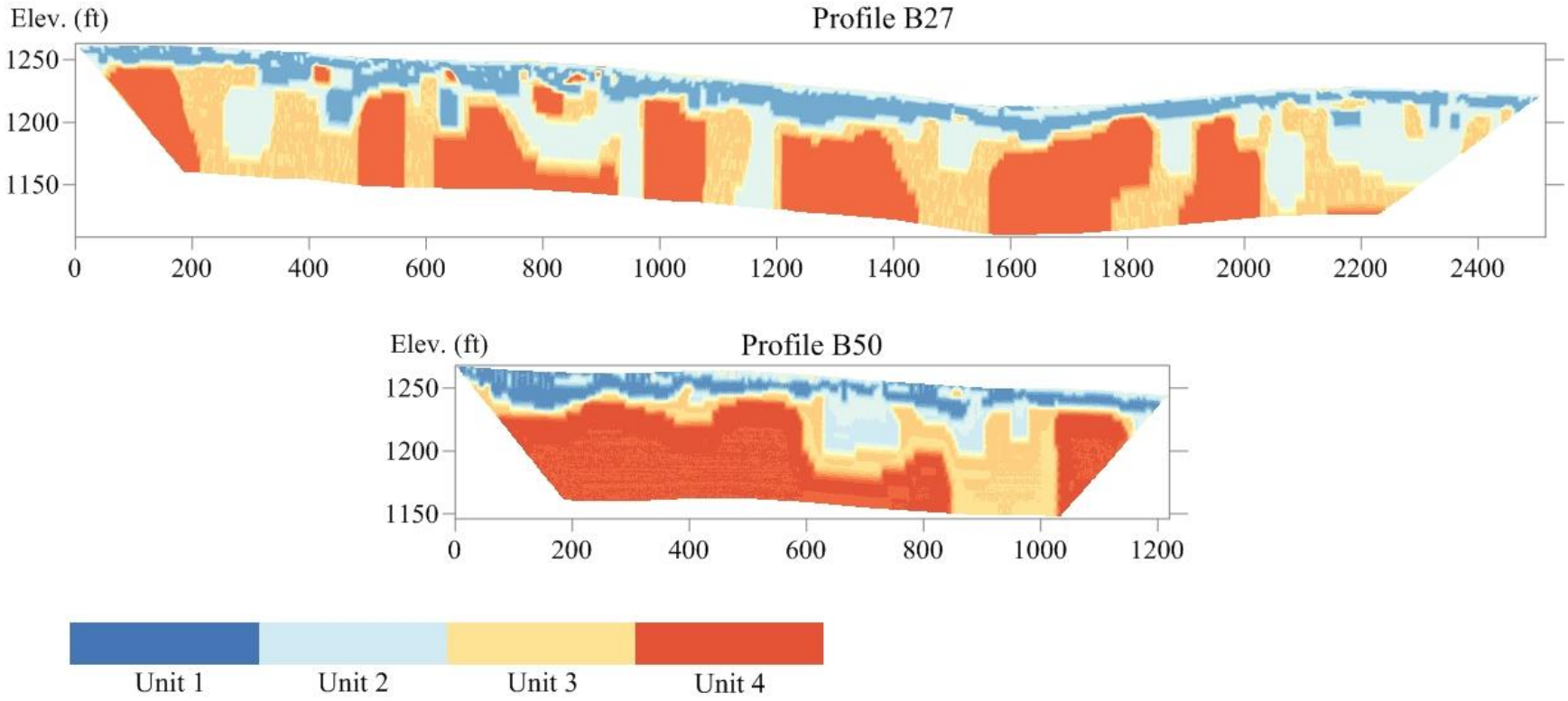

Figure 3.12. Interpreted west-east oriented ERT profile B27 and north-south oriented ERT profile B50

The MASW data were acquired along ERT traverses, at 400 ft. spacing (north-south and west-east), and with the goal of determining engineering properties of the subsurface to a depth of approximately 50 feet (see Figures 3.7 to 3.10). The spacing of the MASW data acquisition location were changed in a few instances due to access issue such as the existence of ponded water, road way and so on.

An active source (a 20 lb. sledge hammer source and metal strike plate) was used to acquire MASW data. The plate was struck (at time = 0) and motion detector was then trigger the seismograph, and the geophones were instantaneously activated. Using an active source allow to generate relatively high frequency seismic energy and this generates a very detailed image of the shallow subsurface. However, an active source do not allow to generate very low frequency energy and hence the depth of investigation generally will be restricted to about 100-120 feet [56].

Vertical stacking was done do to enhance the amplitude of the desired signal which is the surface wave and to minimize the background. The ground was stroked 5 times with the sledge hammer generating a new record each time. Then all the records were added together. Therefore surface wave signal was added in phase and its amplitude was increased by a factor of 5.

Low-frequency vertically-polarized geophones were used to record surface wave data. They are able to record extremely low-frequency data. These geophones also are designed to attenuated higher frequency signals. The desired surface wave energy to analyze in MASW ranges usually between 5 Hz and 40 Hz. The higher frequency signal is mostly refracted energy and refracted energy noises. The other advantaged of using low-frequency vertically-polarized geophones is that they are much more stable than higher

frequency geophones; they are physically coupled to the earth and they simply place on the surface [56].

A multiple number of receivers (24) were deployed with even spacing along a linear survey line with receivers connected to a multichannel recording device (seismograph). Each channel records vibrations from one receiver. One multichannel record (commonly called a shot gather) consists of a multiple number of time series (called traces) from all the receivers in an ordered manner.

In Figures 3.13 to 3.16 four representative MASW data set has been compared to the 2-D ERT profile B27. MASW array BM34 was centered at the 900 foot mark on ERT profile B27, MASW array BM35 was centered at the 1300 foot mark on ERT profile B27, MASW array BM36 was centered at the 1700 foot mark on ERT profile B27, and MASW array BM37 was centered at the 2100 foot mark on ERT Profile B27.

The MASW top-of-rock was interpreted based on the contrast in acoustic properties of soil and rock. As indicated in the figures, top of rock is as interpreted at MASW locations along ERT profile B27 consistent with the top of rock as interpreted at corresponding 2-D ERT locations. As it was mentioned previously, the unit 1-unit 2 contact indicates the top of rock in ERT profiles.

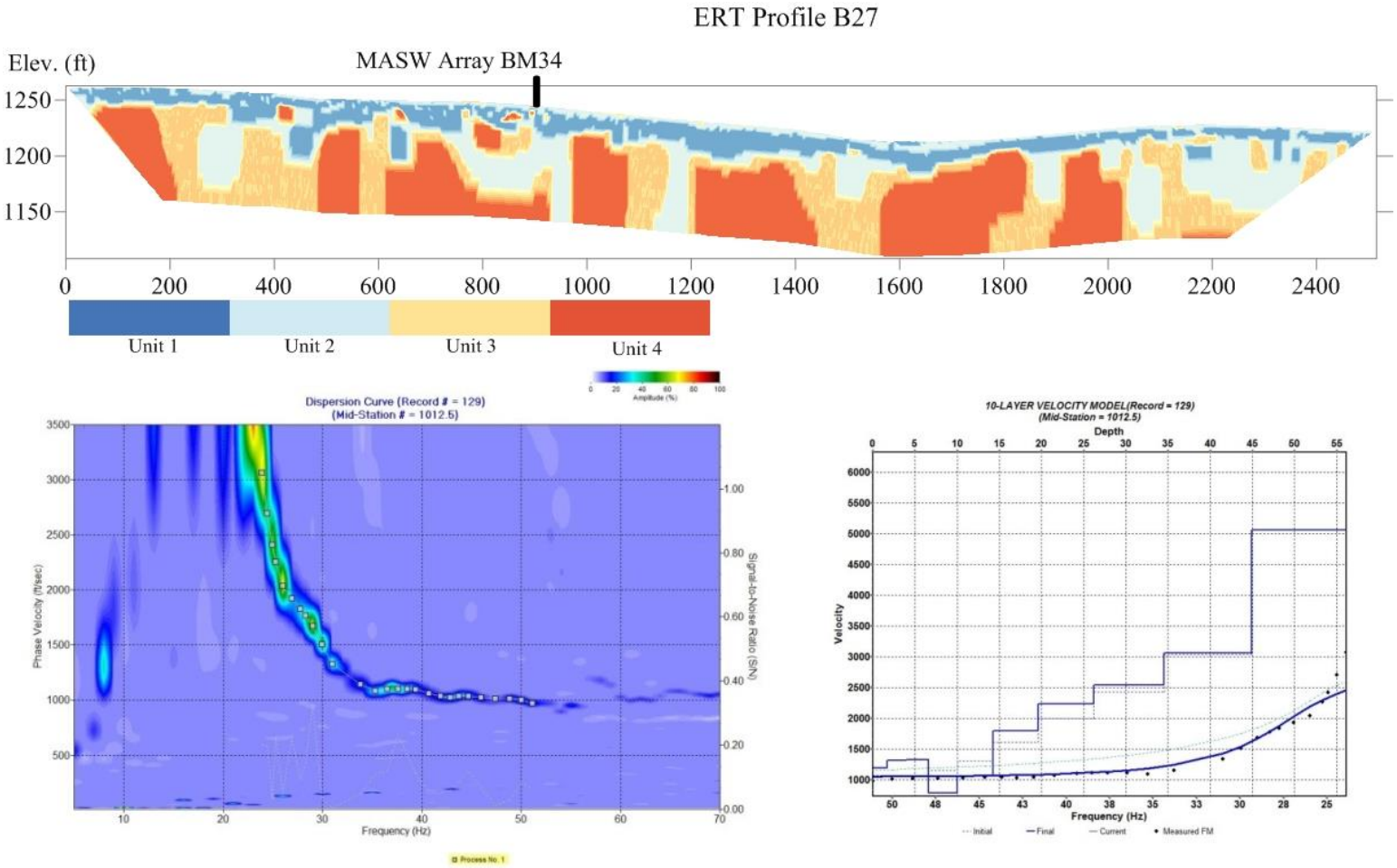

MASW-eatimate of depth to top of rock ~ 14 ft.

ERT-eatimate of depth to top of rock ~ 12 ft.

Array BM34 ties profile B27 at approximately 900 foot mark

MASW-estimate of soil velocity ~ 1200 ft/sec.

Figure 3.13. Top- MASW array BM34 centered at 900 foot mark on ERT profile B27, Left- MASW array BM34 dispersion curve, and Right- Shear wave velocity sounding MB34

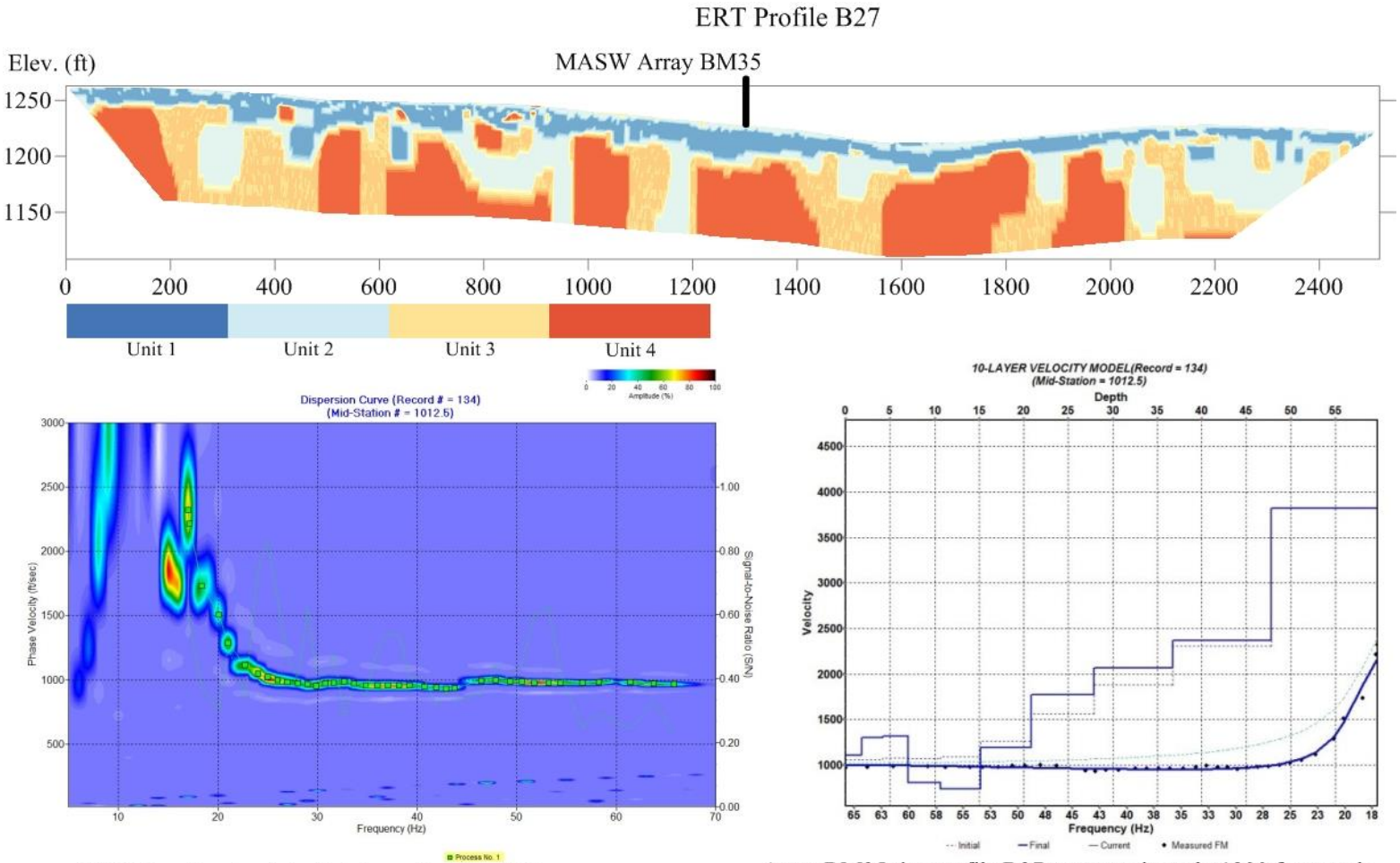

MASW-eatimate of depth to top of rock ~ 21 ft.

ERT-eatimate of depth to top of rock ~ 20 ft.

Array BM35 ties profile B27 at approximately 1300 foot mark

MASW-estimate of soil velocity ~ 1000 ft/sec.

Figure 3.14. Top- MASW array BM35 centered at 1300 foot mark on ERT profile B27, Left- MASW array BM35 dispersion curve, and Right- Shear wave velocity sounding MB35

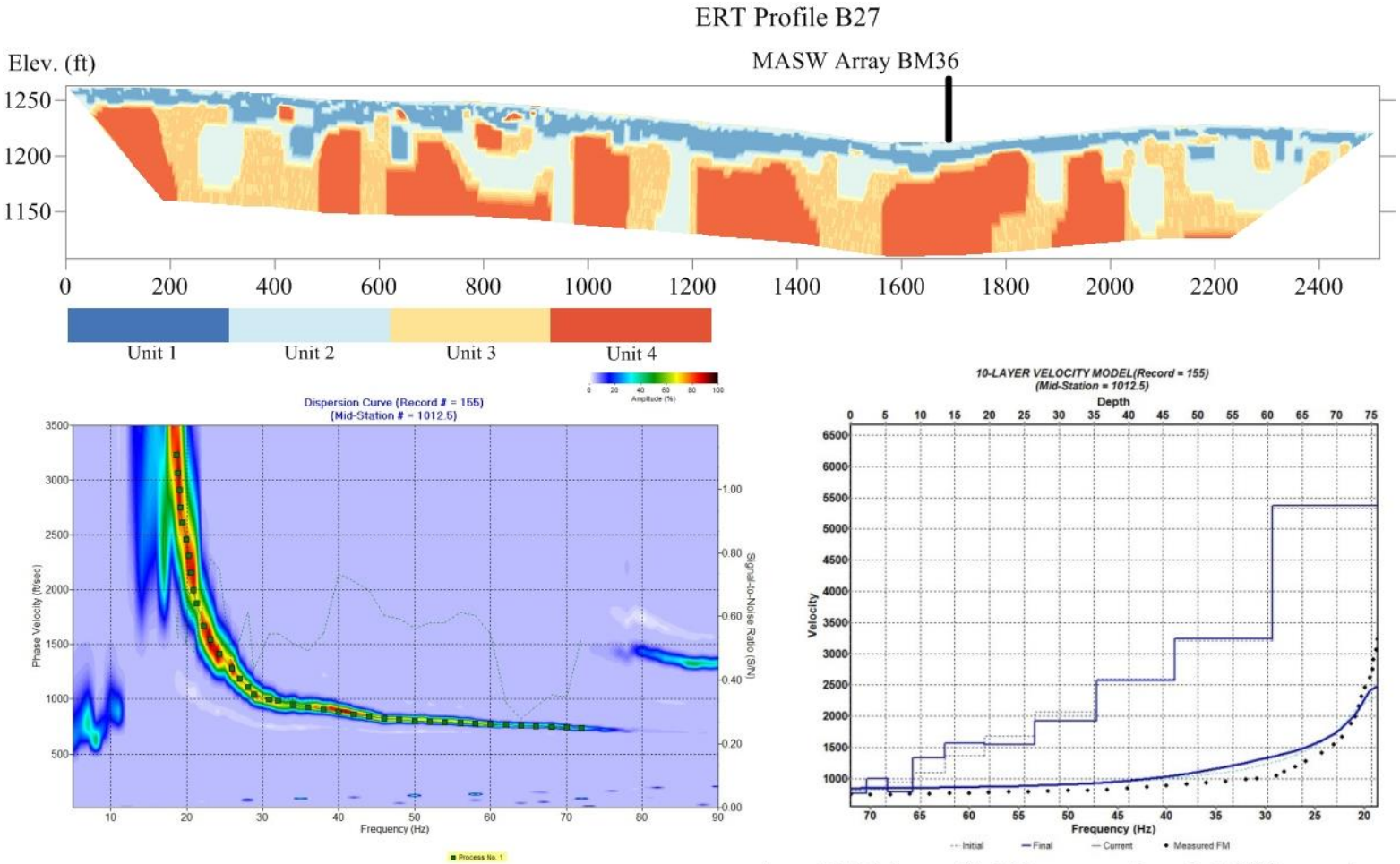

MASW-eatimate of depth to top of rock ~ 13 ft.

ERT-eatimate of depth to top of rock ~ 14 ft.

Array BM36 ties profile B27 at approximately 1700 foot mark

MASW-estimate of soil velocity ~ 1200 ft/sec.

Figure 3.15. Top- MASW array BM36 centered at 1700 foot mark on ERT profile B27, Left- MASW array BM36 dispersion curve, and Right- Shear wave velocity sounding MB36

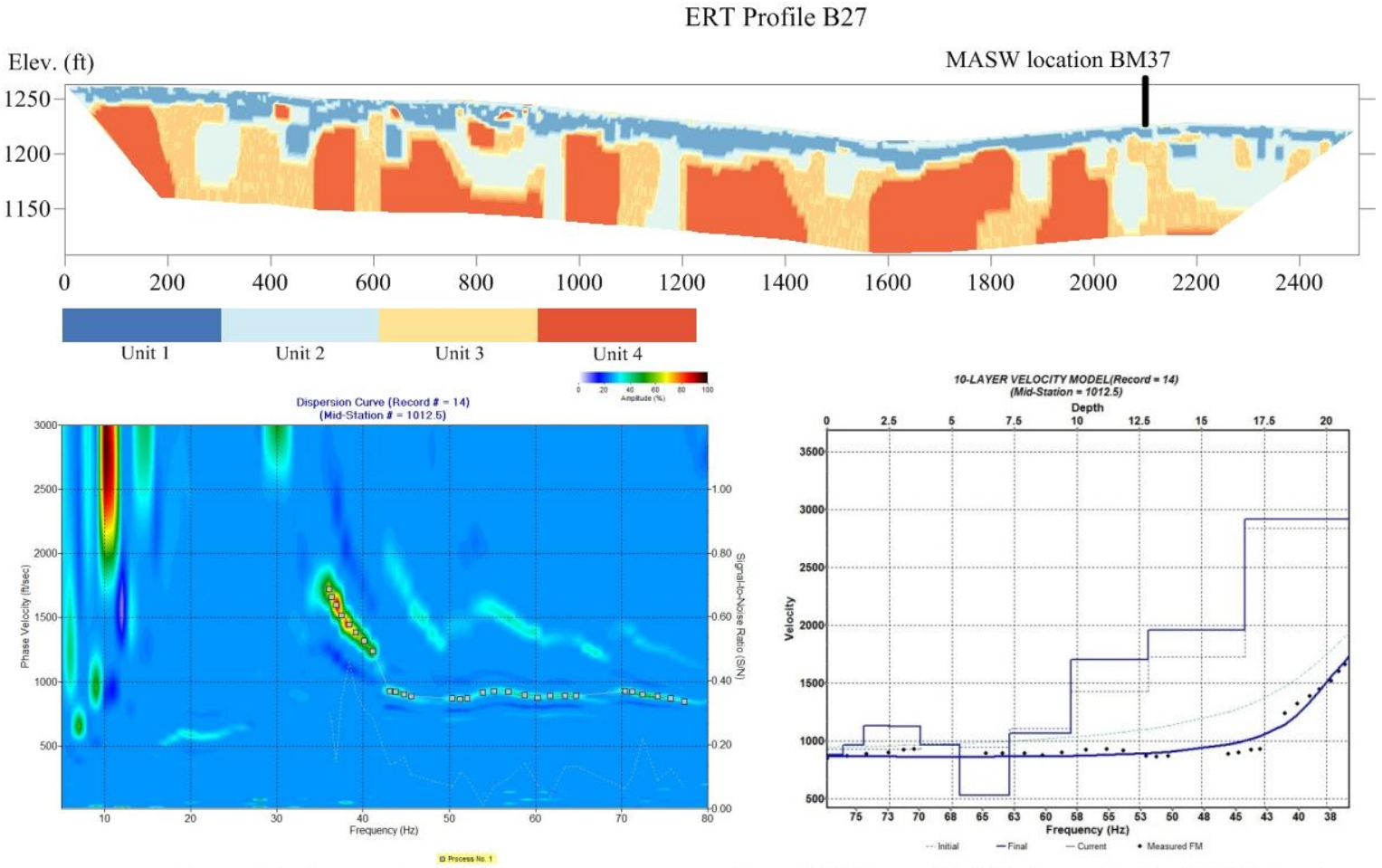

MASW-eatimate of depth to top of rock ~ 9 ft.

ERT-eatimate of depth to top of rock ~ 11 ft.

Array BM37 ties profile B27 at approximately 2100 foot mark

MASW-estimate of soil velocity ~ 1200 ft/sec.

Figure 3.16. Top- MASW array BM37 centered at 2100 foot mark on ERT profile B27, Left- MASW array BM37 dispersion curve, and Right- Shear wave velocity sounding MB37

4. RESULT AND DISCUSSION

4.1. PATTERN, ORIENTATION AND DENSITY OF JOINT SETS

After all the ERT data were interpreted, zones of high moisture content were identified in each area by arranging the interpreted profiles along their original layout. These zones are areas where rock is very moist. In some of these areas rock is probably more fractured. Elsewhere it is simply that moisture is present. Figures 4.1 depict the north-south trending joint sets identified on west-east oriented interpreted ERT profiles in Area B.

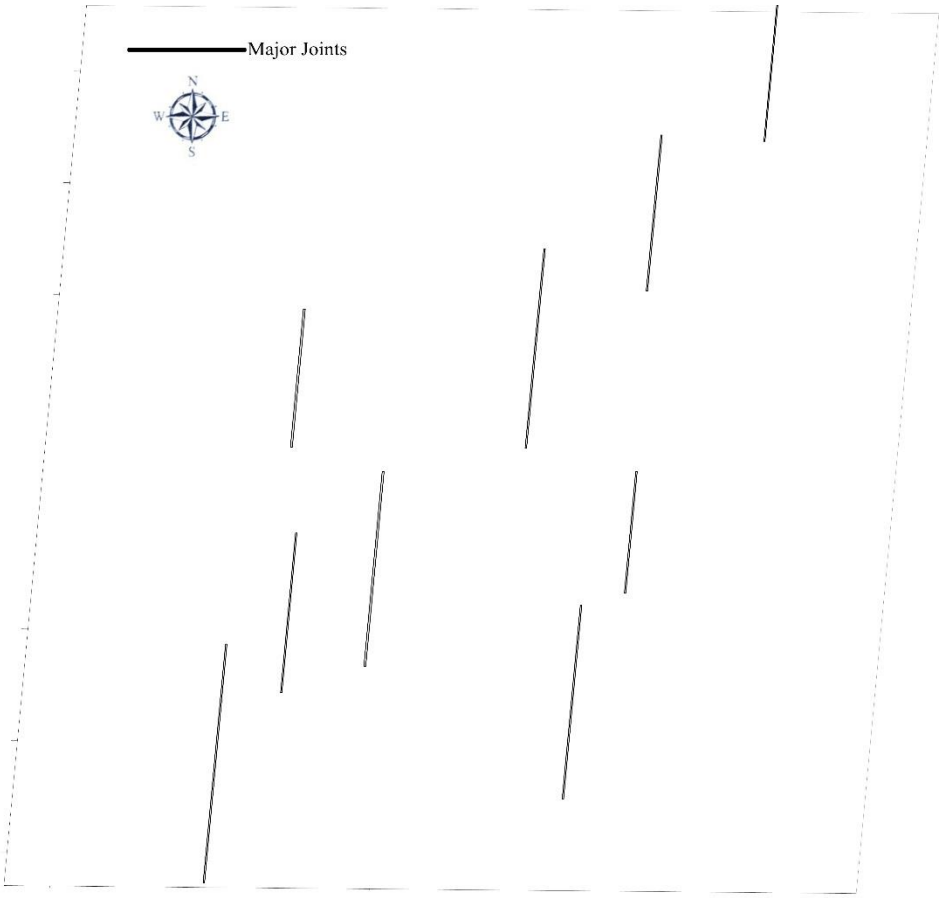

Figure 4.1. Visually prominent north-south trending joint sets in Area B

Visually prominent joint sets have been interpreted along the most anomalous zones (in term of low resistivity) those are prominently imaged on the ERT profiles. Two set of visually prominent orthogonal joints have been identified: north-south trending joint sets and west-east trending joint sets. Figure 4.2 shows the west-east trending joint sets identified on north-south oriented interpreted ERT profiles in the investigation site.

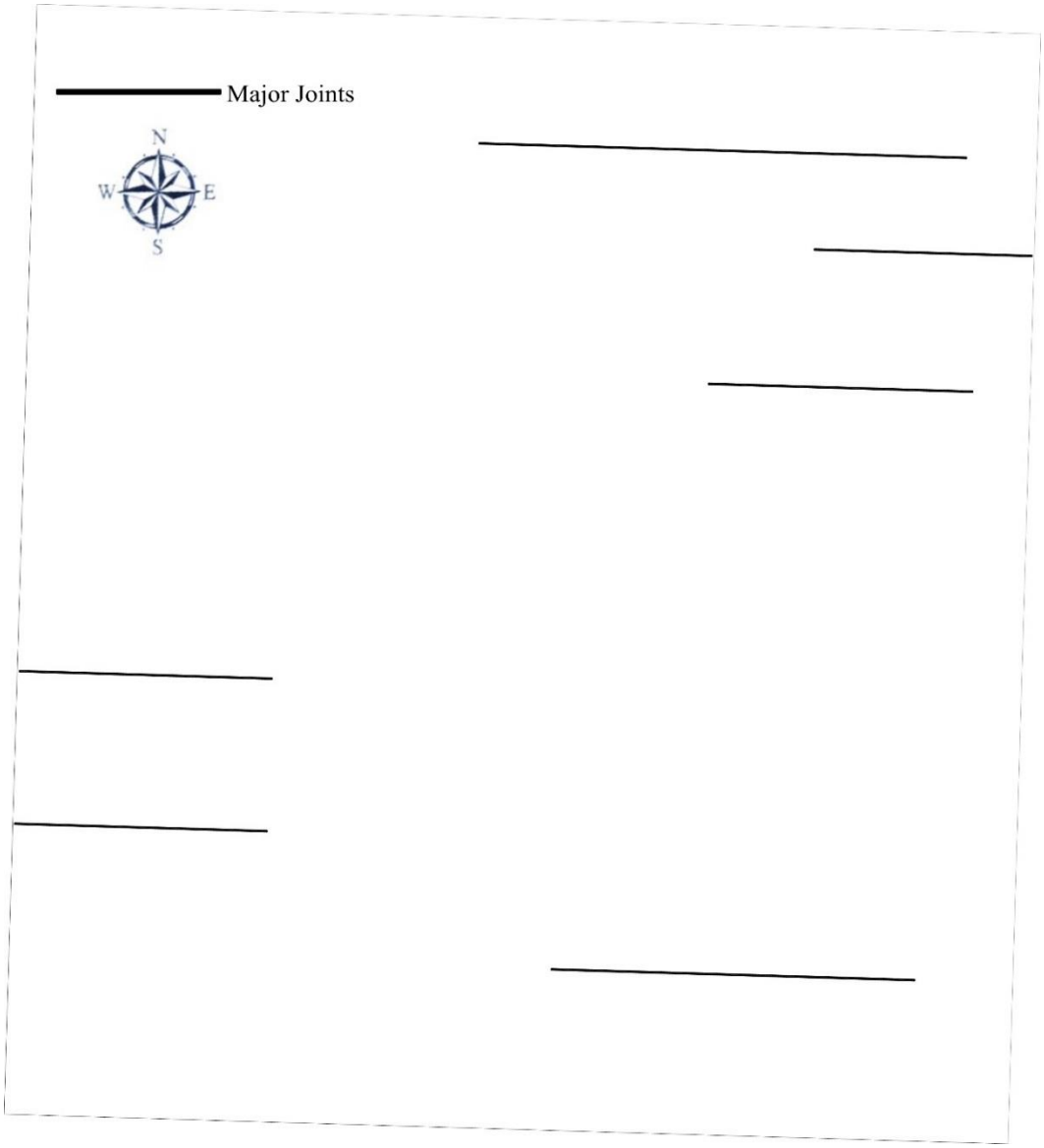

Figure 4.2. Visually prominent west-east trending joint sets in the investigation site

The north-south trending joint sets are more prevalent in the investigation site, with a density of approximately one pre hundred feet. The density of the west-east trending joints sets is approximately one per two hundred feet. A reliable correlation cannot be made between adjacent north-south oriented ERT profiles to determine the west-east trending joint set because of the greater spacing of the north-south oriented ERT profiles (500 feet or more).

Figure 4.3.a depicts ERT profile B17 and the core C14 drilled on it. An anomalous low resistivity zone was selected to drill core C14. The resistivity of the interpreted units and average percentage of RQD or rock quality were compared at the core location. Rock core sample photographs (figure 4.3.d) and calculated RQD have been illustrated in figure 4.3.c and 4.6.d. The top of rock is at 17 ft. depth at core C14 location and the quality of rock is good to excellent along this core (figure 4.3.c). The quality of rock was determined good to excellent for other core rock samples acquired in the investigation site.

Borehole control acquired on the investigation site indicates that anomalous low resistivity zone cannot be interpreted as a single dissolution-enlarged joint filled with clayey soil, as it was expected. It is the presence of the conductive moisture and conductive moist piped clay in rock that causes the elongated anomalies appear on the ERT profiles as zones of relatively low resistivity. The greater the moisture/clay content, the more prominent the low resistivity ERT signature. Other core holes on the investigation site indicates that rock within the interpreted join sets are statistically competent but more extensively fractured than rock in areas do not appear to be dissected by possible join sets.

Most of the interpreted north-south trending joint set appear to extend across the entirety of Areas A, B, C, and D. However, joints are only visually identifiable on some

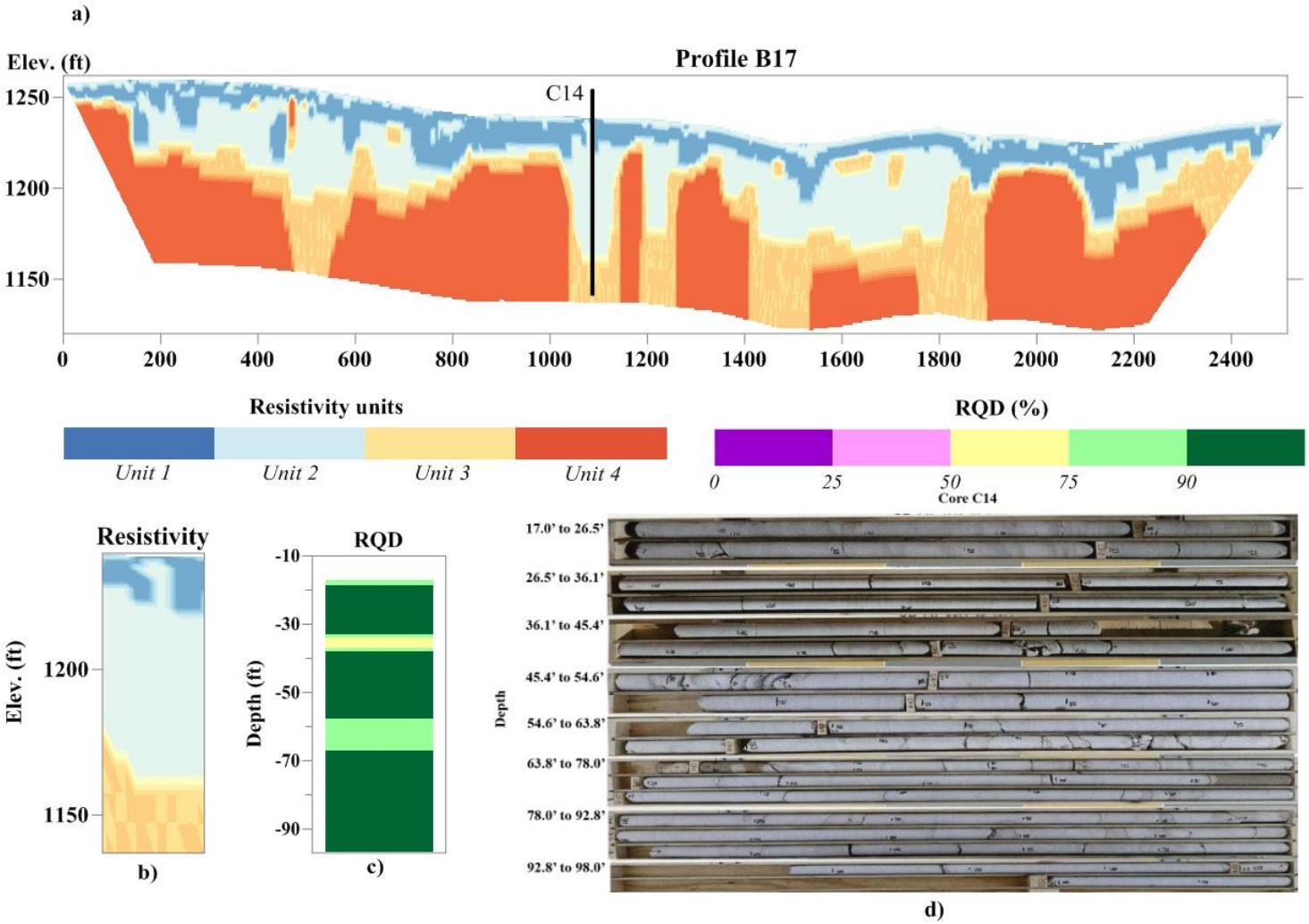

Figure 4.3. Validating the interpreted ERT data at Core hole C14; a) C14 on the ERT profile B17, b) Section of ERT data at C14, c) Average percentage of RQD at C14, d) Rock core sample photographs

ERT profiles but not on the others. One explanation could be that the intensity of fracturing varies and therefore the concentrations of moisture and clay content vary laterally along joints sets. Another reason is the variability of water presence in rock fractures. The amount of existent water is laterally variable beneath the interpreted prominent north-south trending and west-east trending joint sets. In some areas rock fractures are filled with more water, while fractures in other areas contains less water.

As illustrated by interpreted ERT profiles in figure 3.12, joint sets in the investigation site appear to be near-vertical and are characterized by 20 to 40 ft. wide zone of low resistivity. Zones of low resistivity are appear to be wider than 40 feet in some instances. A plausible explanation is that the joint sets are more closely spaced at the areas with wider low resistivity zone. Another explanation could be that joint sets intersect ERT profiles at angle of much less than 90 degree where the low resistivity zone appear wider. The width of lower resistivity zones or interpreted joint sets typically broaden with depth (Figure 4.4.a); however the width of some joint sets is constant (Figure 4.4.b). This pattern might be caused by increase in moisture concentration and clay content. Also, water flow both in horizontal and vertical directions through the rock fractures. An increase in horizontal movement of water could increase the width of low resistivity zones on ERT profiles.

A number of possible joint sets were determined above, however all of the interpreted sets in the investigation site are associated with either man-made features such as roadways, parking lots, hedges and ponds, or confirmed sinkholes. Figure 4.5 depicts the interpreted possible joint sets superposed on the aerial photograph of the investigation site.

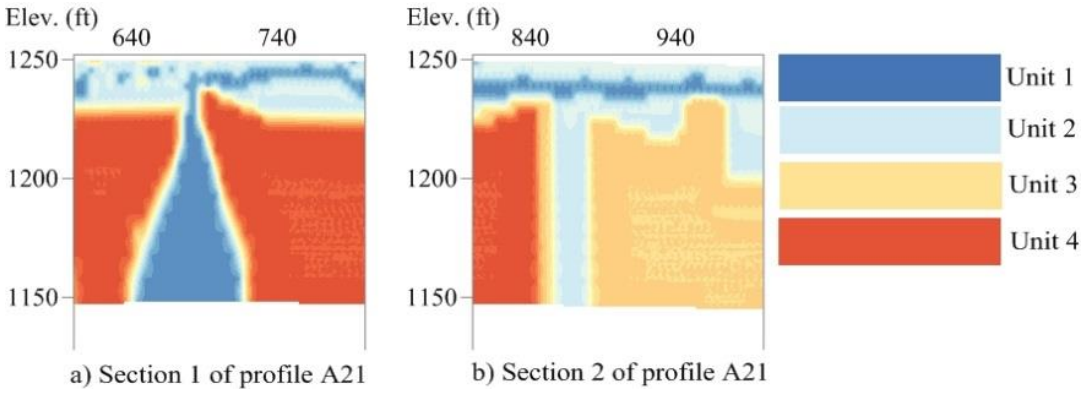

Figure 4.4. Interpreted ERT image of prominent joint sets; a) Section 1 of interpreted ERT profile A21 (from 600 to 800 ft.): Typical broadening with depth b) Section 2 of interpreted ERT profile A21 (from 800 to 100 ft.)

Aerial photographs of Area A indicates that joint set J4 is coincident with north-south trending man-made roadways. The anomalously low resistivity zones associated with J4 can be attributed to the presence of water in roadway drainage ditches. Joint set J2 is coincident with the western edge of a man-made parking lot and an adjacent north-south trending hedgerow. The hedgerow acts as a temporary barrier to surface water flowing to the east-northeast and can be therefore caused by the anomalously low resistivity zones associated with J2. Joint set J6 is coincident with northern and southern edge of a parking lot. The low resistivity zones associated with J6 might be caused, at least in part, by infiltration of edge of parking lot.

Aerial photographs of Area B indicates that joint sets J9, J14 and J15 are coincident with north-south trending manmade roadways. The anomalously low resistivity zones associated with J9, J14 and J15 can be attributed to the presence of water in roadway drainage diches. The anomalously low resistivity zones associated with J7 can be attributed to the presence of surface drainage features.

Aerial photographs of Area C indicates that joint sets J21 and J24 are coincident with north-south trending manmade roadways. The anomalously low resistivity zones associated with J21 and J24 can be attributed to the presence of water in roadway drainage diches. Joint J19 and J20 are coincident with an adjacent north-south trending hedgerow. As noted in the preceding text, the hedgerow acts as a temporary barrier to surface water flowing to the east-northeast and can be therefore caused by the anomalously low resistivity zones associated with J19 and J20.

Aerial photographs of Area D indicates that joint sets J27, J28 and J29 are coincident with north-south trending manmade roadways. The anomalously low resistivity zones associated with J27, J28 and J29 can be attributed to the presence of water in roadway drainage diches. Joint set J30 is coincident with the western edge of a manmade parking lot.

The low resistivity zones associated with J30 might be caused, at least in part, by infiltration of parking lot. Joint set J33 is coincident with the eastern edge of a manmade parking lot and an adjacent north-south trending hedgerow. As noted in the preceding text, the hedgerow acts as a temporary barrier to surface water flowing to the east-northeast and can be therefore caused by the anomalously low resistivity zones associated with J33.

2D contour map of interpreted soil-rock contact (the top of rock) elevation in the investigation site has been illustrated in figure 4.6. Figure 4.7 depicts the 3D surface map of the elevation of soil-rock contact in the investigation site. A good correlation can be observed between the interpreted north-south trending and west-east trending of visually prominent joint sets and areas with lower elevation which are shown in white or lighter blue colors.

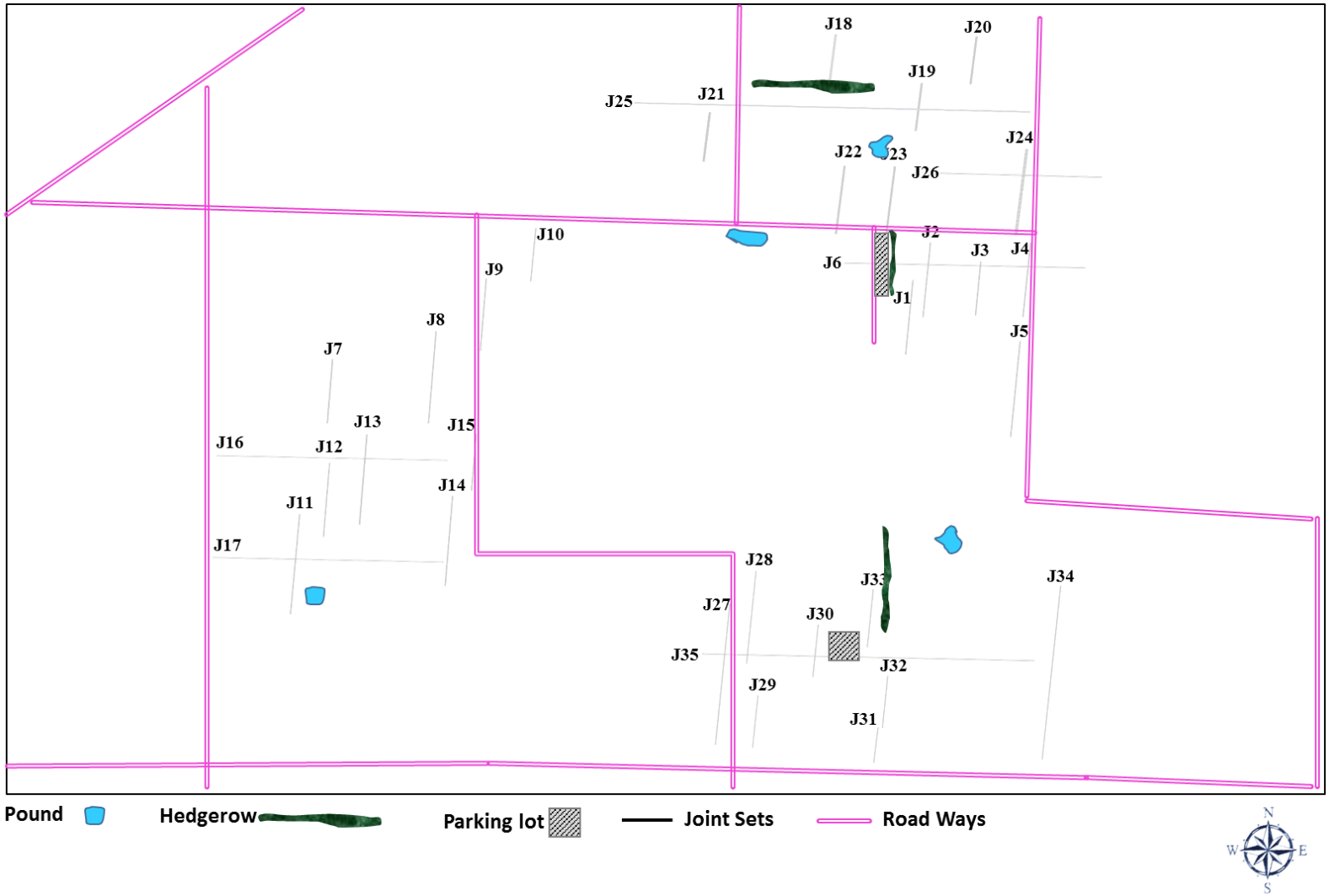

Figure 4.5. Visually prominent joint sets associated with man-made features in the study area

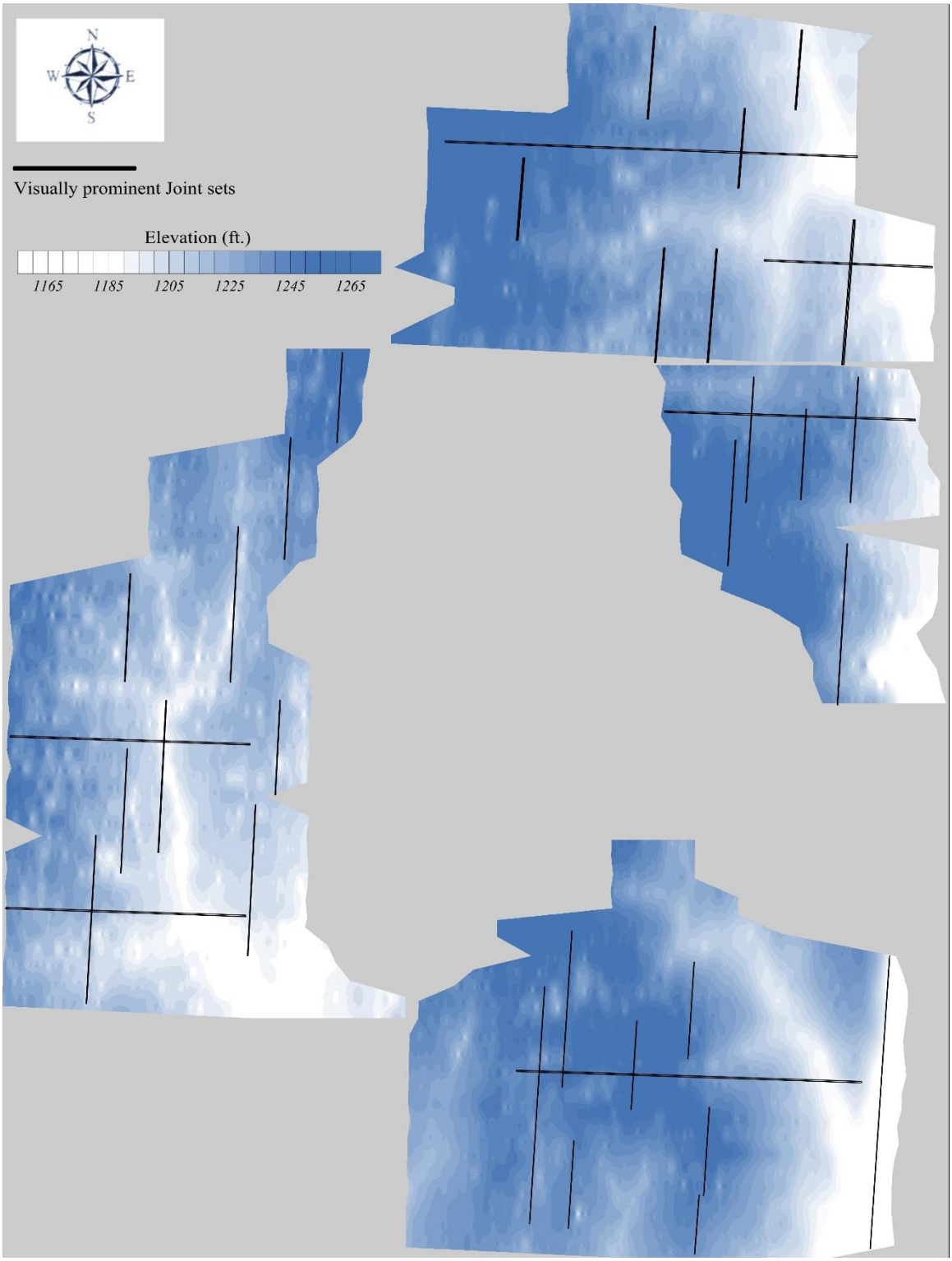

Figure 4.6. Soil-rock contact (top of rock) elevation contour map in the investigation site

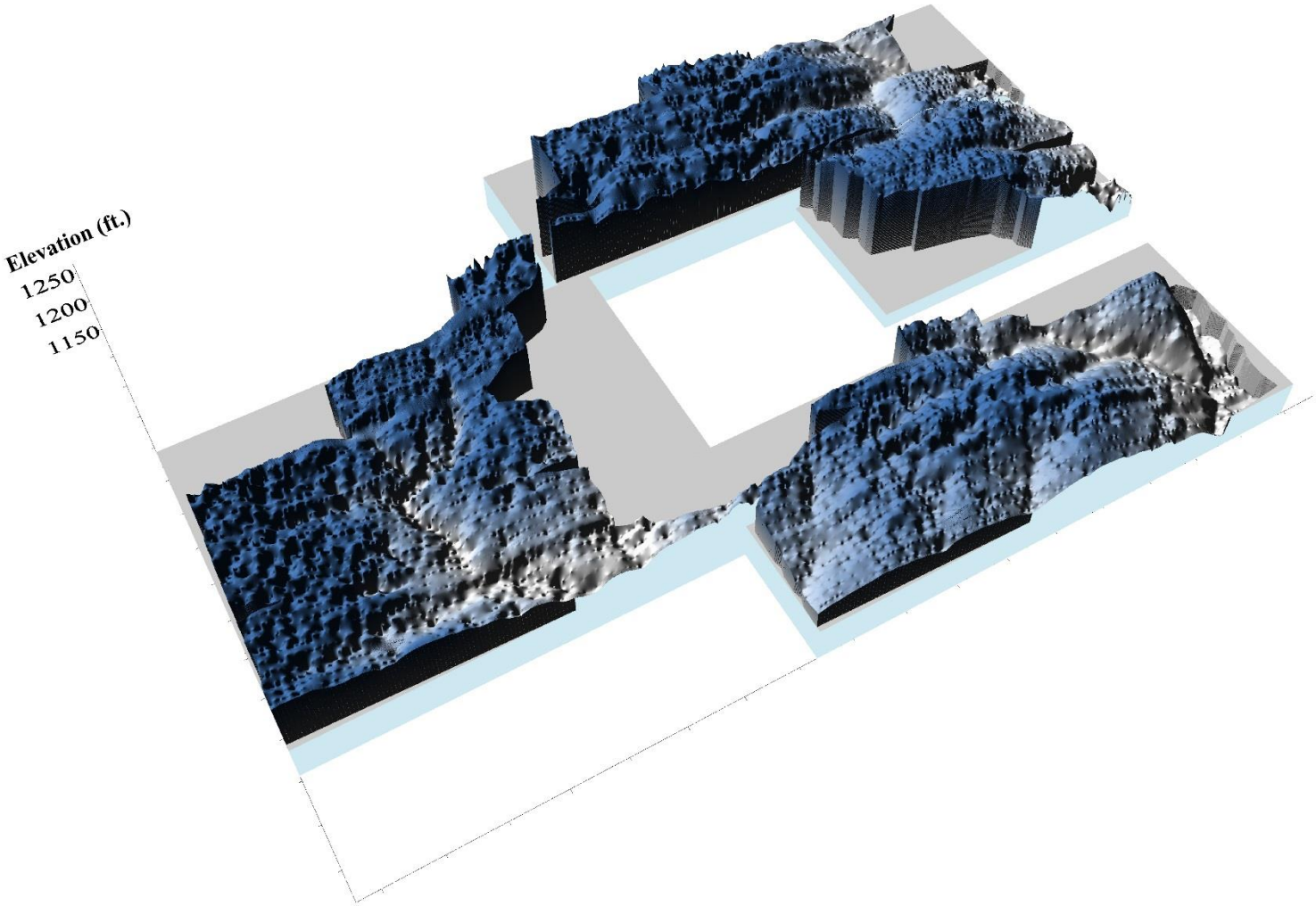

Figure 4.7. 3D surface map of soil-rock contact (top of rock) elevation in the investigation site

4.2. MASW AND BORING CONTROL DATA

MASW data were acquired along ERT traverses and (mostly) at 400 ft. intervals with a goal of exploring the subsurface to a depth of nearly 50 feet. Moreover, a number of core-holes were drilled to correlated with and validate the interpretation of ERT cross-section data.

The depth of soil-rock interface (top-of-rock) was defined from both MASW data and ERT interpreted data at MASW location. Table 4.1 summarizes a comparison between the results from two MASW and ERT methods at some of the MASW arrays location.

Table 4.1. Estimated depth to top of rock from interpreted ERT and MASW data

Data from ERT Profiles		Data from MASW		Differences (ft.)	Data from ERT Profiles		Data from MASW		Differences (ft.)
ERT Profile	Depth (ft.)	MASW Array	Depth (ft.)		ERT Profile	Depth (f.t)	MASW Array	Depth (f.t)	
A2	18	AM1	16.5	1.5		22	BM10	22	0
	11	AM2	11	0	B12	12	BM11	11.5	0.5
	12	AM3	11	1		12	BM12	11	1
	15	AM4	12	3		12	BM13	13.5	1.5
	12	AM5	11	1	B15	19	BM14	16	3
A10	15	AM6	21	6		16	BM15	16.5	0.5
	10	AM7	10	0		15	BM16	18.5	3.5
	15	AM8	13	2		8	BM17	7.5	0.5
	13	AM9	11	2		12	BM18	10	2
	14	AM10	12.5	1.5		17	BM19	17.5	0.5
A13	15	AM11	16	1	B19	19	BM21	12	7
	10	AM12	12	2		17	BM22	17.5	0.5
	8	AM13	9	1		10	BM23	10	0
	6	AM14	6.5	0.5		9	BM24	11.5	2.5
	11	AM15	13	2		13	BM25	10	3

Eighty four percent of the data points have difference less than 5 ft. Difference is less than 1 ft. for twenty percent of the ERT and MASW data. Only 4.4 percent of data have difference larger than 10 ft.The MASW top-of-rock was interpreted based on the contrast in acoustic properties of soil and rock, whereas the ERT top-of-rock was based on contrast in resistivities of soil and rock (or contrast in moisture content). Moreover, top-of-rock was determined based on the first rejection of the drill rig at cores location.

The depth of soil-rock interface was also defined from both boring data and ERT interpreted data at core holes location. Table 4.2 summarizes a compression between the results from two borings and ERT methods. Eighty percent of the data points have errors less than 5 ft. Error is less than 1 ft. for twenty percent of the boring data. Only 6.6 percentage of data have error larger than 10 ft.

Table 4.2. Estimated depth to top of rock from interpreted ERT data and cores

Core hole data		Electrical resistivity tomography (ERT) data		Differences (ft.)
Core Boring	Elevation (ft.)	ERT Profile	Elevation (ft.)	
C1	15.5	B10	16.00	0.50
C2	10.5	B11	16.00	5.50
C3	6.5	B12	16.00	9.50
C4	10.15	B13	13.00	2.50
C5	10	B20	8.00	2.00

A statistical analysis was performed on extracted data from interpreted resistivity data and boring data (Table 4.3). A relatively good correlation was found between the interpreted resistivity units and their geotechnical properties.Unite 1 have an average Rock

Quality Designation (RQD) percentage of 27.89 with average resistivity of 60 ohmmeter ($\Omega.m$). Average RQD is 62.98% for data of Unit 2 with an average resistivity of 345 $\Omega.m$. An average RQD of 87.20% indicates Unit 3 with an average resistivity of 2574 $\Omega.m$. Rocks of unit 4 are characterized by an average RQD of 92.13% and average resistivity of 19794 $\Omega.m$. However, further information about the moisture and clay content is required to confidently describe the geotechnical properties of the soil and rock in the study area. In addition, the quality of rock might varies horizontally between the cores which could result to a different correlation between the resistivity and RQD. Moreover, both MASW data and boring information show that the quality of rock increases with depth. The main reason is rock weathering. Shallow rock is generally weathered and weaker, while rock at depth are non-weathered and in overall less fractured.

Table 4.3. Statistical analysis of data extracted from core holes and interpreted ERT data

Resistivity units		Resistivity ($\Omega.m$)	RQD (%)								
		ERT data	C1		C2	C3		C4	C5		Ave
Unit 1	Min	33	0	-	0	0	-	0	0	0	9
	Max	127	0	-	90	82	-	75	0	100	56
	Ave	60	0	-	26	44	-	12	0	83	28
Unit 2	Min	151	0	76	76	0	78	50	0	93	49
	Max	1425	0	76	100	0	98	90	0	100	72
	Ave	345	0	76	92	0	88	83	0	99	62
Unit 3	Min	204	76	-	-	70	-	75	-	-	75
	Max	13820	89	-	-	100	-	90	-	-	95
	Ave	2574	85	-	-	87	-	81	-	-	87
Unit 4	Min	4667	88	-	-	-	-	-	-	-	88
	Max	73595	96	-	-	-	-	-	-	-	96
	Ave	19794	92	-	-	-	-	-	-	-	92

4.3. THREE DIMENSIONAL ERT DATA

Although pattern, orientation and density of join sets may be identified from 2D ERT data, a complete description of joints is difficult because of their three-dimensional nature. Joint density is a rough inaccurate measure based upon spacing of the dominant joint set. There do not exist rules how to correct the measure where several joints sets are present. One and two dimensional measurements are made perpendicular to the dominant joint sets and these methods also give an inaccurate estimate of orientation of joint sets in many cases [62, 63 and 64].

Three dimensional geophysical methods could be used to study jointing, however indirect observations have limited accuracy. Three dimensional electrical resistivity tomography survey was undertaken at the northern part of Area B for the purpose of validating interpreted results from two dimensional ERT data. Figure 4.8 depicts the layout of ERT traverses in Area B for both 2D and 3D surveys.

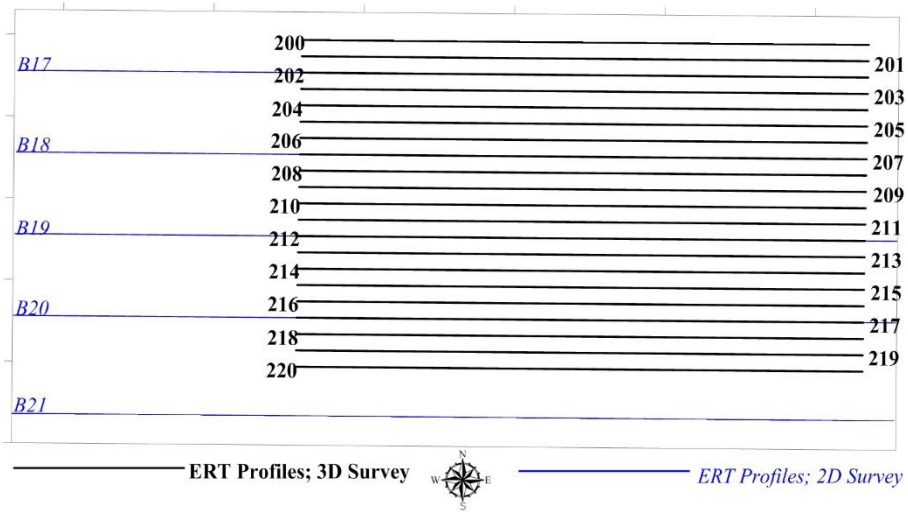

Figure 4.8. Layout of ERT traverses at the northern section of Area B, 2D ERT data acquired along blue lines were processed two dimensionally, 2D ERT data acquired along black lines were processed three dimensionally

A total of 39,585 linear feet of two dimensional ERT data were acquired along 20 separate traverse. ERT data were acquired mostly along parallel west-east oriented traverses nearly spaced at 20 ft. intervals using dipole-dipole array. The electrode spacing along each traverse was 5 feet. Five feet inter-electrode spacing was used to reach the goal of imaging subsurface to a depth approximately 100 ft. The length of the traverses were 1885 ft.

The collected 2D ERT data along black lines in figure 4.8 were combined to a 3D resistivity data model. The 3D resistivity data then were processed to produce a 3D model of the subsurface using Res3Dinv software version 3.10.10 [57 and 58]. Figure 4.9 depicts the vertical sections of the three dimensionally inverted ERT data. Vertical sections were plotted at 20 ft. intervals. Three dimensionally inverted ERT data indicate north-south trending joint sets on vertical sections where the anomalously low resistivity zone appear.

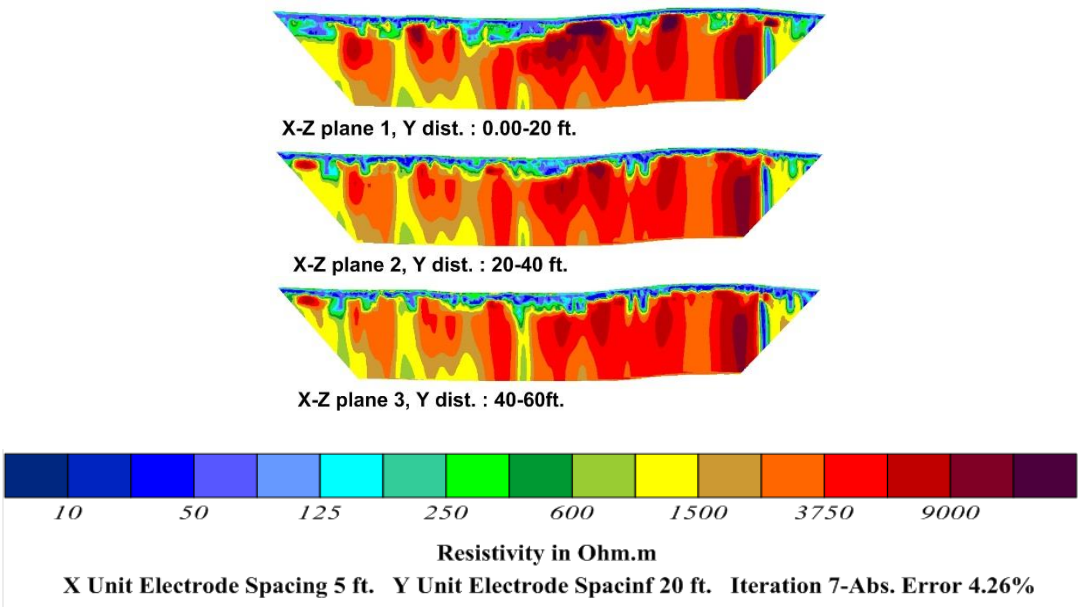

Figure 4.9. Vertical sections of 3D inverted ERT data of profiles 200 to 220 in Area B

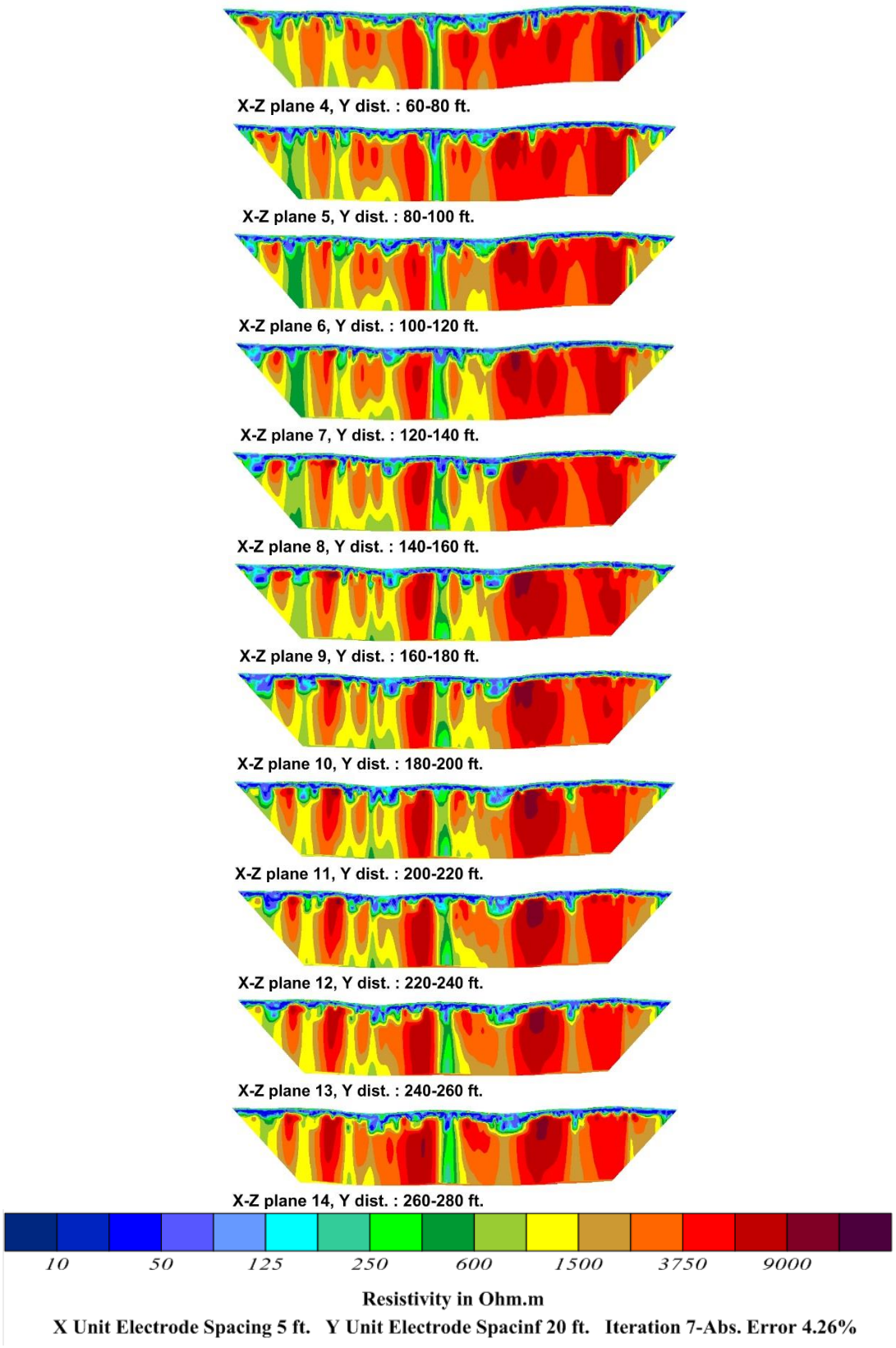

Figure 4.9. Vertical sections of 3D inverted ERT data of profiles 200 to 220 in Area B (cont.)

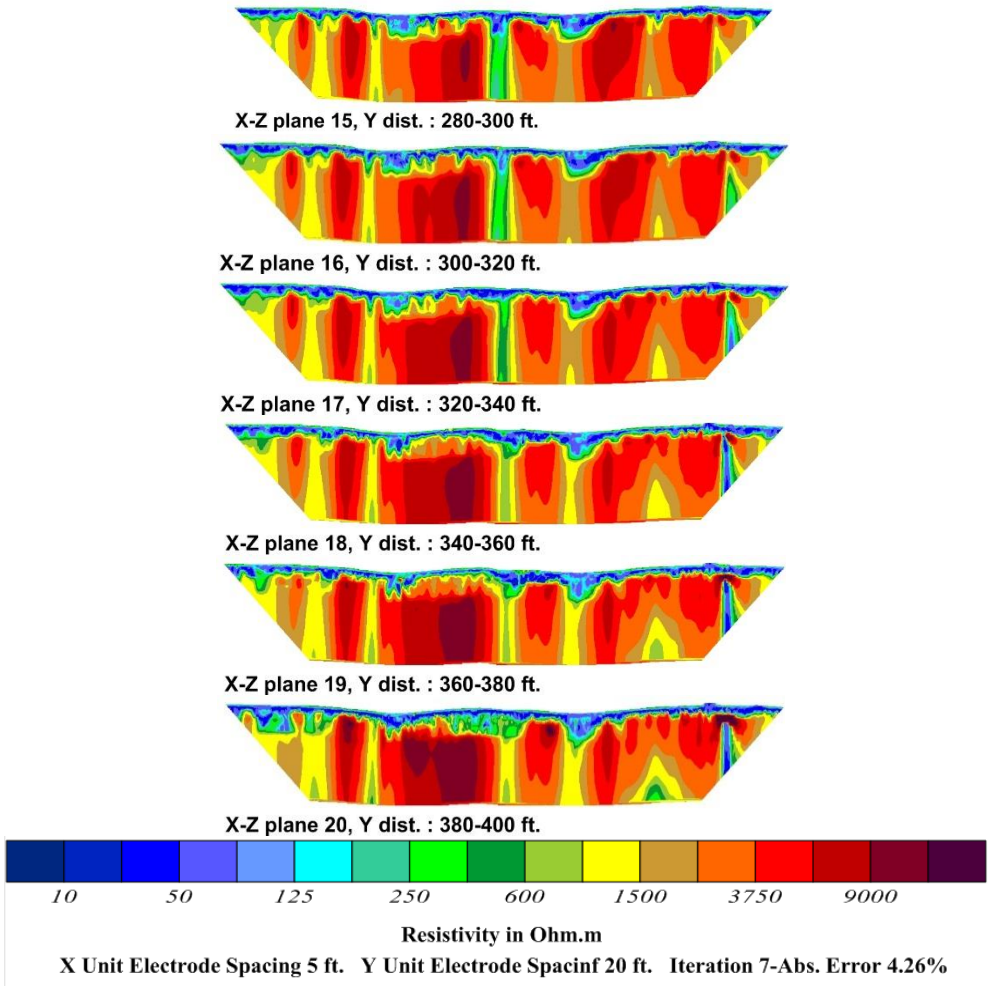

Figure 4.9. Vertical sections of 3D inverted ERT data of profiles 200 to 220 in Area B (cont.)

4.4. COMPARISON WITH OTHER STUDIES

In this section, results are compared to that of three other geophysical investigation near the study area. Site #1 is located at the intersection of Missouri Highway 65 and three Springfield Underground cross tunnels, south of Kearney Street, Springfield, Missouri [59]. Site #2 is located at is located at the proposed intersection of Route 125 over Route 60, Greene County, Missouri [60].And site #3 is located at US Route 60, Springfield,

Missouri [61]. Figure 4.10 depict the location of Site #1, Site #2, and Site #3 relative to the study area.

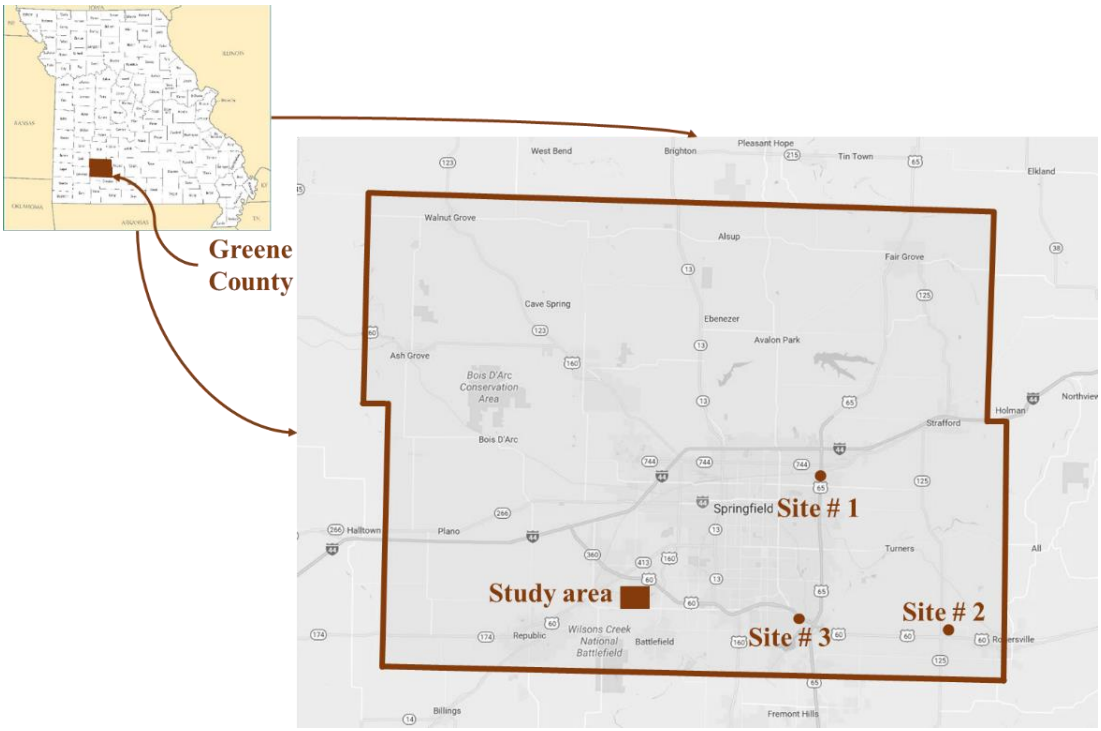

Figure 4.10. The location map of the Site #1, Site #2, and Site #3 relative to the study area

Site #1: At the request of Missouri Department of Transportation (MoDOT) in 2007, a geophysical investigation has been performed to study the near-surface geological formations beneath Highway 65 in the vicinity of the Springfield Underground aggregate mine. Highway 65 is a four-lane, divided highway that runs north and south over three east-west oriented tunnels that connect Springfield Underground facilities on either side of the highway. ERT data have been acquired along four parallel north-south traverses on the surface. ERT data have also been collected along two east-west traverses on the rock ceiling of the southernmost cross tunnel (Figure 4.11).

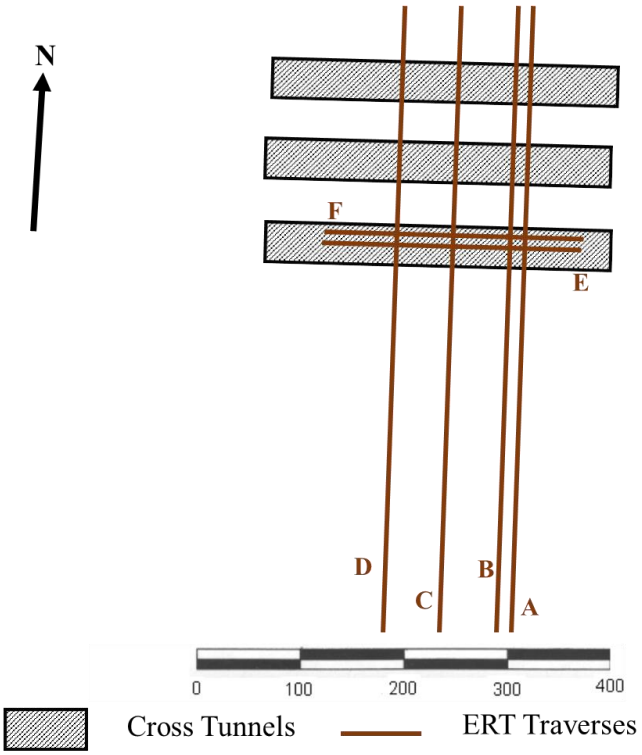

Figure 4.11. Layout of ERT traverses at site #1 [Modified after 59]

Figure 4.12 illustrate the result of ERT modeling in site #1. Authors have interpreted several near-vertical dissolution-enlarged joints or faults from ERT models that oriented approximately north-south and east-west, respectively. However, the orientation of identified features in site #1is not certain due to limited number of boring control and variation of geological features between ERT profiles.

Site #2: ERT data have been acquired at site #2 with the intent of locating any and all substantive air-filled cavities. Dissolution-enlarged fractures have been also studied, because it is anticipated that above mentioned cavities would have developed along these fractures. ERT data have been acquired along two grids of traverses: gird "1A" and grid "1B". Gird "1A"involves 11 west-east oriented traverses spaced at 25 ft. intervals and grid "1B" consists of 8 west-east oriented traverses spaced at 10 ft. intervals (Figure 4.13).

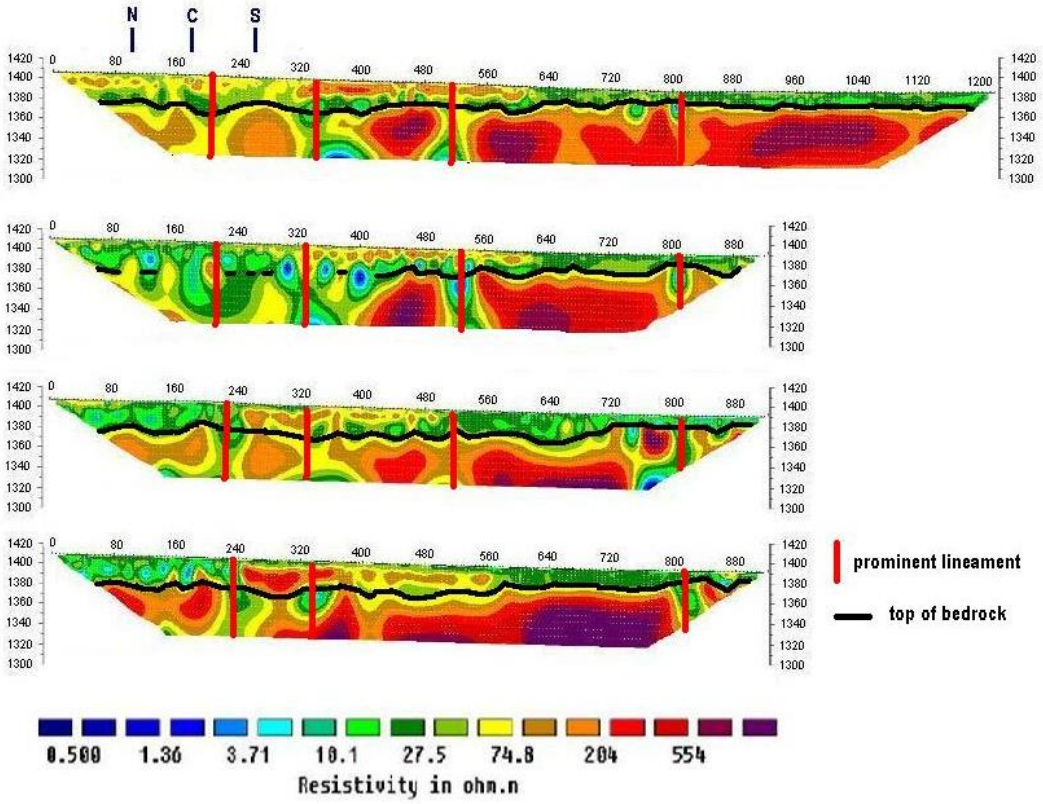

Figure 4.12. Interpreted electrical resistivity Profiles A, B, C, and D at site #1 [Adopted from 59]

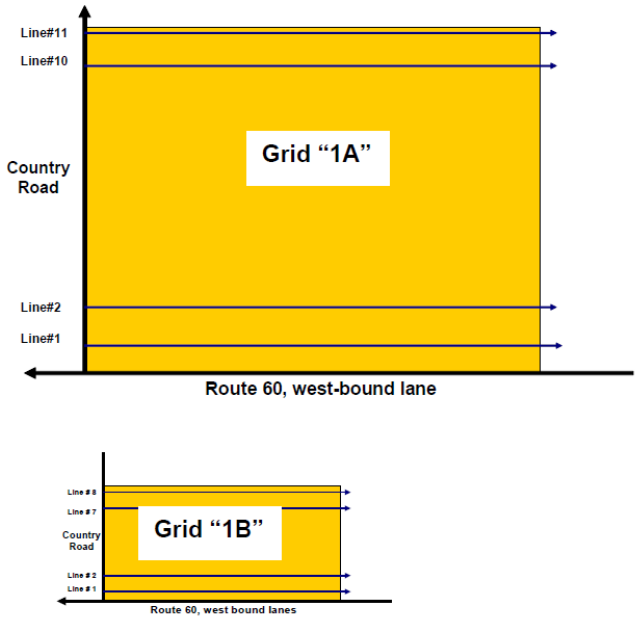

Figure 4.13. Layout of ERT traverses at site #2 [Adopted from 60]

Figure 4.14 illustrate the result of ERT modeling in site #2. Authors have interpreted at least four dissolution-enlarged joint sets oriented in north-south. The interpretation of orientation of the dissolution-enlarged fractures in site #2 is more reliable due to relatively dense grid so f ERT traverses.

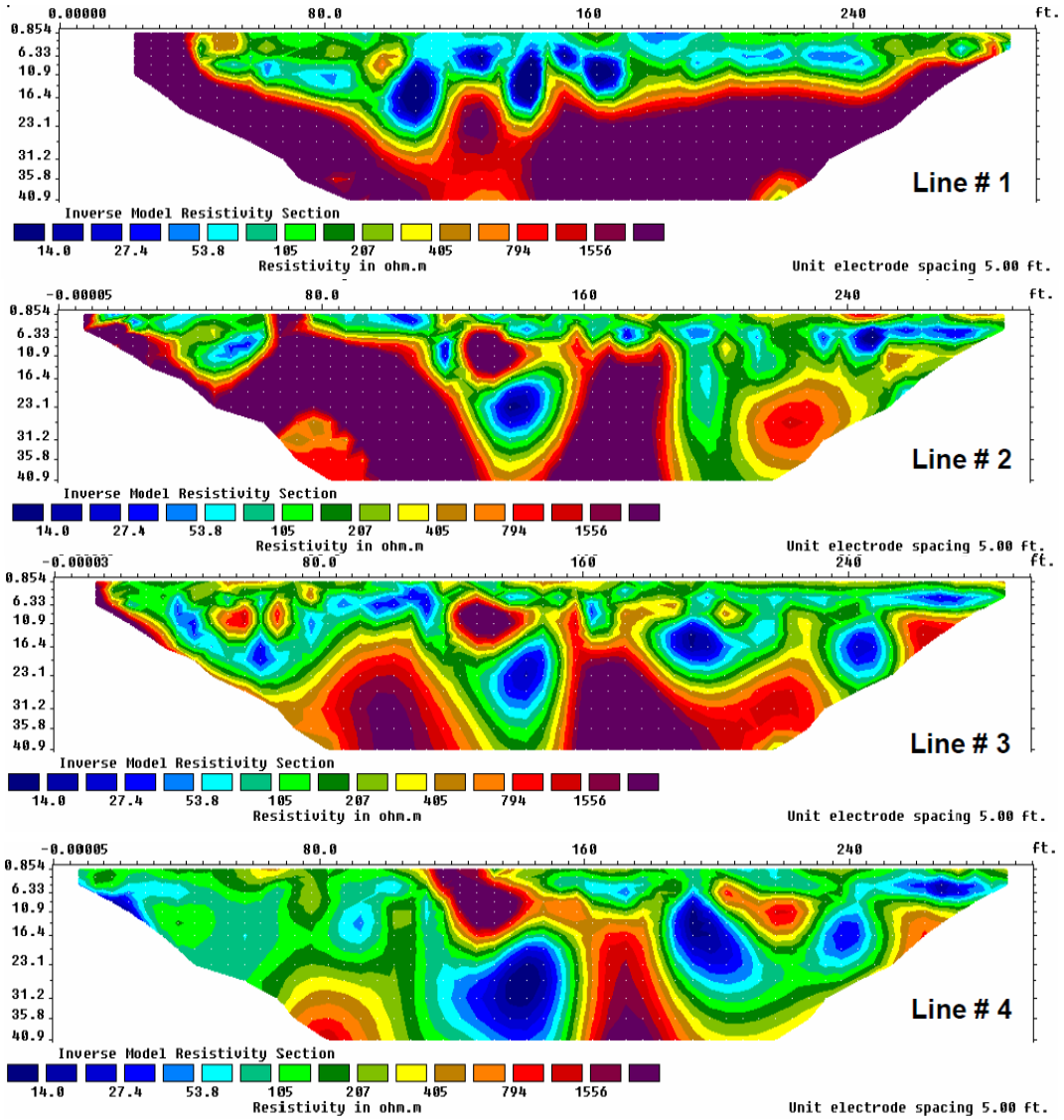

Figure 4.14 Interpreted electrical resistivity lines 1 to 9 of grid "1A" at site #1 [Adopted from 60]

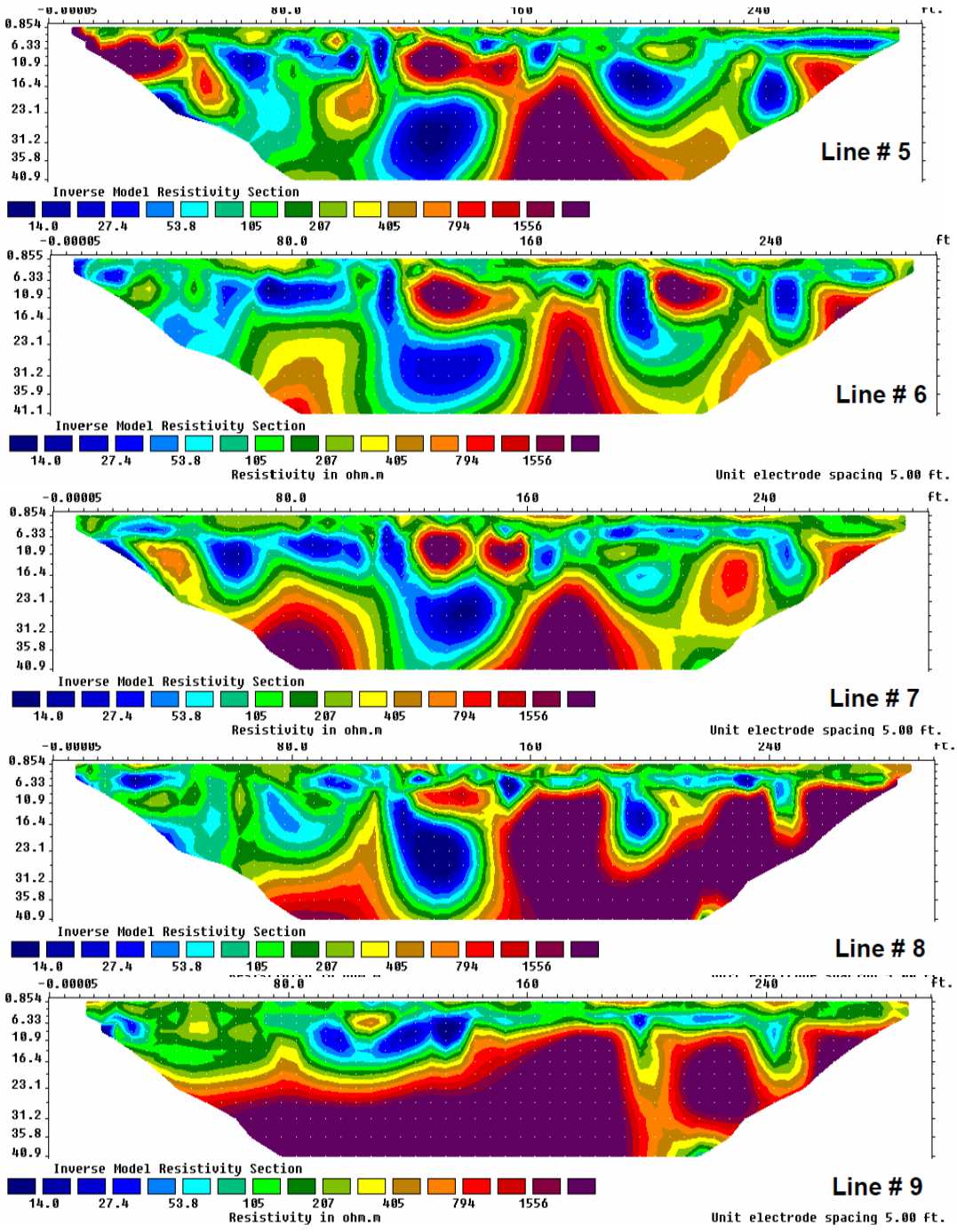

Figure 4.14 Interpreted electrical resistivity lines 1 to 9 of grid "1A" at site #1 [Adopted from 60] (cont.)

Site #3: A geophysical investigation has been carried out at site #3 to first study the air-filled cavities of probable karstic origin and dissolution-enlarged fractures. ERT data have been acquired along 6 parallel traverses. Figure 4.15 depict the layout of ERT traverses at site #3.

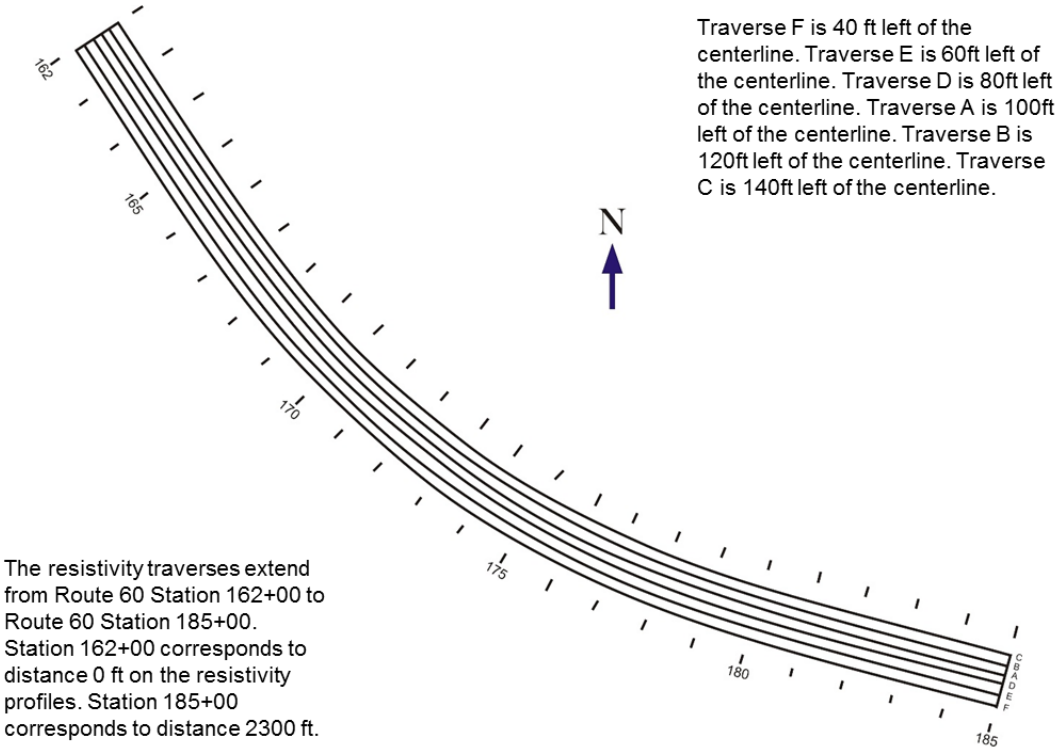

Figure 4.15. Layout of ERT traverses A, B, C, D, E, F at site #3 [Adopted from 61]

Figure 4.16 illustrate the result of ERT modeling in site #3. Authors have interpreted two primary sets of near orthogonal dissolution-enlarged joint sets oriented north-south and east-west.

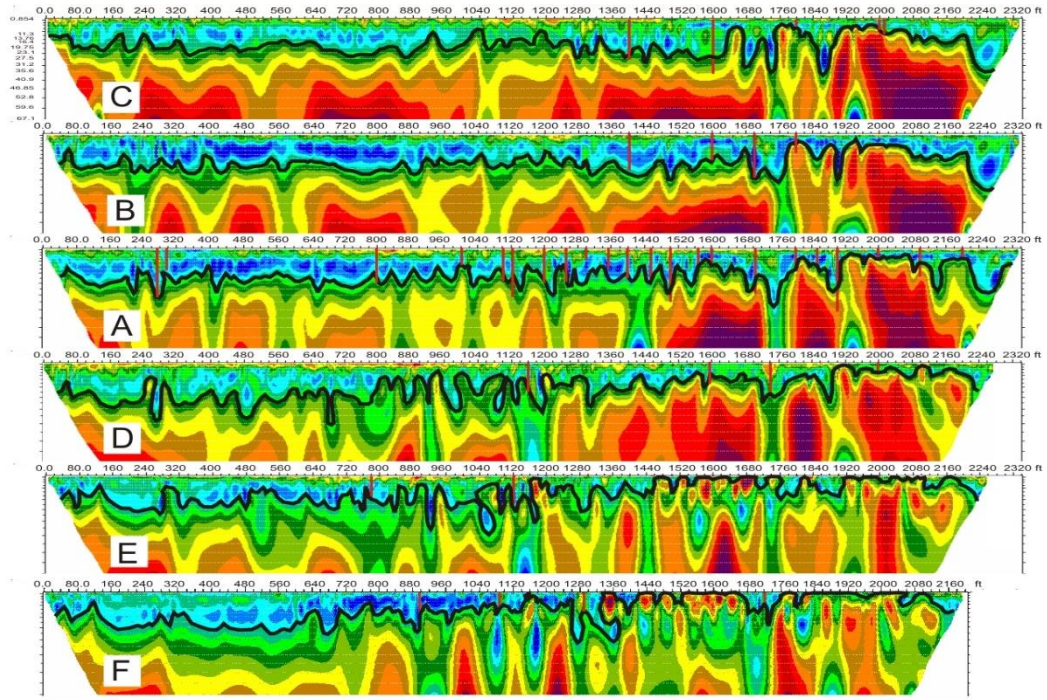

Figure 4.16. Interpreted electrical resistivity Profiles C, B, A, D, E and F at site #3 [Adopted from 61]

5. CONCLUSIONS

Electrical resistivity tomography (ERT) was used to image the subsurface in a karst terrain. This research study was limited to the study of the jointing pattern, orientation and density in a karst terrain in Greene County, Missouri. However, the theoretical underpinning of this study can be applied to other karst environments and features.

Two sets of visually prominent orthogonal joints have been identified in the investigation site: the north-south trending joint sets, and the west-east trending joint sets. The north-south trending joint sets are more prevalent in the investigation site, with a density of approximately one pre hundred feet. The density of the west-east trending joints sets is approximately one per two hundred feet.

A number of joint sets were identified, however aerial photographs of the investigation site revealed that most of the visually prominent joint sets are associated with either cultural features that concentrate runoff, natural surface drainage features, natural surface drainage features or confirmed sinkholes. Over half of the identified visually prominent joint sets are culturally influenced and more than 80% are definitely cultural or drainage influenced.

Furthermore, the soil-rock contacts were determined from interpreting ERT data. The variation of the interpreted soil-rock contacts in the investigation site was compared to the interpreted prominent joint sets in the study area. A good correlation was found between the orientation of joint sets and interpreted soil-rock contact variation.

The Multi-channel Analysis of Surface Wave (MASW) method and coring were employed to validate the interpretation results. A comparison between interpreted soil-rock contact from MASW data and ERT data revealed that 84% of the data points have a

difference less than 5 ft. While only 4.4% of data have a difference larger than 10 ft. The same comparison between the interpreted soil-rock contact from ERT data and cores revealed that 80% of the data points have errors less than 5 ft. And Only 6.6% of data have errors larger than 10 ft. It should be noted that different parameters have been used to estimate the top-of-rock form MASW data, ERT data, and core holes while interpreting the errors.

A statistical analysis was performed on the extracted data from both the interpreted resistivity data and boring data. A relatively good correlation was found between the interpreted resistivity units and their geotechnical properties. However, further information about the moisture and clay content is required to confidently describe the geotechnical properties of the soil and rock in the study area. In addition, the quality of rock might varies horizontally between the cores which could result to a different correlation between the resistivity and RQD. Moreover, both MASW data and boring information show that the quality of rock increases with depth. The main reason is rock weathering. Shallow rock is generally weathered and weaker, while rock at depth are non-weathered and in overall less fractured.

Three dimensional electrical resistivity tomography surveys were undertaken at a section of the investigation site, for the purpose of validating the interpreted results from two dimensional ERT data. Both the horizontal and vertical sections of 3D inverted ERT data indicate north-south trending joint sets.

In addition, results were compared to those of three other geophysical investigations near the study area as follows:

In site #1, a geophysical investigation has been performed to study the near-surface geological formations in the vicinity of an underground aggregate mine. ERT data have been acquired along four parallel north-south traverses and two west-east traverses. Authors have interpreted several north-south and west-east trending joint set in site #1.

ERT data have been acquired at site #2 with the intent of locating any and all substantive air-filled cavities. Authors have interpreted at least four north-south trending joint sets in site #2.

Another geophysical investigation has been carried out at site #3 to study the air-filled cavities of a probable karstic origin. Authors have interpreted two near orthogonal joint sets oriented north-south and east-west.

This PhD research contributes to knowledge and frontier advances in applying the electrical resistivity tomography method to study dissolution-enlarged fractures. This is the first attempt to study the geometry of dissolution-enlarged fractures. The large scale of the investigation (352,015 linear feet of ERT data have been acquired, and MASW data have been acquired at 181 locations) resulted in a reliable interpretation of the pattern, orientation, and density of the joint sets. The new knowledge provides a potential basis for developing geotechnical design methods based on subsurface explorations. It also contributes to understanding the karst development processes.

MASW data and core holes data have been used to validate the research results. The coring data include the soil and rock types and RQD. Electrical resistivity of rocks is influenced by other parameters such as moisture and clay contents. It is recommended, therefore, to further study the relationship between other geotechnical and hydrological

parameters of soil and rock and their electrical resistivity. Knowing this relationships improve the reliability of ERT data interpretations.

The interpretation of geophysical models is highly subjective because of our incomplete knowledge of the subsurface, non-unique processing solutions, and the variation of model resolution. It is thus beneficial to examine multiple geophysical methods to investigate an area of interest. However, joint interpretation studies have been mostly carried out in a qualitative and descriptive manner, as in our study. Further studies are required to enhance the work carried out in this study by employing more objective techniques for integrated interpretation of geophysical models.

APPENDIX A
FRACTURE CRITERIA

In a typical rock deformation experiment, a piece of rock is cut into a cylinder with a diameter ranging from less than 1 centimeter to tens of centimeters in some cases, and a length typically two to four times the diameter. The sample is placed between two pistons of hardened steel or similar material, which are forced together by a device such as a hydraulic ram. The axial stress on the sample is then increased until the sample fails, and the experiment provides data on the stress state required to cause failure [22].

Failure of a sample occurs when the sample is unable to support a stress increase without permanent deformation. The stress at which failure occurs is a measure of the strength of the material. Because failure can occur in a number of different ways, there are a variety of different measures of material strength. Brittle failure occurs with the formation of a brittle fracture, which is a surlace or zone across which the material loses cohesion, that is, it breaks apart. Ductile failure occurs when the material deforms permanently without losing cohesion.

Experiments on brittle failure reveal two fundamentally different types of fracture: extension fractures and shear fractures. These two fracture types mimic natural fractures in rocks. Each type is characte1ized by a different direction of displacement relative to the fracture surface and a different orientation of the fracture plane relative to the principal stresses.

For extension fractures (Figure 1.a, b, c), the fracture plane is perpendicular to the minimum principal stress $\hat{\sigma}_3$ and parallel to the maximum principal stress $\hat{\sigma}_1$• Displacement is approximately normal to the fracture surface. Extension fractures are tension fractures (Figure 1.a) if the minimum principal stress $\hat{\sigma}_3$ is tensile, as in uniaxial tension. They form by longitudinal splitting (Figure 1.b) if the minimum principal stress is equal or close to

zero and the maximum compressive stress $\hat{\sigma}_1$ is the axial stress, as in uniaxial compression. Fractures that form by longitudinal splitting tend to be more irregular in orientation and shape than other extension fractures. Extension fractures may also form under conditions of extensional stress (Figure 1.c) in which the unique axial stress is the minimum compressive stress $\hat{\sigma}_3$.

Shear fractures form in confined compression at angles of less than 45° to the maximum compressive stress $\hat{\sigma}_1$ (Figure 1.d). Displacement is parallel to the fracture surface. If the state of stress is triaxial, the shear fractures are parallel to the intermediate principal stress $\hat{\sigma}_2$, and the fracture planes form a conjugate pair of orientations at angles less than 45° on either side of the maximum compressive stress $\hat{\sigma}_1$. If $\hat{\sigma}_2 = \hat{\sigma}_3$, the possible orientations of shear fractures are tangent to a cone of less than 45° about the $\hat{\sigma}_1$ axis.

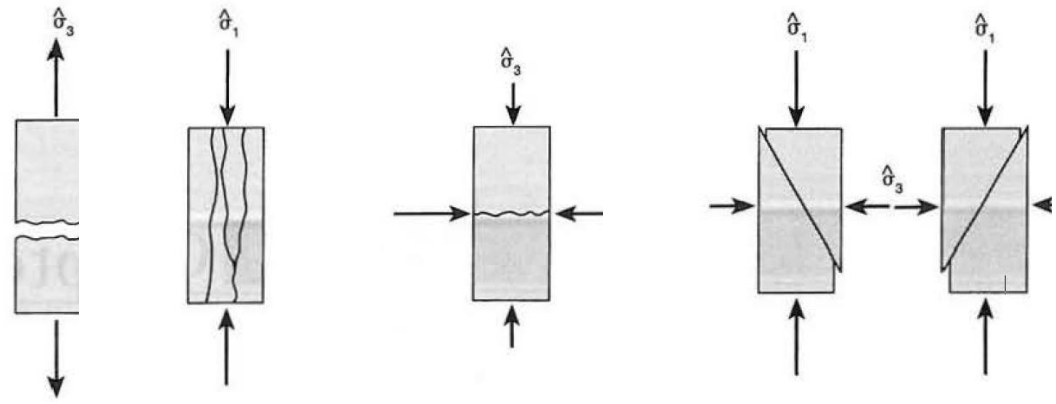

a. Tension fracture

b. Longitudinal splitting

c. Extension fracture

d. Conjugate shear fracture

Figure 1. Types of fractures during experiments on brittle rock [Adopted from 25]

A fracture criterion for tension fractures [22]**:** Experiments on rocks under uniaxial tension show that, for each rock type, there is a characteristic value of tensile stress (T_0) at which tension fracturing occurs. A rock is stable at tensile stress smaller than T_0 , but it cannot support larger tensile stresses. T_0 is the tensile strength of the material. Figure 2 shows a Mohr diagram. In Mohr diagram, horizontal axis is the value of the normal stress (σ_n) and the vertical axis is the value of shear stress (σ_s). The boundary between stable and unstable states of tensile stress is called the tension fracture envelope (Figure 2.a). It is a line perpendicular to the σ_n axis at T_0 and is represented by the equation

$$\sigma_n^* = T_0 \qquad (1)$$

where σ_n^* is the critical normal stress required to produce fracture. A Mohr circle that lies to the right of the line represents a stable stress state (Figure 2.a). A Mohr circle tangent to the line (a critical Mohr circle) represents a state of stress that causes tension fracturing (Figure 2.b). Mohr circles that cross the line represent unstable states of stress that the material cannot support (Figure 2.c).

We can describe the orientation of a fracture plane relative to the principal stresses by the fracture plane angle α_f, which is the angle between the maximum principal stress $\hat{\sigma}_1$ and the fracture, or by the fracture angle θ_f, which is the angle between the maximum principal stress $\hat{\sigma}_1$and the normal to the fracture plane. For a given plane, $|\alpha_f - \theta_f| = 90^\circ$, and if both angles are acute, they are opposite in sign.

In experiments, the tension fracture plane is normal to the maximum tensile stress $\hat{\sigma}_3$. Thus the fracture plane angle α_f is 0° and the fracture angle θ_f is 90° (Figure 2.d). On the Mohr diagram (Figure 2.e), the stress on the fracture plane plots at an angle of $2\theta_f =$

180° from $(\hat{\sigma}_1, 0)$. The normal stress and shear stress components on the fracture plane thus plot exactly at the point of tangency between the critical Mohr circle and the tension fracture envelope.

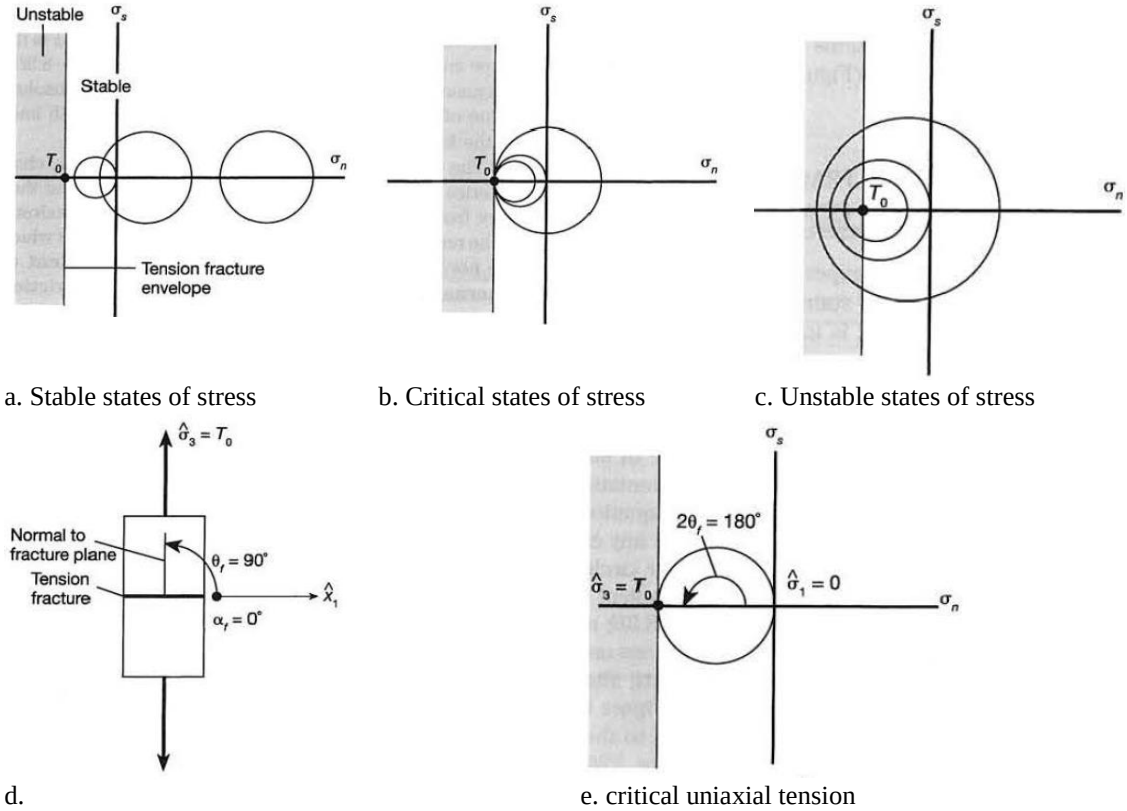

a. Stable states of stress b. Critical states of stress c. Unstable states of stress

d. e. critical uniaxial tension

Figure 2. Fracture criterion for uniaxial tension [Adopted from 22]

According to above fracture criterion, therefore, a tension fracture forms on any plane in the material on which the normal stress reaches the critical value T_0, and the fracture plane is perpendicular to the maximum tensile stress $\hat{\sigma}_3$. This fracture criterion, however, applies only to tension fractures formed under conditions of tensile stress. It does

not account for the occurrence of extension fractures that develop under conditions in which none of the principal stresses are tensile such as longitudinal splitting.

The Coulomb fracture criterion for confined compression [22]**:** In confined compression experiments, the relationship between the state of stress and the occurrence of shear fracturing is more complicated than for uniaxial tension. Fracture experiments on different samples of the same rock show that the initiation of fracturing depends on the differential stress ($\sigma^{(Dif)} = \hat{\sigma}_1 - \hat{\sigma}_3$) and that the magnitude of the differential stress necessary to cause shear fracture increases with increasing confining pressure. The fracture angle θ_f between $\hat{\sigma}_1$ and the normal to the fracture plane is generally around $\pm 60^{\circ}$, so the fracture plane angle α_f between the fracture plane itself and the maximum compressive stress $\hat{\sigma}_1$ must be about $\pm 30^{\circ}$ (Figure 1.d).

Experimental data show that it is possible to construct on the Mohr diagram a shear fracture envelope that separates stable from unstable states of stress. This envelope commonly approximates a pair of straight lines that are symmetric across the σ_n axis (Figure 3.a-c), although in fact the lines may be slightly concave toward that axis. Any Mohr circle contained between the two lines of the fracture envelope represents a stable stress state (Figure 3.a). A Mohr circle tangent to the lines represents a critical state of stress that causes fracturing (Figure 3.b). A Mohr circle that crosses the fracture envelope represents an unstable state of stress that cannot be supported by the material (Figure 3.c); before the Mohr circle reaches this state, fracturing would already have occurred. On any critical Mohr circle, the points of tangency with the shear fracture envelope (Figure 3.b) indicate the surface stress components on the actual fracture plane at the time of fracture.

The straight line approximation to the shear fracture envelope is the *Coulomb fracture criterion*, and it states that the critical shear stress $|\sigma_s^*|$ is equal to a constant *c* plus the tangent of the slope angle ϕ of the line times the normal stress σ_n, or

$$|\sigma_s^*| = c + \mu\sigma_n \qquad (2)$$

where

$$\mu = \tan\phi \qquad (3)$$

and where σ_s^* is the critical shear stress; μ and *c* are the slope and intercept of the lines, respectively; and ϕ is the slope angle of the line, taken to be positive (Figure 3.b). Because the equation is written in terms of the absolute value of the critical shear stress, it describes both lines of the fracture criterion.

The Coulomb fracture criterion states that whenever the state of stress in a rock is such that on a plane of some orientation, the surface stress components (σ_n, σ_s) satisfy Equation (2), that plane can become a shear fracture. For any critical stress state, there are two points on the Mohr circle at angles of $\pm 2\theta_f$ from $\hat{\sigma}_1$ where the circle is tangent to the two lines given by Equation (2) (Figure 3.b; note that $2\acute{\theta}_f = -2\theta_f$). These points define the stresses on two differently oriented planes called the conjugate shear planes (Figure 3.d, e). On the Mohr circle (Figure 3.b), the angles between the σ_n axis and the radii to the points of tangency with the fracture criterion are $\pm 2\theta_f$. Thus in physical space, the normals to the two coajugate shear fractures must be at angles of $\pm\theta_f$ to the $\hat{x}_1$ axis (and to $\hat{\sigma}_1$), and the fracture planes themselves make an angle of $\pm\alpha_f$ with $\hat{\sigma}_1$ (Figure 3.d, e). The fracture criterion does not predict which orientation of fracture should actually form.

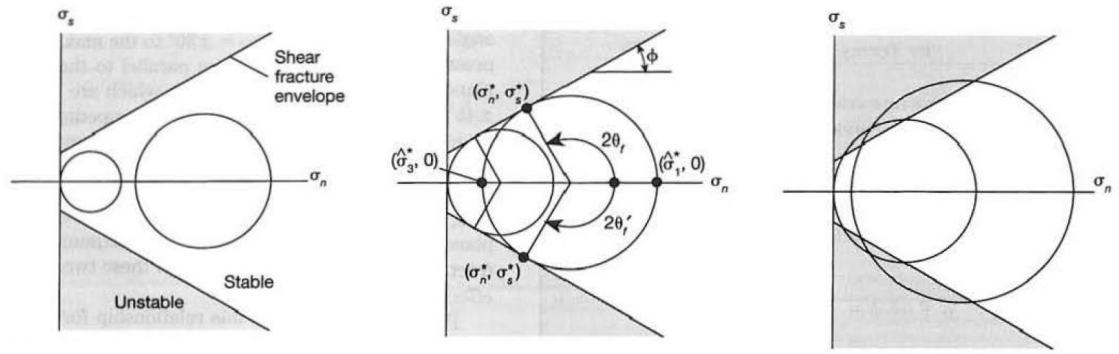

a. Stable states of stress b. Critical states of stress c. Unstable states of stress

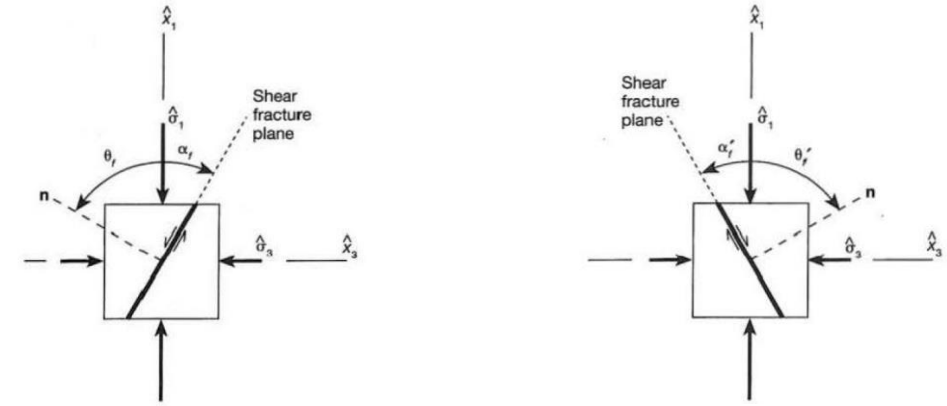

d. e.

Figure 3. Coulomb fracture criterion for axial compression [Adopted from 22]

On the Mohr circle, the radius to the tangent point must be perpendicular to the fracture envelope, so the angles θ_f and α_f are related to the slope angle of the fracture envelope ϕ by the following equations:

$$\left|2\theta_f\right| = (90 + \phi) degrees = \left(\frac{\pi}{2} + \phi\right) radians$$

(4)

$$\left|2\alpha_f\right| = (90 - \phi) degrees = \left(\frac{\pi}{2} - \phi\right) radians$$

Thus the fracture envelope defines both the critical stress required for fracture and the orientation of the shear fracture that develops.

APPENDIX B

FRACTURES AND FRATURING

Fractures are the most common geologic features and hardly any outcrops of rock exist that does not have some fractures through it. Fractures are surfaces along which rocks have broken. Fractures are distinguished by the relative motion that has occurred across the fracture surface during formation [22].

*Extension fractures***:** For extension fractures, or Mode I fractures, the relative motion is perpendicular to the fracture walls (Figure 1.a).

*Shear fractures***:** For shear fractures the relative motion is parallel to the surface. For mode II shear fractures, the motion is a sliding motion perpendicular to the edge of the fracture (Figure 1.b); for mode III shear fractures, it is a sliding motion parallel to the fracture edge (Figure 1.c).

*Mixed mode fractures***:** Mixed mode fracture or oblique extension fracture has components of displacement both parallel and perpendicular to the fracture surface.

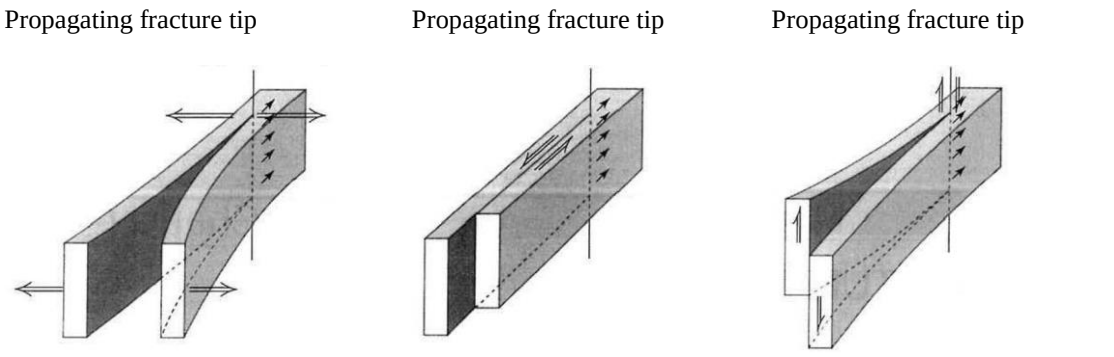

Figure 1. Major types of fractures based on relative displacement of the material on opposite side of the fracture [Adopted from 22]

Joints: fractures that shows very small displacement normal to their surfaces and no, or very little, displacement parallel to their surfaces. If there is no shear displacement, a joint is an extension fracture. A joint with very small shear displacement, however, may be an extension fracture on which shear displacement has later accumulated.

Joint set: If many adjacent joints have a similar geometry, the fractures collectively are called a Joint Set.

Systematic joints: Systematic joints are characterized by roughly planar geometry, regular parallel orientations, and regular spacing.

Nonsystematic joints: Nonsystematic Joints are curved and irregular in geometry, although they may occur in distinct sets of regional extent. Nonsystematic joints nearly always terminate against older joints which commonly belong to a systematic set. Because most joints we see are systematic, the term joint is generally used to refer to them.

Joint zone: A joint Zone is a quasi-continuous fracture that is composed of a series of closely associated parallel fractures and that extends much further than any of the individual fractures. In practice, such a joint zone is also called simply a joint.

Joint system: Most outcrops contain more than one set of joints, each with a characteristic orientation and spacing. Two or more joint sets affecting the same volume of rock constitute a joint system.

Cross joints: If systematic joints of one set consistently terminate against the joints of another set, they are referred to as cross joints. Joints that cut a fold or some other linear feature at high angles are also called cross joints, and those in other orientations are Oblique Joints or Diagonal Joints.

Strike joints: Strike joints are vertical joints parallel to the strike of the bedding.

Dip joints: Dip joints are vertical joints parallel to the dip of the bedding

Bedding joints: Bedding joints are parallel to the bedding.

Sheet joints: Sheeting, or exfoliation joints, are curved extension fractures that are subparallel to the topography and result in a characteristic smooth, rounded topography. Sheet joints may be found in many kinds of rocks, but the characteristic topography is best displayed in plutonic rocks in mountainous regions where the joints appear to cut the rock into sheets like the layers of an onion. Many sheet joints apparently formed later than other joints sets, although is some cases they predate late phase of intrusive activity, as evidenced by dikes present along the joints.

Columnar joints: Columnar joints are extension fractures characteristics of shallow tabular igneous intrusions, dike or sills, or thick extrusive flow. The fractures separate the rock into roughly hexagonal or pentagonal columns, which are often oriented perpendicular to the contact of the igneous body with surrounding rock.

Veins: Veins are extension fractures that are filled with mineral deposits. The deposit may be massive or composed of fibrous crystal grains such as quartz or calcite. The fibrous filling can be very useful in interpreting the deformation associated with opening of the vein.

Pinnate fractures: Pinnate fractures, or Feather fractures, are extension fractures that form *en echelon* array along brittle shear fractures (Figure 2). The acute angle between the extension fracture and the fault plane is a unique indicator of the sense of shear along the fault, and it points in the direction of relative motion of the block containing the fractures.

Gash fractures: Gash fractures are extension fractures, usually mineral-filled, that may form along zones of ductile shear in the same orientation as the pinnate fractures. They are generally S- r Z-shaped, depending on the sense of shear along the zone. The orientation of planar gash fractures can be used in the same way as feather fractures to determine the sense of shear on the associated shear zone.

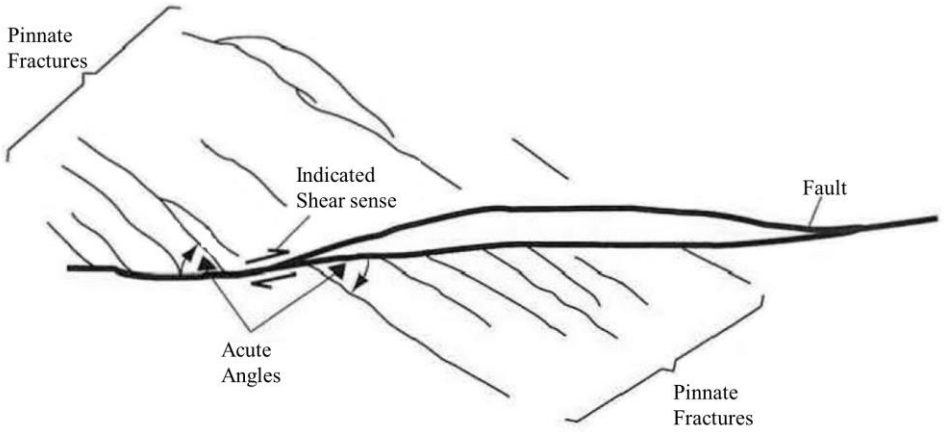

Figure 2. Pinnate fractures, or feather fractures, in an *en echelon* array along a brittle fault. The sense of rotation through the acute angle from the fault plane to the pinnate fracture plane has the same sense as the shear sense on the fault (clockwise in this case) [Adopted from 22]

Fractures associated with faults [22]: Fractures often form as subsidiary features spatially related to other structures. In some cases, faults are accompanied by two sets of small-scale shear fractures at an angle of approximately 90° to each other with opposite senses of shear. These are called conjugate shear fractures. Figure 3 shows data for a system of conjugate fractures that developed in an area closely associated with a known fault. The rose diagram shown in Figure 3.b is plotted in the vertical plane normal to the strike of the

fault, and the distribution of fracture dips is plotted below the horizontal line. The orientation of the fault is also indicated on the figure. The major set of fractures is clearly parallel to the fault; the second and less well developed set is approximately 65° from the first set. Extension fractures associated with faulting include pinnate fractures and gash fractures, which were described above.

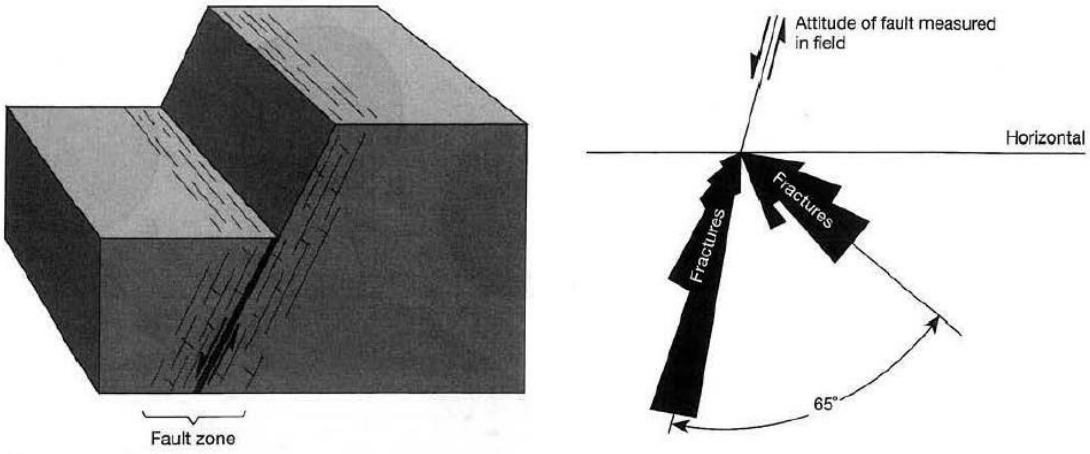

a. Normal fault with dominant parallel shear fractures (long lines) and subordinate conjugate shear fractures (short lines)

b. Rose diagram plotted in the vertical plane, showing the distribution of dips of two sets of fractures associated with a normal fault

Figure 3. Shear fractures associated with faulting [Adopted from 22]

Fractures associated with folds [22]: Fracture often develop in rocks in association with folding. A variety of orientations, related symmetrically to the fold, have been reported. Figure 4 is a diagrammatic illustration of the orientations of fractures that have been reported from folds. It is convenient to refer the orientations to an orthogonal system of coordinates (a, b, c) related to the fold geometry and bedding. The b axis is parallel to the fold axis, which in general is the line about which the bedding planes are

folded. A line parallel to the fold axis is parallel to the bedding regardless of where on the fold it lies. Thus the b axis has a constant orientation for all the (a, b, c) axes. The c axis is everywhere perpendicular to the bedding and the a axis lies in the bedding plane perpendicular to the fold axis (b) and the c axis.

Fractures parallel to the plane of the a and c axes and to the plane of the b and c axes are called ac fractures and bc fractures, respectively. The fractures shown in sets A, B, and D are all perpendicular to the bedding. In sets A and B, the ac fractures and the bc fractures, respectively, bisects the acute angle between the two other fracture sets, which are oblique fractures. In set D, the fractures bisects the obtuse angle between the oblique fractures. The inclined fractures in sets C and E are parallel to the fold axis b. Those in set C make a low angle with bedding, and those in set E make a high angle with bedding.

Fractures in sets A and D are particularly common on fold limbs. Sets B and E tend to be associated with the convex sides of a fold where the curvature is strongest. And set C occurs on the strongly curved concave side of folds.

It is possible that the fractures of all these orientations formed in association with folding, that the ac and bc fractures are extension fractures, and that the oblique and inclined fractures are shear fractures. That interpretation is not justified, however, simply on the basis of fracture pattern and orientation. Such fractures have been shown to predate the folding in some cases, and to postdate it in others, and as we have remarked before, the presence of shear displacement on a fracture does not necessarily mean that the fracture originated as a shear fracture. In order to make a well-documented interpretation of complex fractures systems, it is critical to describe all the characteristics of the various fracture sets that we have discussed. This includes citing specific evidence for extensional

or shear displacement and fracturing, the spatial distribution of fractures, and evidence suggesting the relative sequences of formation of the fractures in different sets.

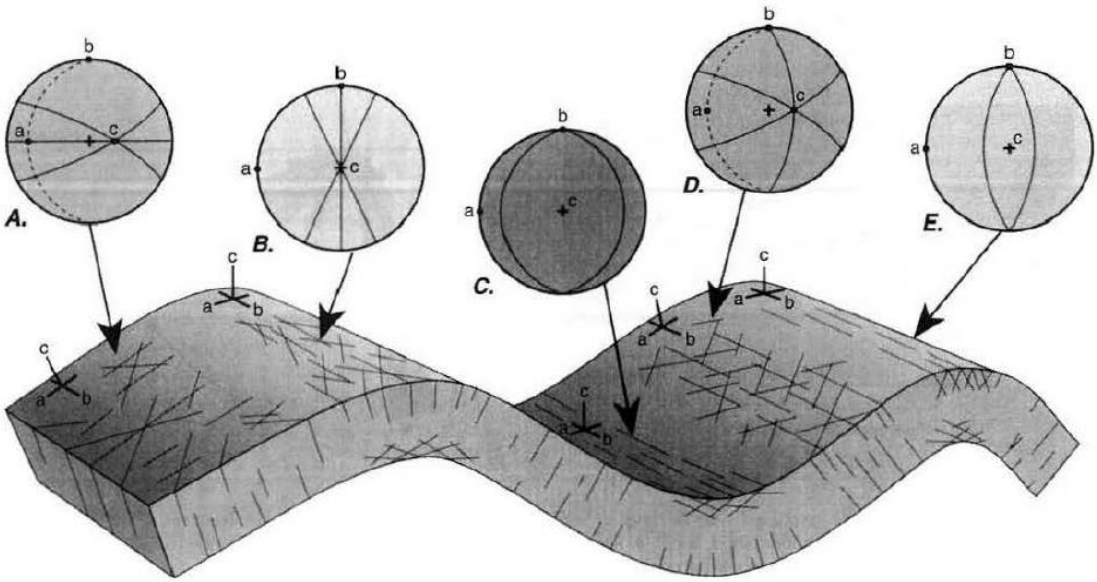

Figure 4. Fractures associated with folds. The stereographic projections show the orientation of the reference coordinate system (a, b, c), the bedding where it is not horizontal (dotted great circles), and the fractures (solid great circles) [Adopted from 22]

Fractures associated with igneous intrusions [22]: Fractures form an association with intrusions, and some types occur only within the igneous rock. In many cases, the internal structure of plutonic rocks is related in a simple manner to the orientation of other fractures that develop. Especially near the margins of plutonic bodies, platy minerals such as mica and tabular mineral grains may be aligned parallel to one another, creating a planar structure in the rock called a foliation. Elongate mineral grains also may be aligned parallel to one another within the foliation, creating a linear structure called a lineation.

Stress histories and the origin of joints:

The study of geologic history of fractures is notoriously difficult. Evidence bearing on the mode of fracture formation and relative time of formation of different fractures is often ambiguous. As planes of weakness in the rock, fractures are subject to reactivation in later tectonic events, so some of the observable features of a fracture may be completely unrelated to the time and mode of its formation [22].

A wide variety of mechanisms induct and change the stress condition in the Earth's crust and therefore fractures have numerous origin. All stresses that have been measured directly in the Earth are compressive; true tensile stresses are rare. For extension fractures to form, therefore, two conditions must be met. Pre fluid pressure must be large enough for the effective minimum principal stress to become tensile, and the differential stress must be small enough so that, at the critical pore fluid pressure, extension fractures form rather than shear fractures. It is probable that hydrofracture in rocks should often result in extension. Stress arises in the Earth because of the overburden, the driving mechanisms of plate tectonic processes, horizontal and vertical motions, changes (over space and time) in temperature and pressure, the inhomogeneous mechanical properties of the crust, and pore fluid pressure. Possible origin of fractures can be explained by models of loading histories. A summary of possible loading histories that form the joints are discussed in the following:

Joint formation during burial [22]: In tectonically quiescent sedimentary basins, at depths less than about 3 km, measures fluid pressure are generally not greater that hydrostatic pressure, which suggest that flow of fluid throughout the rock is unrestricted above that level. With increasing depth of burial, flow becomes restricted, and compaction and equathermal pressuring can increase the fluid pressure more rapidly than the minimum compressive stress increases. Eventually hydrofracture results.

Joint formation during uplift and erosion [22]**:** During uplift and erosion, we assume that the principal stress are horizontal and vertical and that the vertical stress equals the overburden. The vertical normal stress decreases as the overburden diminishes, and the temperature also decreases. The change in horizontal stress component during uplift determine whether jointing occurs in this phase of the rock history. The important factors determining horizontal stresses are the Poisson and thermal affects, which tend to counteract each other, and bending stresses.

If the rock behave as an elastic material, the Poisson effect predicts that a decrease in the vertical load will cause extension in the vertical direction and contraction in the horizontal direction. The rocks are not free to change horizontal dimensions, however, so the horizontal components of stress decrease sufficiently to offset exactly the Poisson contraction.

Thermal contraction of the rock associated with a decrease in temperature, however, competes with and commonly overwhelms the Poisson effect. Because the rocks cannot change horizontal dimensions, the horizontal compressive stress decrease by an amount that exactly offset the thermal contraction.

The net effect of most conditions of uplift and erosion is that horizontal stress becomes the minimum compressive stress, and the vertical stress the maximum compressive stress. As long as one of the horizontal effective stresses is tensile, however, vertical joints that are normal to that stress component can form. Again, the effect of the pore fluid pressure plays a critical role in producing an effective tensile stress in a compressive stress regime. The development of one set of vertical joints relived the effective tensile stress normal to those joints. If the other horizontal principal effective

stress is tensile, then it becomes the maximum effective tensile stress, and a second set of vertical joints may form orthogonal to the first set. Such systems of orthogonal vertical joints are a common feature, for example, of the flat-lying sediments in the midcontinent region of the United States.

Tectonic joints [22]: If tectonic stress are imposed on a rock during burial, then compaction and restriction of the pore fluid circulation may occur at shallower depth than is possible under lithostatic loading. The resulting high pore fluid pressure can cause hydrofracturing at depths. Tectonic stresses can, of course, affect rocks during uplift as well as during burial. Such stresses can govern the orientation of new joints by changing the value of one of the horizontal components of stress. If a horizontal stress became the minimum compressive stress, and to that were added a horizontal tensile tectonic stress, then vertical joints would form, normal to the tectonic stress. If the horizontal tectonic stress were the maximum compressive stress, vertical joints would form parallel to it.

Sheet joints [22]: Sheet joints are subparallel to the topographic surface. Either the topography controls the orientation of the sheet joints, or the orientation of the sheet joints is controlled by preexisting stresses in the rock, and the joints affect the evolution of the topography.

Under some circumstance, the maximum compressive stress can remain horizontal and the minimum compressive stress vertical during uplift, as might result if a tectonic compression were applied. As the vertical stress approaches zero, horizontal joints could propagate in a manner similar to longitudinal splitting. The topography would affect the local orientation of the stress field, because the topographic surface is a free surface that must be a principal surface of stress. Thus the principal stresses locally must be

perpendicular or parallel to the topography. This model predicts that the joints should tend to parallel topography.

The alternative hypothesis assumes that topography is controlled by the orientation of joints, which are in turn the result of residual stresses in the rock. For example, in a plutonic igneous body, cooling at depth concentric with the boundary of the pluton could produce residual thermal stresses within the body with the maximum compressive stress subparallel to the boundary. As the minimum compressive stress decreases toward zero during uplift, sheet joining could develop by longitudinal splitting, the orientations of the joints would reflect the shape of the boundary or cooling surfaces in the pluton. Subsequent erosion is controlled by the orientation of the joints. The interpretation of sheet joints is not clear-cut, and both hypothesis could be occur in different cases.

Columnar joints [22]: The polygonal fracture pattern, or columnar joints, that are common features of many igneous extrusions and shallow intrusions probably result from thermal stresses set up by unequal cooling and thermal contraction between the igneous body and the country rock. After solidification, the higher temperature of the igneous rock means that its thermal contraction would be considerably greater than that of the adjacent country rock if the contact were free to slip. A welded contact makes any relative displacement between the two rock masses impossible. In this case, as the two rocks cool, stress build up on both sides of the contact sufficient to prevent displacement along the contact. Normal stress component that are parallel to the contact are tensile in the igneous rock, preventing it from contracting as much as thermal contraction would require; these stress components are balanced by a compressive stress in the country rock, which force it to contract more than thermal contraction would require. In general, the tensile stresses in

the igneous rock become oriented parallel to the isothermal surfaces during cooling. Because rocks are weaker in tension than in compression, the igneous rocks tend to form tensile fractures perpendicular to the surface of equal temperature.

The origin of the hexagonal shape of the columns is not well understood. More than one set of fractures is required to relieve the tensile stress in two orthogonal directions. Such a system of fractures can fill a volume with close-packed fracture-bounded prisms if the prism cross section is triangular, rectangular, or hexagonal. Of these, the hexagonal prisms have the smallest fracture area per unit volume of prism. Thus fracture-bounded prisms with a hexagonal cross section requires less energy to produce than other prism shapes, and this form of columnar joint is dominant. In principle, however, two set of fracture should suffice to relive tensile stresses in two orthogonal directions. Consequently, we do not at present understand mechanisms of development of the three sets of tensile fracture that define the hexagonal prisms

BIBLIOGRAPHY

1. Ford, D.C. and Williams, P., Karst hydrology and geomorphology, John Wiley & Sons, Chichester, England, 2007.
2. Klimchouk, A.B., Ford, D.C., Palmer, A.N., Dreybrodt, W., Speleogenesis. Evolution of karst aquifers, National Speleological Society, Huntsville, Alabama, 2000.
3. Palmer, A.N., Cave geology, Cave books, Dayton, USA, 2007.
4. Palmer, A.N., Origin and morphology of limestone caves: Geological Society of America Bulletin, v. 103, p. 1-21, 1991.
5. McCracken, M.H., Structural features of Missouri: Mo, Geol. Survey and Water Resources, Rept. Inv. 49, vi+100p., 11figs, 1971.
6. Graves, H.B., The Pre-Cambrian structures of Missouri, Transaction of the Academy of Science of St. Louis, v. 29, pp. 111-161, 1938.
7. Ball, S.H. and Smith, A.F., The geology of Miller County, Missouri Bureau of geology and Mines, 2nd series, v. 1, 207 p, 1903.
8. Van Horn, F. B., Geology of Moniteau County, Missouri Bureau of geology and Mines, 2nd series, v. 3, 104 p, 1905.
9. Hinds, H. and Greene, F. C., The stratigraphy of the Pennsylvanian Series in Missouri, Missouri Bureau of geology and Mines, 2nd series, v. 13, 407 p, 1915.
10. Bretz, J. H. , Caves of Missouri, Missouri Geological Survey and Water Recourses, 2nd series, v. 39, 490 p., 1956.
11. Barnholtz, S., Influence of jointing on cavern development in Miller County, Missouri Speleogy, v. 3, n. 4, pp 66-73, 1961.
12. Van Nostrand, R.G. and Cook, K.L., Interpretation of resistivity data, United States Geological Survey professional paper 499, United States government printing office, Washington: 1966.
13. Frankline A.G., Patrick D.M., Butler D.K., Storhm W.E. Jr, Hynes-Griffin M.E, Foundation considerations in siting of nuclear facilities in karst terrains and other areas susceptible to ground collapse, Geotechnical Laboratory, U.S. Army Engineer Waterways Experiment Station (Technical report NUREG/CR-2062), Vicksburg, MS, 1981.
14. Zhou, W., Beck, B.F., Stephenson, J.B., Reliability of dipole-dipole electrical resistivity tomography for defining depth to bedrock in covered karst terranes, Environmental geology, 39 (7), 2000.
15. Branson, E. B., The Geology of Missouri, University of Missouri, Columbia, 1944.
16. Vandike, J.E., Groundwater level data for Missouri: Water year 1991-1992. Missouri Department of Natural Resources. Division of Geology and Land Survey. Water Resource Report No.42. Rolla, Missouri, 1993.
17. Thornbury, W.D., Regional Geomorphology of the United Staes, John Wiley & Sons, Inc., New York. London. Sydney, 2nd edition, 1965.

18. Eardley, A.J., Structural geology of North America, Harper & Brothers publications. New York, 1951
19. Unklesbay, A.G. and Vineyard, J.D., Missouri geology: Three billion years of volcanoes, seas, sediments, and erosion, University of Missouri press, Columbia and London, 1992.
20. Missouri Division of Natural Resource.
21. McCracken, M.H., Major structural features of Missouri, Missouri Department of Natural Resource: Division of geology and land survey, 1966.
22. Twiss, R.J. and Moores, E.M., Structural geology, 2nd edition, W. H. Freeman and Company, New York, 2007.
23. Palmer, A. N. and Palmer, M. V., Cave and Karst of the USA: Missouri, National Speleological Society, Inc., Huntsville, Alabama, 2009.
24. Miller, D.E. and Vandike, J.E., Groundwater resources of Missouri, Missouri state water plan series, Missouri Department of Natural Resources, v. 2, 210 p, 1997.
25. White, W.B., Geomorphology and hydrology of karst terrains, New York: Oxford University Press, 1988.
26. Waele, J.D, Gutierrez, F., Parise, M., Plan, L., Geomorphology and natural hazards in karst areas: A review, Geomorphology, 134 (2001) 1-8.
27. Runkel, A.C., Tipping, R.G., Alexander, E.C., Jr., Green, J.A Mossler, J.H., Alexander, S.C., hydrogeology of the paleozoic bedrock In southeastern Minnesota, Minnesota geological survey, 2003.
28. International Society for Rock Mechanics (ISRM), Commission on Terminology, Symbols and Graphic Representation, Terminology. Int. Soc. Rock Mech. secretary, Lisbon, 1975.
29. Sharma, V.M. and Saxena, K.R., In-Situ characterization of rocks, a. A. Balkema publishers, 2001.
30. Archie, G.E., The electrical resistivity log as an aid in determining some reservoir characteristics, Petroleum Transactions of AIME 146: 54–62. 1942.
31. Reynolds, J.M., An introduction to Applied and Environmental Geophysics, John Wiley & Sons, Chichester, England, 1997.
32. Chalikakis, K., Plagnes, V., Guerin, R., Valois, R., and Bosch, F.P., Contribution of geophysical methods to karst-system exploration: an overview, Hydrogeology Journal (2011) 19: 1169–1180.
33. Griffiths, D.H., Turnbull, J., A multi-electrode array for resistivity surveying, First Break 3(7), 16-20, 1985.
34. Griffiths, D.H., Turnbull, J., Olayinka, A.I., Two-dimensional resistivity mapping with a computer-controlled array, First Break 8(4), 121–129, 1990.
35. Loke, M.H., Barker, R.D., Rapid least-squares inversion of apparent resistivity pseudosections by a quasi- Newton method, Geophysical Prospecting 44, 131–152, 1996.
36. Griffiths, D.H., Barker, R.D., Two-dimensional resistivity imaging and modelling in areas of complex geology. J. Appl. Geophys. 29, 211–226, 1993.

37. Dahlin, T., 2D resistivity surveying for environmental and engineering applications, First Break 14 (7), 275–283, 1996.

38. Pánek, T.A, Margielewski, W., Tábořík, P., Urban, J., Hradecký, J, and Szura, C., Gravitationally induced caves and other discontinuities detected by 2D electrical resistivity tomography: Case studies from the Polish Flysch Carpathians, Geomorphology 123 (2010) 165–180.

39. Frid, V., Averbach, A., Frid, M., Dudkinski, D., and Liskevich, G., Statistical Analysis of Resistivity Anomalies Caused by Underground Caves, Pure and Applied Geophysics, 2015.

40. Zhou, W., Beck, B. F., Adams, A. L., Effective electrode array in mapping karst hazards in electrical resistivity tomography, Environmental Geology 42, 922–928, 2002.

41. Dahlin, T., and Zhou, B., A numerical comparison of 2D resistivity imaging with 10 electrode arrays, Geophysical Prospecting 52, 379–398, 2004.

42. Pelton, W.H., Rijo, L. and Swift, C.M.,Jr., Inversion of two-dimensional resistivity and induced polarization data, Geophysics, 43. 788-803, 1973.

43. Tripp, A.C., Hohmann, G.W. and Swift, C.M., Jr., Two-dimensional resistivity inversion, Geophysics, 49, 1708-1717, 1984.

44. Tong, L.T. and Yang, C.H., Incorporation of topography into two-dimensional resistivity inversion, Geophysics, 55, 354-361, 1990.

45. Shima, H., 2-D and 3-D resistivity image reconstruction using crosshole data, Geophysics, 57, 1270-1281, 1992.

46. Sasaki, Y., Resolution of resistivity tomography inferred from numerical simulation, Geophysical Prospecting, 40, 453-463, 1992.

47. Barker, R.D., A simple algorithm for electrical imaging of the subsurface, First, Break, 10, 53-62, 1992.

48. GeoEngineers, Preliminary geophysical investigation, City Utilities John Twitty Energy Center, Springfield, Missouri, 2015.

49. http://nationalmap.gov/small_scale/printable.html, 1997-2014 Edition of The National Atlas of the United States

50. GeoEngineers, Site Health and Safety plan: Detailed Site Investigation, City Utilities John Twitty Energy Center, Springfield, Missouri, 2014.

51. Middendorf, M. A., Thomson, K. C., Eason, G.L., and Sumner, H. S., Bedrock geologic map of the Springfield 1 degree × 2 degrees quadrangle, Missouri: U.S. Geological Survey, Miscellaneous Field Studies map MF-1830-D, scale 1:250,000, 1987.

52. Martin, J. A. and Prat, W. P., Geology and Mineral Resource Assessment of Springfield 1 °X2° quadrangle, Missouri, As Appraised in September 1985, U.S. Geological Survey Bulletin, 1942.

53. Whitfield, J. W., Ward, R. A., Denne, J. E., Holbrook, D. F., Bush, W. V., Lineback, J. A., Luza, K. V., Jensen, K. M., Fishman, W. D., Richmond, G. M., and Wiede, D. L., Quaternary geologic map of the Ozark Plateau 4 degrees × 6 degrees quadrangle, United States: U.S. Geological Survey, Miscellaneous Investigation Series Map I-1420(NJ-15), scale 1:1,000,000, 1993.

54. Park, C.B., Miller, R.D., Xia, J., Multichannel analysis of surface waves, GEOPHYSICS, v. 64, n. 3, pp. 800–808, 1999.

55. Park, C.B., MASW: Horizontal Resolution in 2D Shear-Velocity (Vs) Mapping, Kansas Geological Survey open file report, 2005.

56. Anderson, N.L., MASW and GPR lecture Notes, Missouri S&T, 2014

57. Loke, H.M., Tutorial: 2-D and 3-D electrical imaging surveys. Retrieved January 27th, 2010, Geotomo: http://www.geoelectrical.com

58. Loke, M.H., Barker, R.D., Practical techniques for 3-D resistivity surveys and data inversion. Geophysical Prospecting v. 44, pp.499–523, 1996.

59. Anderson, N.L., Highway 65/Springfield Underground Geophysical Investigation, SCI Engineering, 2008.

60. Anderson, N.L., Apel, D.B, Ismail, A., Assessment of Karst Activity at Highway Construction Sites Using the Electrical Resistivity Method, Missouri Department of Transportation, 2006.

61. Myat, M.T., Muchaidze, I., Wamweya, A., Anderson, N.L., Robison, J.L, Assessment of karst activity at Springfield route 60 study site, ASCE: Sinkholes and the Engineering and Environmental Impacts of Karst, pp 714-723, 2008.

62. Terzaghi R., Sources of error in joint surveys, Geotechnique, v. 15, pp. 287-304, 1965.

63. Palmström A., RMi - a rock mass characterization system for rock engineering purposes, Ph.D thesis, University of Oslo, Norway, 409 p, 1995.

64. Palmström A., The volumetric joint count - a useful and simple measure of the degree of rock mass jointing, IV congress international association of engineering geology, v. 2, pp. 221-228, 1982.

VITA

Elnaz Siami-Irdemoosa was born in Tehran, Iran. She graduate from Amirkabir University of Technology at Tehran with a Bachelor of Science in Mining Engineering in 2006. She obtained her Master of Science in Rock Mechanics from the Amirkabir University of Technology, Iran form 2008 to 2011. In August 2013, she joined the PhD program in Geological Engineering at Missouri University of Science and Technology in Rolla, MO, formerly known as University of Missouri Rolla. During her PhD candidacy, she worked as a research assistant on integrated interpretation of resistivity and seismic data under the guidance of Dr. Neil L. Anderson. In May 2017, she received her PhD in Geological Engineering from Missouri University of Science and Technology.